Variational Methods for Control and Design of Bipedal Robot Models

Thesis by

David N. Pekarek

In Partial Fulfillment of the Requirements

for the Degree of

Doctor of Philosophy

California Institute of Technology

Pasadena, California

2010

(Submitted June 4, 2010)

Acknowledgments

Foremost, I wish to acknowledge and thank my advisor Jerrold E. Marsden. His kind-hearted guidance throughout my graduate studies has been an invaluable contribution to my academic and professional development. For this I am truly grateful.

I wish to thank the members of my thesis committee, Joel Burdick, Richard Murray, and Mathieu Desbrun. Their interaction and advice has certainly improved the quality and direction of my research. I would also like to thank additional Caltech faculty, John Doyle, Jim Beck, and David Boyd for their time and interest.

I have had so many postdocs and fellow graduate students make a positive impact on my stay at Caltech. In no particular order, I would like to acknowledge John Delacruz, Morgan Putnam, Noel du Toit, Glenn Garrett, Anne Dekas, John Matson, Andy Downard, Justus Brevik, Jeff Hanna, Dominic Rizzo, Nok Wongpiromsarn, Peter Trautman, Elisa Franco, Pablo Abad-Manterola, John Meier, Chris Kovalchick, Andrea Leonard, Nick Hudson, Michael Wolf, Julia Braman, Jeremy Ma, Tony Roy, Molei Tao, Ashley Moore, Philip du Toit, Ari Stern, Katalin Grubits, Nawaf Bou-Rabee, Sigrid Leyendecker, Marin Kobilarov, Sina Ober-Blöbaum, Andy Lamperski, and surely several others. Part of the joy of life at Caltech was a working environment that included each of them.

I must also thank the Caltech Masters and Rose Bowl Aquatic Center Masters swim teams for providing good company and serene waters whenever I could afford a break. I would especially like to acknowledge Mo, Si, Nikki, Bucky, Jim, Zuma, Mike, Holly, Tom, Jess, and Kaspar. A long way from home, they have been my family.

Certainly, I must acknowledge my parents, Charles and Kathy, my brothers, Joe and Will, and my grandparents, William and Mary. They have loved and supported me longer than anyone, regardless of my faults. I have also been supported by newer family members, my step parents, Mark and Margaret, sisters-in-law, Meeah and Andrea, step siblings, Leah and Spencer, and step grandfather, Pierre. The more the merrier.

Finally, I thank Christina for her love, humor, companionship, and patience. We've a long journey ahead and I can't wait.

Abstract

This thesis investigates nonsmooth mechanics using variational methods for the modeling, control, and design of bipedal robots.

The theory of Lagrangian mechanics is extended to capture a variety of nonsmooth collision behaviors in rigid body systems. Notably, a variational impact model is presented for the transition of constraints behavior that describes a biped switching stance feet at the conclusion of a step.

Next, discretizations of the impact mechanics are developed using the framework of variational discrete mechanics. The resulting variational collision integrators are consistent with the continuous time theory and have an underlying symplectic structure.

In addition to their role as integrators, the discrete equations of motion capturing nonsmooth dynamics enable a direct method for trajectory optimization. Upon specifically defining the optimal control problem for nonsmooth systems, examples demonstrate this optimization method in the task of determining periodic gaits for two rigid body biped models.

An additional effort is made to optimize bipedal walking motions through modifications in system design. A method for determining optimal designs using a combination of trajectory optimization methods and surrogate function optimization methods is defined. This method is demonstrated in the task of determining knee joint placement in a given biped model.

Contents

List of Figures

Chapter 1

Introduction

It is an exciting time to study bipedal walking robots. Driven by nature's examples in animals and humans alike, engineers and roboticists have persistently worked at synthetically capturing the abilities and efficiencies associated with legged locomotion. The last decade has seen a number high profile industry successes, notably Sony's Qrio [35] and Honda's Asimo [78], pushing the boundaries of robotic capabilites in walking. At first glance, the performance of these robots can make it seem that the major challenges in the field are foregone. In fact, these robots have given rise to new problems and have motivated new research directions.

The robots mentioned above are state of the art, but use a tremendous amount of energy. Each of these bipeds walks flat footed with severe constraints on its motion in order to control its center of pressure, a weighted average of its ground reaction forces. The result is a robot that walks impressively and stably, but also inefficiently. In response to this, a large body of research has aimed at producing controllers for efficient walking motions. Works that focus on stabilizing controllers appear in [4, 41, 26, 38, 28], while others approach the problem using optimal control techniques in [25, 82, 76]. This thesis fits in the context of the latter group, providing a new framework in which to model, design, and produce optimal controllers for bipedal robot models.

1.1 Nonsmooth Mechanics

The dynamics of a walking robot are nonsmooth as a result of the change in ground contacts required to take a step. Assuming a model with no compliance at the contact, these dynamics require the modeling of rigid body impact mechanics. This is a task for which there are multiple approaches.

Perhaps the most popular approach is the use of measure differential inclusions. This tool extends the familiar framework of differential equations to allow measure-valued forces, namely impulses. Mathematically, differential inclusions were first considered by Filippov [33, 34] and gained traction in the area of rigid body dynamics with the sweeping process of Moreau [70, 71]. The method is particularly popular for its ability to produce powerful existence and uniqueness results, notably Stewart's work [85] resolving the paradox of Painlevé. A control theoretic approach for systems described with measure differential inclusions is provided by Brogliato [19, 21].

A simpler approach to rigid body impact mechanics, and one that is more prevelant in the engineering literature on biped control, is the use of hybrid system descriptions. This method, best used on systems with isolated incidences of contact, describes impacts with a guard and a reset map. The guard is a function detecting contact and the reset map modifies the system's phase applying an impulsive force. In practice, the reset map is often defined with algebraic impact models [24, 43], but may also recast measure differential inclusion results [20]. A hybrid system description does not modify the framework of differential equations, but makes use of it in the creation of a hybrid automaton. This model specifies a set of differential equations, one for each possible set of engaged contacts in the system. Existence and uniqueness results for hybrid automata have been provided by Lygeros et al. [64]. A control theoretic framework for hybrid systems is discussed by Bemporad and Morari [8], Branicky et al. [17], and Skaikh and Caines [79]. The use of hybrid systems to describe bipeds

appears in numerous works [41, 26, 25, 4, 40, 44, 39, 38, 81, 76].

In this thesis, we make use of a third approach, variational nonsmooth mechanics. Similar to measure differential inclusions, this method can be considered as its own modeling framework or as a means to generate reset maps in the hybrid systems approach. The variational methodology used traces its roots to Young [87], and has been used in the context of rigid body impacts in [54, 23, 32]. The work of Fetecau et al. [32] features the symplectic structure underlying this description of impacts, one of the method's main advantages. However, existence and uniqueness results are a significant challenge when using this method, an issue that remains deferred in this thesis.

1.2 Discrete Mechanics

Capturing nonsmooth mechanics with variational methods enables their representation in discrete time as variational integrators. An excellent account of variational integrators and their derivation for standard smooth mechanics problems is provided in [42]. The geometric structure of variational integrators is discussed in the context of the discrete mechanics framework in Marsden and West [68]. This framework has been succesfully applied in describing a wide range of areas within mechanics: constrained systems [68, 61, 59, 69], solid mechanics [57, 59], mechanical systems on Lie groups [16, 55], electromagnetics [83], and nonsmooth mechanics [32, 27].

The variational collision integrators derived in this thesis build on the work of Fetecau et al. [32] and extend those methods to a wider range of rigid body impact behaviors. The numerical integrators produced are in contrast to two more common approaches in the simulation of nonsmooth dynamics, numerical methods for measure differential inclusions [2, 84] and integration using smoothing and penalty functions [80, 50]. Using the variational approach is often more computationally expensive than

these methods, but benefits from the discrete symplectic structure at its foundation.

The discrete mechanics framework, in addition to developing variational integrators, provides a means to solve optimal control problems. First explored in Junge et al. [47], the method of discrete mechanics and optimal control (DMOC) recasts a standard optimal control problem as a finite-dimensional optimization problem. In doing so, the DMOC method fits in the class of direct methods for trajectory optimization. A wealth of literature exists regarding solution methods for trajectory optimization, direct methods and otherwise. We highlight the surveys provided in [13, 12].

1.3 Design Optimization with Surrogates

In addition to optimizing walking motions for bipedal robots, another approach to improving their efficiency is through their design. This thesis considers the design problem of finding design parameters to reduce the cost of optimal control. Cost function evaluations for this problem, which are determined by solving a trajectory optimization problem, are computationally expensive and provide no gradient information. These properties are present in other types of engineering design problems, for instance the aeroacoustic shape design performed by Marsden et al. [65] and the fuel assembly optimization performed by Raza and Kim [75]. In each of these works, the gradient free optimization was performed efficiently using surrogate methods [45, 6]. Surrogate methods approximate the cost function with a structured surrogate model and choose additional sample locations based on information provided by the surrogate. In the hands of an experienced user these methods offer rapid convergence in comparison to other popular gradient-free methods such as pattern search methods [5], trust region methods [3], and evolutionary algorithms [37]. Although, surrogate methods alone do not provide convergence guarantees. The work

of Booker et al. [15] has extended them to do so with the incorporation of pattern search steps.

1.4 Contributions and Thesis Outline

Chapter 2 provides a review of smooth mechanical systems, both free and holonomically constrained, using a nonautonomous variational approach. This review sets the stage for the variational development of rigid body impact mechanics. Variational principles lead to nonsmooth dynamics for systems, both free and holonomically constrained, undergoing elastic, inelastic, and perfectly plastic collisions. Dynamics are also derived for impacts causing a transition of constraints, the case that is pertinent for modeling walking. Additionally, the chapter makes use of null space descriptions [60, 10, 9] in the nonsmooth dynamics wherever possible. The merging of variational methodologies for constraints and nonsmooth behaviors is a notable contribution.

Chapter 3 extends all of the derivations from Chapter 2 to a discrete time setting. The resulting discrete time equations of motion are suitable for use as variational integrators. A nonautonomous approach is required in the variational methodology, but can also lead to infeasibility during integration. Hence, a discussion is maintained to indicate when adaptive time stepping is advisable during integration. The development and demonstration of variational collision integrators is the primary contribution in this chapter.

Chapter 4 incorporates the discrete equations of motion from Chapter 3 into the DMOC method. After a review of DMOC for smooth systems, an optimization problem for systems with nonsmooth dynamics is defined and discretized. The discrete form is numerically tractable as demonstrated with trajectory optimization results providing locally optimal periodic gaits for two biped models. Coupled with the author's previous work [73], this demonstration of DMOC on systems with nonsmooth

dynamics is the first of its kind.

Chapter 5 addresses the task of design optimization for bipedal robots. Specifically, the previous chapter's DMOC results are leveraged in a search for design parameters that reduce the cost of optimal control. A framework utilizing surrogate methods to sample and optimize design parameters is outlined. This framework is then demonstrated, utilizing the "strawman" surrogate method, in the task of designing the knee joint placement in a 4-link biped. This use of surrogate methods to optimize designs for improved optimal control is a notable contribution.

Chapter 6 is devoted to outlining future research directions stemming from this thesis.

Chapter 2

Variational Collision Mechanics

In this chapter, we develop a framework by which variational mechanics describes a variety of collision behaviors in rigid body mechanical systems. We begin by reviewing smooth mechanical systems, both free and holonomically constrained, in a nonautonomous setting. This lays the foundation necessary to explore collisions of constrained systems, and finally collisions allowing or even causing changes in system constraints. These behaviors are essential when describing the dynamics of bipedal robots.

2.1 Smooth Systems

Before delving into impact mechanics, we conduct a quick review of free and holonomically constrained Lagrangian mechanics. Examining these systems in a nonautonomous setting yields redundant results; however, we labor through this nonetheless in order to build familiarity with the approaches that will be applied in the nonsmooth case.

2.1.1 Free Systems

Consider a mechanical system with an n-dimensional configuration manifold Q, this manifold's associated tangent bundle TQ, and a Lagrangian $L : TQ \to \mathbb{R}$. In the

nonautonomous approach we consider a "time-like" variable τ on the interval $[0,1]$ and define parameterizations of time and trajectories in configuration space as mappings $c_t(\tau)$ and $c_q(\tau)$, respectively. More formally, consider the ***path space***

$$\mathcal{M} = \mathcal{T} \times \mathcal{Q}([0,1], Q),$$

where

$$\mathcal{T} = \{c_t \in C^\infty([0,1], \mathbb{R}) \mid c_t' > 0 \text{ in } [0,1]\},$$
$$\mathcal{Q}([0,1], Q) = \{c_q \in C^2([0,1], Q)\}.$$

Notice that the elements $c \triangleq (c_t, c_q)$ in $\mathcal{M}$ do not just define paths on the configuration manifold Q, but rather paths on an ***extended configuration manifold*** $Q_e = \mathbb{R} \times Q$. For any path $c \in \mathcal{M}$ on Q_e, we can invert the parameterization $t = c_t(\tau)$ to recover an associated curve on Q in the time domain as

$$q(t) = c_q(c_t^{-1}(t)).$$

Noting that $\mathcal{M}$ is a smooth manifold, we define an ***extended action map*** on path space $\bar{\mathfrak{G}} : \mathcal{M} \to \mathbb{R}$ as

$$\bar{\mathfrak{G}}(c_t, c_q) = \int_0^1 \bar{L}\left(c(\tau), c'(\tau)\right) d\tau,$$

where we have introduced the ***extended Lagrangian*** $\bar{L} : TQ_e \to \mathbb{R}$ defined as

$$\bar{L}\left(c(\tau), c'(\tau)\right) = L\left(c_q(\tau), \frac{c_q'(\tau)}{c_t'(\tau)}\right) c_t'(\tau).$$

Remark 2.1: *Notice the factor of c_t' that appears in $\bar{L}$ after the (autonomous) Lagrangian term. The inclusion of this term is such that a change of variables $t = c_t(\tau)$ produces the correct autonomous action in the time domain $\mathfrak{G} : \mathcal{Q}([0,1], Q) \to \mathbb{R}$ of*

the form

$$\mathfrak{G}(q) = \int_{c_t(0)}^{c_t(1)} L\,(q, \dot{q})\,dt.$$

This factor of c_t' will be pervasive in the future instances that we recast autonomous concepts in the nonautonomous setting.

Finally, we define the ***second-order submanifold*** of Q_e as

$$\ddot{Q}_e = \left\{ \frac{d^2c}{d\tau^2}(0) \in T(TQ_e) \mid c : [0,1] \to Q_e \text{ is a } C^2 \text{ curve} \right\}.$$

Now we have all of the necessary elements in place to describe variations of the action with respect to the path.

Theorem 2.1: *Given a C^k Lagrangian, $k \geq 2$, there exists a unique C^{k-2} mapping $EL : \ddot{Q}_e \to T^*Q_e$ and a unique C^{k-1} one-form Θ_L on TQ_e, such that for all variations $\delta c \in T_c\mathcal{M}$ of c we have:*

$$d\bar{\mathfrak{G}}(c) \cdot \delta c = \int_0^1 EL(c'') \cdot \delta c\, d\tau + \Theta_L(c') \cdot \hat{\delta} c(\tau)\Big|_0^1, \tag{2.1.1}$$

where

$$\begin{aligned}
EL(c'') &= \left[\frac{\partial L}{\partial q} c_t' - \frac{d}{d\tau}\left(\frac{\partial L}{\partial \dot{q}}\right)\right] dc_q + \left[\frac{d}{d\tau}\left(\frac{\partial L}{\partial \dot{q}}\frac{c_q'}{c_t'} - L\right)\right] dc_t, \\
\Theta_L(c') &= \left[\frac{\partial L}{\partial \dot{q}}\right] dc_q - \left[\frac{\partial L}{\partial \dot{q}}\frac{c_q'}{c_t'} - L\right] dc_t, \\
\hat{\delta} c(\tau) &= \left(\left(c(\tau), \frac{\partial c}{\partial \tau}(\tau)\right), \left(\delta c(\tau), \frac{\partial \delta c}{\partial \tau}(\tau)\right)\right).
\end{aligned}$$

As in [32], we term EL the **Euler-Lagrange derivative** *and Θ_L the* **Lagrangian one-form**. *The latter of these expressions is consistent with the terminology in [67].*

PROOF: Considering $\delta c \in T_c\mathcal{M}$ with components δc_t and δc_q, we take variations of

the action as

$$d\bar{\mathfrak{G}}(c)\cdot\delta c=\int_0^1\left[\frac{\partial L}{\partial q}\delta c_q+\frac{\partial L}{\partial\dot{q}}\left(\frac{\delta c_q'}{c_t'}-\frac{c_q'\delta c_t'}{(c_t')^2}\right)\right]c_t'\,d\tau+\int_0^1 L\delta c_t'\,d\tau.$$

Using integration by parts on all instances of $\delta c_q'=\frac{d}{d\tau}\delta c_q$ and $\delta c_t'=\frac{d}{d\tau}\delta c_t$ produces the desired result. ■

Hamilton's principle indicates that trajectories of the mechanical system will correspond with stationary points of the action. That is, a solution $c\in\mathcal{M}$ will yield $d\bar{\mathfrak{G}}(c)\cdot\delta c=0$ for variations $\delta c\in T_c\mathcal{M}$ that vanish at the boundaries 0 and 1. Utilizing (2.1.1), we see that setting variations to zero at the boundaries eliminates the influence of the $\Theta_L(c')$ term, and it is sufficient for solutions to produce $EL(c'')=0$ for all $\tau\in(0,1)$. This yields the ***extended Euler-Lagrange equations***, which, when expressed in the time domain, take the form

$$\frac{\partial L}{\partial q}-\frac{d}{dt}\left(\frac{\partial L}{\partial\dot{q}}\right)=0 \tag{2.1.2}$$

$$\frac{d}{dt}\left(\frac{\partial L}{\partial\dot{q}}\dot{q}-L\right)=0 \tag{2.1.3}$$

for all $t\in(c_t(0),c_t(1))$.

Remark 2.2: *For a given $q(t)$ satisfying the extended Euler-Lagrange equations, there actually exists an equivalence class of paths (c_t,c_q) such that $q(t)=c_q(c_t^{-1}(t))$. For a detailed explanation of how to quotient this redundancy out of the results, see [31].*

Perhaps unsurprisingly, in (2.1.2), we have revealed the standard Euler-Lagrange equations one would deduce in the autonomous setting. Noting that the ***energy*** of a Lagrangian system is $E=\left(\frac{\partial L}{\partial\dot{q}}\dot{q}-L\right)$, (2.1.3) implies energy conservation. While Hamilton's principle in the autonomous setting does not produce this equation, we

know it to be true of autonomous systems obeying (2.1.2) (see [68] or [32]). Thus, the additional variational machinery involved in using a nonautonomous approach on smooth systems has yielded one additional redundant equation. While this is somewhat unrewarding, we will see greater merits of this approach in Section 2.2 and beyond.

2.1.2 Holonomic Constraints

In many instances, we may encounter mechanical systems where it is necessary, or perhaps simply advantageous, to describe the system using constraints. In general, these constraints take a variety of forms and are often classified according to different fundamental structures and dependencies (see [7] for instance). Here, we will only consider holonomic constraints of the form $g(q) = 0$, where $g : Q \to \mathbb{R}^m$, $m < n$, is a ***constraint function*** for which 0 is assumed to be a regular value such that $N = g^{-1}(0) \subset Q$ is a ***constraint submanifold***. As we remain in a nonautonomous setting, we will often view the above as an ***extended constraint function*** $\bar{g} : Q_e \to \mathbb{R}^m$ defined by $\bar{g}(c) = g(c_q)c_t'$ (recall Remark 2.1), with an associated ***extended constraint submanifold*** $N_e = \bar{g}^{-1}(0) = \mathbb{R} \times N \subset Q_e$.

One of the most accessible and widely used methods to handle such systems is the introduction of Lagrange multipliers. This approach, using the Lagrange multiplier theorem to construct equivalent variational principles, will be our focus in the context of both smooth and nonsmooth trajectories. However, when possible, we will describe results in terms of the null space method [60, 10, 9], which falls into the general class of projection methods. As we will encounter its application repeatedly, we now explicitly state the Lagrange multiplier theorem.

Theorem 2.2: *Consider a smooth manifold M and a function $\Phi : M \to V$ mapping to some inner product space V, such that $0 \in V$ is a regular point of Φ. Set $\mathcal{D} = \Phi^{-1}(0) \subset M$. Given a function $\bar{\mathfrak{G}} : M \to \mathbb{R}$, define $\tilde{\mathfrak{G}} : M \times V \to \mathbb{R}$ by $\tilde{\mathfrak{G}}(c, c_\lambda) =$*

$\bar{\mathfrak{G}}(c) - \langle c_\lambda, \Phi(c)\rangle$. *The following are equivalent:*

1. $c \in \mathcal{D}$ is an extremum of $\bar{\mathfrak{G}}|_{\mathcal{D}}$;

2. $(c, c_\lambda) \in M \times V$ is an extremum of $\tilde{\mathfrak{G}}$.

PROOF: See [1]. ∎

Using the manifold structure of N_e, we can consider restrictions of the extended Lagrangian of the form $\bar{L}^{N_e} = \bar{L}|_{TN_e}$. We will be comparing the dynamics of $\bar{L}^{N_e}$ resulting from an action principle on $\mathcal{T} \times \mathcal{Q}([0,1], N)$ with the dynamics of an ***augmented Lagrangian*** $\tilde{L}^{\bar{g}} : T(Q_e \times \mathbb{R}^m) \to \mathbb{R}$ derived in the higher dimensional ***constrained coordinate path space***

$$\mathcal{M}_{cc} = \mathcal{T} \times \mathcal{Q}([0,1], Q) \times \mathcal{L},$$

where $\mathcal{T}$ and $\mathcal{Q}([0,1], Q)$ are as previously defined and $\mathcal{L}$ is the space of square-integrable curves $c_\lambda : [0,1] \to \mathbb{R}^m$.

Theorem 2.3: *Given an extended Lagrangian system $\bar{L} : TQ_e \to \mathbb{R}$ with an extended holonomic constraint $\bar{g} : Q_e \to \mathbb{R}^m$, denote $\tilde{Q}_e = Q_e \times \mathbb{R}^m$, $N_e = \bar{g}^{-1}(0) \subset Q_e$, and $L^{N_e} = L|_{TN_e}$. The following are equivalent:*

1. $c \in \mathcal{T} \times \mathcal{Q}([0,1], N)$ extremizes $\bar{\mathfrak{G}}^{N_e} = \bar{\mathfrak{G}}|_{TN_e}$ and thus is a solution of the extended Euler-Lagrange equations for $\bar{L}^{N_e}$;

2. $(c, c_\lambda) \in \mathcal{M}_{cc}$ produces $q(t) = c_q(c_t^{-1}(t))$ and $\lambda(t) = c_\lambda(c_t^{-1}(t))$ satisfying the **extended constrained Euler-Lagrange equations**

$$\frac{\partial L}{\partial q} - \frac{d}{dt}\left(\frac{\partial L}{\partial \dot{q}}\right) = \left(\frac{dg}{dq}\right)^T \cdot \lambda \tag{2.1.4}$$

$$\frac{d}{dt}\left(\frac{\partial L}{\partial \dot{q}}\dot{q} - L + g \cdot \lambda\right) = 0 \tag{2.1.5}$$

$$g = 0, \tag{2.1.6}$$

for all $t \in (c_t(0), c_t(1))$;

3. $(c, c_\lambda) \in \mathcal{M}_{cc}$ extremizes $\tilde{\mathfrak{G}}(c, c_\lambda) = \bar{\mathfrak{G}}(c) - \langle c_\lambda, \Phi(c)\rangle$ and hence solves the Euler-Lagrange equations for the augmented Lagrangian $\tilde{L}^{\bar{g}} : T\tilde{Q}_e \to \mathbb{R}$ defined by

$$\tilde{L}^{\bar{g}}(c, c_\lambda, c', c'_\lambda) = \bar{L}(c, c') - \langle c_\lambda, \bar{g}(c)\rangle.$$

PROOF: We readily apply Theorem 2.2. In the context of that theorem, the full space M is $\mathcal{M} = \mathcal{T} \times \mathcal{Q}([0,1], Q)$, the function to be extremized is $\bar{\mathfrak{G}}$ as defined in Subsection 2.1.1, and $V = \mathcal{L}$ with the L_2 inner product. Set $\Phi : M \to V$ as $\Phi(c)(\tau) = \bar{g}(c(\tau))$ such that $c \in \mathcal{T} \times \mathcal{Q}([0,1], N)$ if and only if $\Phi(c) = 0$ (meaning $\bar{g}(c(\tau)) = 0$ for all $\tau \in [0,1]$). From this it follows $\mathcal{D} = \Phi^{-1}(0) = \mathcal{T} \times \mathcal{Q}([0,1], N)$.

The first condition above corresponds precisely with the first condition in Theorem 2.2. That is, $c \in \mathcal{D}$ is an extremum of $\bar{\mathfrak{G}}|_{\mathcal{D}}$. By the Lagrange multiplier theorem, this is equivalent to $(c, c_\lambda) \in M \times V$ being an extremum of $\tilde{\mathfrak{G}}(c, c_\lambda) = \bar{\mathfrak{G}}(c) - \langle c_\lambda, \Phi(c)\rangle$. Identifying $M \times V$ with $\mathcal{M}_{cc}$ and examining the particular form of $\tilde{\mathfrak{G}} : \mathcal{M}_{cc} \to \mathbb{R}$, we see the augmented Lagrangian $\tilde{L}^{\bar{g}} : T\tilde{Q}_e \to \mathbb{R}$ emerge as

$$\begin{aligned}
\tilde{\mathfrak{G}}(c, c_\lambda) &= \bar{\mathfrak{G}}(c) - \langle c_\lambda, \Phi(c)\rangle \\
&= \int_0^1 \bar{L}\,(c, c')\,d\tau - \int_0^1 \langle c_\lambda(\tau), \Phi(c)(\tau)\rangle d\tau \\
&= \int_0^1 \left[\bar{L}\,(c(\tau), c'(\tau)) - \langle c_\lambda(\tau), \bar{g}(c(\tau))\rangle\right] d\tau \\
&= \int_0^1 \tilde{L}^{\bar{g}}(c(\tau), c_\lambda(\tau), c'(\tau), c'_\lambda(\tau))d\tau.
\end{aligned}$$

As (c, c_λ) extremizes $\tilde{\mathfrak{G}}(c, c_\lambda)$, it is also a solution to the Euler-Lagrange equations for $\tilde{L}^{\bar{g}}$, satisfying the third condition. Finally, the second condition follows from this by solving $d\tilde{\mathfrak{G}} = 0$ and casting the results in the time domain using the same process as in the proof of Theorem 2.1. ∎

We note a few properties of the extended constrained Euler-Lagrange equations and their relation to the unconstrained set (2.1.2) and (2.1.3). We see that (2.1.4) parallels the momentum evolution (2.1.2), although now in the presence of constraint forces $\left(\frac{dg}{dq}\right)^T \cdot \lambda$. These forces maintain that the system remains on N, which is signified by (2.1.6). Noting this condition, we also see that the constrained system's energy, the conserved quantity in (2.1.5), is equivalent to the previously defined energy E. This energy conservation equation, similar to (2.1.3), is redundant in this setting.

In another effort to prepare tools for our treatment of nonsmooth mechanics, we will reconsider the system above using the vakonomic method [58] on the "hidden" (or secondary) constraints [29] associated with g. These constraints are simply the time-differentiated form of $g(q) = 0$; that is, $f : TQ \to \mathbb{R}^m$ such that

$$f(q, \dot{q}) = \frac{dg}{dq} \cdot \dot{q} = 0.$$

In the nonautonomous setting, and in accordance with Remark 2.1, we define an equivalent ***extended hidden constraint*** as $\bar{f} : T(Q_e) \to \mathbb{R}^m$ of the form

$$\begin{aligned} \bar{f}(c, c') &= f\left(c_q, \frac{c'_q}{c'_t}\right) c'_t \\ &= \frac{dg}{dq}\Big|_{c_q} \cdot c'_q. \end{aligned}$$

Given that c'_t is strictly positive, $f = 0$ if and only if $\bar{f} = 0$. One important property that will allow us to draw parallels between the usage of the holonomic constraint g and the hidden constraint f is

$$\frac{dg}{dq} = \frac{\partial f}{\partial \dot{q}}. \tag{2.1.7}$$

Remark 2.3: *The original constraint $g(q) = 0$ and the hidden constraint $f(q, \dot{q}) = 0$ differ slightly in their respective constraint submanifolds. See that $f^{-1}(0)$ is the space of paths satisfying $\frac{d}{dt}(g(q)) = 0$, also written as $g(q(t)) = g(q(c_t(0)))$ for all*

t. We cannot guarantee that this space is N, or even a submanifold at all, without the condition $g(q(c_t(0))) = 0$. We will assume this condition henceforth and thus $f^{-1}(0) = N \in Q$.

We should state that the vakonomic method, often mentioned in the context of nonholonomic constraints on TQ, is often disregarded for the more favorable nonholonomic method [14]. However, in [58], it is shown that these methods are equivalent when applied to an integrable (i.e., holonomic) constraint. We show in the nonautonomous case that the vakonomic method produces c_q and c_t equivalent to those in Theorem 2.3.

Theorem 2.4: *Given an extended Lagrangian system $\bar{L} : TQ_e \to \mathbb{R}$ with an extended holonomic constraint $\bar{g} : Q_e \to \mathbb{R}^m$ and its associated extended hidden constraint $\bar{f} : Q_e \to \mathbb{R}^m$, denote $\tilde{Q}_e = Q_e \times \mathbb{R}^m$, $N_e = \bar{f}^{-1}(0) \subset Q_e$, and $L^{N_e} = L|_{TN_e}$. The following are equivalent:*

1. $c \in \mathcal{T} \times \mathcal{Q}([0,1], N)$ extremizes $\bar{\mathfrak{G}}^{N_e}$ and thus is a solution of the extended Euler-Lagrange equations for $\bar{L}^{N_e}$;

2. $(c, c_\lambda) \in \mathcal{M}_{cc}$ produces $q(t) = c_q(c_t^{-1}(t))$ and $\lambda(t) = c_\lambda(c_t^{-1}(t))$ satisfying the **vakonomic extended constrained Euler-Lagrange equations**

$$\frac{\partial L}{\partial q} - \frac{d}{dt}\left(\frac{\partial L}{\partial \dot{q}}\right) = -\left(\frac{df}{d\dot{q}}\right)^T \cdot \dot{\lambda} \tag{2.1.8}$$

$$\frac{d}{dt}\left(\frac{\partial L}{\partial \dot{q}}\dot{q} - \left(\frac{df}{d\dot{q}}\dot{q}\right) \cdot \lambda - L + f \cdot \lambda\right) = 0 \tag{2.1.9}$$

$$f = 0, \tag{2.1.10}$$

   for all $t \in (c_t(0), c_t(1))$;

3. $(c, c_\lambda) \in \mathcal{M}_{cc}$ extremizes $\tilde{\mathfrak{G}}(c, c_\lambda) = \bar{\mathfrak{G}}(c) - \langle c_\lambda, \Phi(c)\rangle$ and hence solves the Euler-

Lagrange equations for the augmented Lagrangian $\tilde{L}^{\bar{f}} : T\tilde{Q}_e \to \mathbb{R}$ defined by

$$\tilde{L}^{\bar{f}}(c, c_\lambda, c', c'_\lambda) = \bar{L}(c, c') - \langle c_\lambda, \bar{f}(c, c') \rangle.$$

PROOF: The proof of this theorem follows identically the structure of the proof for the previous Theorem 2.3. The only difference is in the form of $\Phi : M \to V$, which is now $\Phi(c)(\tau) = \bar{f}(c(\tau), c'(\tau))$. Again, the Lagrange multiplier theorem provides equivalence of the first and third conditions, and here the augmented Lagrangian appears as $\tilde{L}^{\bar{f}}(c, c_\lambda, c', c'_\lambda) = \bar{L}(c, c') - \langle c_\lambda, \bar{f}(c, c') \rangle$.

The Euler-Lagrange equations associated with $\tilde{L}^{\bar{f}}$ take a slightly more complex form in this case. To see their derivation, examine that $d\tilde{\mathfrak{G}} = 0$ implies

$$\begin{aligned}
0 &= \int_0^1 \left[EL(c'') \cdot \frac{\delta c}{c'_t} - c_\lambda \cdot \frac{\partial f}{\partial q} \delta c_q - c_\lambda \cdot \frac{\partial f}{\partial \dot{q}} \left(\frac{\delta c'_q}{c'_t} - \frac{c'_q \delta c'_t}{(c'_t)^2} \right) - f \delta c_\lambda - c_\lambda \cdot f \frac{\delta c'_t}{c'_t} \right] c'_t \, d\tau \\
&= \int_0^1 \left[\left(\frac{\partial L}{\partial q} - c_\lambda \cdot \frac{\partial f}{\partial q} \right) c'_t - \frac{d}{d\tau} \left(\frac{\partial L}{\partial \dot{q}} - c_\lambda \cdot \frac{\partial f}{\partial \dot{q}} \right) \right] \delta c_q \, d\tau + \int_0^1 -f c'_t \, \delta c_\lambda \, d\tau \\
&\quad + \int_0^1 \left[\frac{d}{d\tau} \left(\left(\frac{\partial L}{\partial \dot{q}} - c_\lambda \cdot \frac{\partial f}{\partial \dot{q}} \right) \frac{c'_q}{c'_t} - L + c_\lambda \cdot f \right) \right] \delta c_t \, d\tau \\
&\quad + \left[\frac{\partial L}{\partial \dot{q}} - c_\lambda \cdot \frac{\partial f}{\partial \dot{q}} \right] \delta c_q \Big|_0^1 + \left[\left(\frac{\partial L}{\partial \dot{q}} - c_\lambda \cdot \frac{\partial f}{\partial \dot{q}} \right) \frac{c'_q}{c'_t} - L + c_\lambda \cdot f \right] \delta c_t \Big|_0^1,
\end{aligned}$$

where $\cdot$ has been used as shorthand for the inner product. The expressions above fully define the Euler-Lagrange derivative and the Lagrangian one-form for the augmented Lagrangian $\tilde{L}^{\bar{f}}$. For future reference, we record their definitions here as

$$\begin{aligned}
\widetilde{EL}(c'', c''_\lambda) &= \left[\left(\frac{\partial L}{\partial q} - c_\lambda \cdot \frac{\partial f}{\partial q} \right) c'_t - \frac{d}{d\tau} \left(\frac{\partial L}{\partial \dot{q}} - c_\lambda \cdot \frac{\partial f}{\partial \dot{q}} \right) \right] dc_q \\
&\qquad + \left[-f c'_t \right] dc_\lambda + \left[\frac{d}{d\tau} \left(\frac{\partial L}{\partial \dot{q}} \frac{c'_q}{c'_t} - L \right) \right] dc_t \qquad (2.1.11) \\
\Theta_{\tilde{L}^{\bar{f}}}(c', c'_\lambda) &= \left[\frac{\partial L}{\partial \dot{q}} - c_\lambda \cdot \frac{\partial f}{\partial \dot{q}} \right] dc_q - \left[\left(\frac{\partial L}{\partial \dot{q}} - c_\lambda \cdot \frac{\partial f}{\partial \dot{q}} \right) \frac{c'_q}{c'_t} - L + c_\lambda \cdot f \right] dc_t \qquad (2.1.12)
\end{aligned}$$

Requiring that $\widetilde{EL}(c'', c''_\lambda)$ is identically zero and recasting that condition in the time

domain provides (2.1.8), (2.1.9), and (2.1.10). In the final steps, the dc_q terms containing f are collected and simplified as

$$-\lambda \cdot \frac{\partial f}{\partial q} - \frac{d}{dt}\left(-\lambda \cdot \frac{\partial f}{\partial \dot{q}}\right) = -\lambda \cdot \frac{\partial f}{\partial q} + \dot{\lambda} \cdot \frac{\partial f}{\partial \dot{q}} + \lambda \cdot \frac{\partial^2 f}{\partial q \partial \dot{q}}\dot{q}$$
$$= \dot{\lambda} \cdot \frac{\partial f}{\partial \dot{q}}.$$

This cancellation produces the right-hand side of (2.1.8). ∎

Corollary 2.1: *The path* $(c, c_\lambda) \in \mathcal{M}_{cc}$ *satisfies the extended constrained Euler-Lagrange equations if and only if there exists* $\breve{c}_\lambda \in \mathcal{L}$ *such that* $(c, \breve{c}_\lambda) \in \mathcal{M}_{cc}$ *satisfies the vakonomic extended constrained Euler-Lagrange equations.*

PROOF: By Theorems 2.3 and 2.4, the given statements are each equivalent to the condition: $c \in \mathcal{T} \times \mathcal{Q}([0,1], N)$ is a solution to the extended Euler-Lagrange equations for the restricted Lagrangian, $\bar{L}^{N_e}$. Hence, they too are equivalent. ∎

Our results in the vakonomic case are nearly identical to the previous results (2.1.4), (2.1.5), and (2.1.6). Equation (2.1.8) is a momentum evolution equation with constraint forces, and noting the property (2.1.7) we see that these forces take nearly an identical form to those in (2.1.4) (there is just $-\dot{\lambda}$ in place of the former λ). Remark 2.3 has already mentioned the equivalence between the respective constraint equations (2.1.6) and (2.1.10). Finally, noting that f is linear in $\dot{q}$, we have

$$\frac{\partial f}{\partial \dot{q}}\dot{q} = f,$$

such that (2.1.9) amounts to conservation of the unconstrained energy E.

Momentarily disregarding the redundant energy equations (2.1.5) and (2.1.9), each set of the paired equations (2.1.4), (2.1.6) and (2.1.8), (2.1.10) has the structure of an $(n+m)$-dimensional set of differential algebraic equations (DAEs) [18] in the variables

(q, λ). The dimension of these systems should be somewhat disconcerting considering that they are capturing $(n-m)$-dimensional dynamics on the submanifold N. Using the null space method [61], we can reduce the dimension of the DAEs and eliminate the presence of any Lagrange multipliers λ.

We introduce the concept of an $n \times (n-m)$ ***null space matrix*** $P(q)$ with $(n-m)$ columns that form a basis of T_qN such that $P(q) : \mathbb{R}^{n-m} \to T_qN$. The term null space matrix is derived from the property of $P(q)$ that

$$\text{range}(P(q)) = \text{null}\left(\frac{\partial g}{\partial q}(q)\right) = T_qN. \tag{2.1.13}$$

Note that there is no unique basis for T_qN and hence $P(q)$ is in general not unique. However, (2.1.13) is a necessary and sufficient condition to define a null space matrix. Any $P(q)$ satisfying this condition can be used as a projection on the DAEs (2.1.4) and (2.1.6) as follows

$$P^T(q)\left[\frac{\partial L}{\partial q} - \frac{d}{dt}\left(\frac{\partial L}{\partial \dot{q}}\right)\right] = 0, \tag{2.1.14}$$

$$g = 0, \tag{2.1.15}$$

for all $t \in (c_t(0), c_t(1))$. Recalling (2.1.7), the same projection applies to the vakonomic equations (2.1.8) and (2.1.10) which results in the DAEs above, just with $f = 0$ in place of the equivalent condition (2.1.15). The DAEs (2.1.14) and (2.1.15) are equivalent to (2.1.4), (2.1.6) and (2.1.8), (2.1.10), but are only n-dimensional. This is still higher than the dimension of the constrained dynamics, $(n-m)$, but is equivalent to the dimension of the constrained coordinates q. A lower dimensional description of the dynamics would only make sense in a lower dimensional coordinate space, for instance, generalized coordinates on N.

2.1.3 External Forcing

In this section, we study a generalization of the extended Euler-Lagrange equations for mechanical systems with external forces (e.g., friction, damping, or control forces). Adding the virtual work of such forces into our variational arguments marks a departure from Hamilton's principle and to the Lagrange-d'Alembert principle. Here, we demonstrate this for the simplest case, the free systems of Subsection 2.1.1. However, the following arguments readily apply to any of the variational principles in this chapter.

As in [67], we define an ***exterior force field*** as a fiber-preserving map $F : TQ_e \to T^*Q_e$ over the identity. Following Remark 2.1, we write this in coordinates a

$$F : (c, c') \to (c, F(c, c')c'_t).$$

Appending the virtual work of $F = (F_t, F_q)$ to our previous Hamilton's principle for free systems yields the ***integral Lagrange-d'Alembert principle***

$$\delta \int_0^1 L\left(c_q(\tau), \frac{c'_q(\tau)}{c'_t(\tau)}\right) c'_t(\tau) d\tau + \int_0^1 F(c(\tau), c'(\tau)) \cdot \delta c \, d\tau = 0,$$

where, as before, variations $\delta c \in T_c\mathcal{M}$ vanish at the boundaries. Taking variations of the action as in Subsection 2.1.1, we see the condition above is equivalent to the ***extended forced Euler-Lagrange equations***

$$\frac{\partial L}{\partial q} - \frac{d}{dt}\left(\frac{\partial L}{\partial \dot{q}}\right) = -F_q, \tag{2.1.16}$$

$$\frac{d}{dt}\left(\frac{\partial L}{\partial \dot{q}}\dot{q} - L\right) = -F_t, \tag{2.1.17}$$

for all $t \in (c_t(0), c_t(1))$. As a direct consequence of the energy evolution equation being redundant for smooth systems, we can derive a necessary consistency condition

between F_q and F_t. This relation appears as

$$\begin{aligned} F_t &= -\frac{d}{dt}\left(\frac{\partial L}{\partial \dot{q}}\dot{q} - L\right) \\ &= -\frac{d}{dt}\left(\frac{\partial L}{\partial \dot{q}}\right)\dot{q} - \frac{\partial L}{\partial \dot{q}}\ddot{q} + \frac{\partial L}{\partial \dot{q}}\ddot{q} + \frac{\partial L}{\partial \dot{q}}\dot{q} \\ &= \left(-F_q - \frac{\partial L}{\partial q}\right)\dot{q} + \frac{\partial L}{\partial q}\dot{q} \\ &= -F_q\dot{q}. \end{aligned}$$

Though mathematically the freedom exists to define forces (F_t, F_q) that violate this condition, physically this would defy the conservation of mechanical energy.

2.2 Elastic Collisions

We now extend the concepts and variational principles in Section 2.1 to a nonsmooth setting. As discussed in [20], there are primarily two qualitatively different approaches for describing nonsmooth mechanics with variational principles. The first involves modifications to the path space [54] such that one takes variations over curves with isolated points of diminished smoothness or continuity. The second uses modifications to the variational principle itself [23] to include impulsive forces at certain configurations. We will be utilizing the former approach, mainly following the notation and methods of [32]. First, we handle the most basic of nonsmooth behaviors, the energy-conserving elastic collision.

2.2.1 Free Systems

To model an unconstrained mechanical system undergoing an elastic collision, we keep our definitions of Q, Q_e, L, $\bar{L}$, and $\bar{\mathfrak{G}}$ from Section 2.1. Furthermore, we define $C \subset Q$, a submanifold with boundary defining ***admissible configurations*** (configurations

that do not intersect any contact surface). The boundary of C, denoted ∂C, defines the set of ***contact configurations***.

Remark 2.4: *Note that this definition of the set contact configurations implies that it is of codimension 1 relative to the set admissible configurations. This is in agreement with a point contact assumption. Cases of higher codimension, such as the case when multiple contacts are made at once, are excluded.*

Nonautonomous trajectories of the above model belong to a ***nonsmooth path space*** defined by

$$\mathcal{M}_{ns} = \mathcal{T} \times \mathcal{Q}_{ns}([0,1], \tau_i, \partial C, Q),$$

where $\mathcal{T}$ remains as previously defined and

$$\begin{aligned}\mathcal{Q}_{ns}([0,1], \tau_i, \partial C, Q) = \{c_q : [0,1] \to Q \mid c_q \text{ is } C^0, \text{ piecewise } C^2, \\ \exists \text{ one singularity in } c_q(\tau) \text{ at } \tau_i, c_q(\tau_i) \in \partial C\}.\end{aligned}$$

While the proof is excluded here, [32] shows that $\mathcal{M}_{ns}$ is in fact a smooth manifold. This path space allows for variations of the collision time $c_t(\tau_i)$ while fixing the moment of impact in τ-space. This property will be extremely useful in the variational arguments to come, and indicates the utility of the nonautonomous approach in handling nonsmooth problems. The trajectory labeled "Elastic" in Figure 2.1 depicts an autonomous trajectory $q(t)$, derived from a path $(c_t, c_q) \in \mathcal{M}_{ns}$, that is subject to the elastic collision model derived below.

Remark 2.5: *While the path space definition does not explicitly exclude the possibility, we will assume that $\dot{q}$ is not tangential to the contact set ∂C at τ_i^- and τ_i^+. Essentially, the following results are not intended to describe "grazing" contacts made by rigid surfaces tangentially approaching each other.*

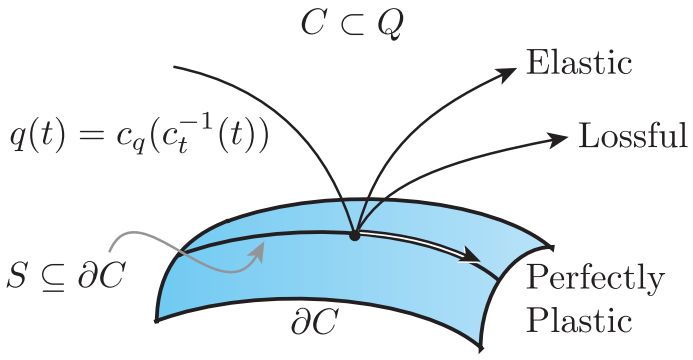

Figure 2.1: Trajectories $q(t)$ representing a variety of collision models for free mechanical systems.

With smoothness properties allowing for the implementation of variational calculus, we return to examining variations of the extended action map. Due to the singularity in c_q ($c_q'(\tau_i)$ does not exist), the action integral must be split at τ_i and integration by parts applied to each of the two resulting integrals. This results in the following for any $\delta c \in T_c\mathcal{M}_{ns}$,

$$\begin{aligned}\mathbf{d}\bar{\mathfrak{G}}(c)\cdot\delta c = &\int_0^{\tau_i} EL(c'')\cdot\delta c\, d\tau + \int_{\tau_i}^1 EL(c'')\cdot\delta c\, d\tau \\ &+ \Theta_L(c')\Big|_0^{\tau_i^-}\cdot\hat{\delta}c(\tau) + \Theta_L(c')\Big|_{\tau_i^+}^1\cdot\hat{\delta}c(\tau).\end{aligned}$$

In the application of Hamilton's principle to the varied action above, the integral terms imply the system obeys the extended Euler-Lagrange equations (2.1.2) and (2.1.3) for all $t \in (c_t(0), c_t(\tau_i)) \cup (c_t(\tau_i), c_t(1))$. That is, the behavior of the system away from the point of impact does not change from the smooth case. To determine the behavior at impact, notice variations δc still vanish at the boundaries 0 and 1 but not necessarily at τ_i. Hence the behavior of the Lagrangian one-form at τ_i has important consequences regarding the system's ***variational jump conditions*** at

impact. These conditions are

$$\left[\frac{\partial L}{\partial \dot{q}} dq - E\, dt\right]_{c_t(\tau_i^-)}^{c_t(\tau_i^+)} = 0, \tag{2.2.1}$$

on $TQ_e|(\mathbb{R}\times\partial C)$. To be exact, we say that an equality of forms holds "on" a particular tangent space if the equation holds upon contraction with any vector in that tangent space. This means the condition above could be written more formally as

$$\begin{aligned}
\frac{\partial L}{\partial \dot{q}}\Big|_{c_t(\tau_i^+)} \cdot v_q &= \frac{\partial L}{\partial \dot{q}}\Big|_{c_t(\tau_i^-)} \cdot v_q, \\
-E\Big|_{c_t(\tau_i^+)} \cdot v_t &= -E\Big|_{c_t(\tau_i^-)} \cdot v_t,
\end{aligned}$$

for all $v = (v_{t,} v_q) \in TQ_e|(\mathbb{R} \times \partial C)$. As we will continually express jump conditions using the equality of forms, it will be useful to retain this underlying meaning.

Noting the tangent space in which it applies, (2.2.1) indicates both conservation of energy and conservation of momentum tangent to ∂C across the moment of impact. These jump conditions provide no information regarding the momentum normal to ∂C, which we know is impulsively changing at impact in order for the system to remain in the set of admissible configurations C.

Remark 2.6: *The jump conditions defined in* (2.2.1) *admit the trivial solution*

$$\frac{\partial L}{\partial \dot{q}}\Big|_{c_t(\tau_i^+)} = \frac{\partial L}{\partial \dot{q}}\Big|_{c_t(\tau_i^-)},$$

but we readily disregard this as it yields inadmissible configurations $q(t) \notin C$ *for* $c_t(\tau) > c_t(\tau_i)$.

Geometrically speaking, we could express the momentum jump condition in (2.2.1) as

$$i^*\left(\frac{\partial L}{\partial \dot{q}}\Big|_{\tau_i^-}^{\tau_i^+}\right) = 0,$$

where $i^* : T^*Q \to T^*\partial C$ is the cotangent lift of the embedding $i : \partial C \to Q$. To formulate this condition in terms of the null space matrices of Subsection 2.1.2, let us assume (for notational purposes) that the manifold ∂C can be expressed as the level set $g_{\partial C}^{-1}(0)$ of some function $g_{\partial C} : Q \to \mathbb{R}$. Then, if we define an $n \times (n-1)$ null space matrix $P_{\partial C}(q) : \mathbb{R}^{n-1} \to T_q\partial C$ that satisfies (2.1.13) for $g = g_{\partial C}$ and $N = \partial C$, we can express the momentum jump condition as

$$P_{\partial C}^T(q) \left[\frac{\partial L}{\partial \dot{q}} \right]_{c_t(\tau_i^-)}^{c_t(\tau_i^+)} = 0. \tag{2.2.2}$$

Essentially with $P_{\partial C}(q)$ as defined above, its transpose provides a mapping $P_{\partial C}^T(q) : T_q^*Q \to T_q^*\partial C$. We will maintain this use of the null space notation in our jump conditions for the constrained cases ahead.

2.2.2 Holonomic Constraints

To model a holonomically constrained mechanical system undergoing an elastic collision we retain all of the notation and definitions from Subsections 2.1.2 and 2.2.1. We assume that $R = (N \cap C) \subset Q$ is a submanifold with boundary defining the set of ***constrained admissible configurations*** that lie in C and satisfy the holonomic constraint g. In the nonautonomous setting, we will make regular reference to $R_e = \mathbb{R} \times R$. Furthermore, we assume the set of ***constrained contact configurations*** ∂R, the boundary and a submanifold of R, is a submanifold of ∂C as well. These manifolds, as well as a constrained trajectory undergoing an elastic collision (labeled "Elastic"), are shown in Figure 2.2. Finally, we assume at all points of contact $q \in \partial R$ the manifolds R and ∂C are not tangential, i.e., the tangent spaces T_qR and $T_q\partial C$ are not equivalent nor is either a subset of the other. This assumption is similar to the condition assumed in Remark 2.5.

We will utilize the vakonomic method on a ***constrained coordinate nonsmooth***

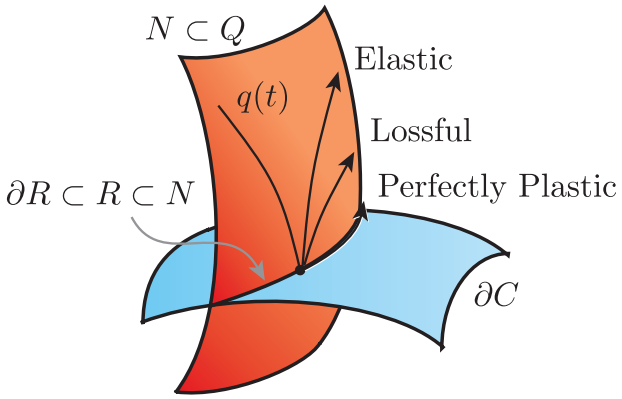

Figure 2.2: Trajectories $q(t)$ representing a variety of collision models for holonomically constrained mechanical systems. For simplicity, $U = \partial R$ has been used in the perfectly plastic case.

path space of the form

$$\mathcal{M}'_{ccns} = \mathcal{M}'_{ns} \times \mathcal{L},$$

where $\mathcal{L}$ is as previously defined and $\mathcal{M}'_{ns} = \mathcal{T} \times \mathcal{Q}_{ns}([0,1], \tau_i, \partial R, Q)$. Note that $\mathcal{Q}_{ns}([0,1], \tau_i, \partial R, Q)$ uses our previous definition of $\mathcal{Q}_{ns}([0,1], \tau_i, \partial C, Q)$, but replaces ∂C with ∂R. The path space $\mathcal{M}'_{ccns}$ restricts the point of contact to lie in ∂R unlike the more general $\mathcal{M}_{ccns} = \mathcal{M}_{ns} \times \mathcal{L}$, which would only restrict it to ∂C. The choice between these two definitions is a subtle issue, one we will revisit later. For now, we give the following theorem relating the nonsmooth dynamics of $\bar{L}^{R_e} = \bar{L}|_{TR_e}$ resulting from an action principle on $\mathcal{T} \times \mathcal{Q}_{ns}([0,1], \tau_i, \partial R, N)$ with the dynamics of the augmented Lagrangian $\tilde{L} : T(Q_e \times \mathbb{R}^m) \to \mathbb{R}$ on $\mathcal{M}'_{ccns}$.

Theorem 2.5: *Given an extended Lagrangian system $\bar{L} : TQ_e \to \mathbb{R}$ on an admissible set C, with a contact set ∂C, subject to an extended hidden constraint $\bar{f} : Q_e \to \mathbb{R}^m$ associated with an extended holonomic constraint $\bar{g} : Q_e \to \mathbb{R}^m$, denote $N_e = \bar{f}^{-1}(0) \subset Q_e$, $R_e = \mathbb{R} \times (N \cap C)$, and $L^{R_e} = L|_{TR_e}$. The following are equivalent:*

1. $c \in \mathcal{T} \times \mathcal{Q}_{ns}([0,1], \tau_i, \partial R, N)$ extremizes $\bar{\mathfrak{G}}^{R_e}$ and thus is a solution of the extended Euler-Lagrange equations and variational jump conditions associated with $\bar{L}^{R_e}$;

2. $(c, c_\lambda) \in \mathcal{M}'_{ccns}$ produces $q(t) = c_q(c_t^{-1}(t))$ and $\lambda(t) = c_\lambda(c_t^{-1}(t))$ satisfying the vakonomic extended constrained Euler-Lagrange equations for all $t \in (c_t(0), c_t(\tau_i^-)) \cap (c_t(\tau_i^+), c_t(1))$, as well as the variational jump conditions

$$\left[\frac{\partial L}{\partial \dot{q}} dq - E\, dt\right]_{c_t(\tau_i^-)}^{c_t(\tau_i^+)} = 0, \tag{2.2.3}$$

   on $TQ_e|(\mathbb{R} \times \partial R)$.

3. $(c, c_\lambda) \in \mathcal{M}'_{ccns}$ extremizes $\tilde{\mathfrak{G}}(c, c_\lambda) = \bar{\mathfrak{G}}(c) - \langle c_\lambda, \Phi(c) \rangle$ and hence solves the Euler-Lagrange equations for the augmented Lagrangian $\tilde{L}^{\bar{f}} : T(Q_e \times \mathbb{R}^m) \to \mathbb{R}$ defined by

$$\tilde{L}^{\bar{f}}(c, c_\lambda, c', c'_\lambda) = \bar{L}(c, c') - \langle c_\lambda, \bar{f}(c, c') \rangle.$$

PROOF: In the context of Theorem 2.2, our full space M is $\mathcal{M}'_{ns}$. Keep in mind the distinction between this space and $\mathcal{M}_{ns}$; paths in this full space cannot stray from ∂R at the point of contact. The function to be extremized is $\bar{\mathfrak{G}}$ as defined in Subsection 2.1.1, and again $V = \mathcal{L}$ with the L_2 inner product. Set $\Phi : M \to V$ as $\Phi(c)(\tau) = \bar{f}(c(\tau))$ such that for paths c in the full space, we have $c \in \mathcal{T} \times \mathcal{Q}_{ns}([0,1], \tau_i, \partial R, N)$ if and only if $\Phi(c) = 0$. Hence, we have $\mathcal{D} = \Phi^{-1}(0) = \mathcal{T} \times \mathcal{Q}_{ns}([0,1], \tau_i, \partial R, N)$.

The first condition and third conditions are equivalent by Theorem 2.2. That is, $c \in \mathcal{D}$ extremizing $\bar{\mathfrak{G}}|_{\mathcal{D}}$ is equivalent to $(c, c_\lambda) \in M \times V$ extremizing $\tilde{\mathfrak{G}}(c, c_\lambda) = \bar{\mathfrak{G}}(c) - \langle c_\lambda, \Phi(c) \rangle$. Identifying $M \times V$ with $\mathcal{M}'_{ccns}$, the structure of $\tilde{\mathfrak{G}} : \mathcal{M}'_{ccns} \to \mathbb{R}$ yields an augmented Lagrangian of the same form in Theorem 2.4. In order to show the second and third conditions are equivalent, we evaluate $d\tilde{\mathfrak{G}} = 0$ using the same procedure as in Subsection 2.2.1. Recalling (2.1.11) and (2.1.12), we split the action

integral such that variations of $\tilde{\mathfrak{G}}(c, c_\lambda)$ have the form

$$\mathbf{d}\tilde{\mathfrak{G}}(c, c_\lambda) \cdot \delta c = \int_0^{\tau_i} \widetilde{EL}(c'', c_\lambda'') \cdot \delta(c, c_\lambda)\, d\tau + \int_{\tau_i}^1 \widetilde{EL}(c'', c_\lambda'') \cdot \delta(c, c_\lambda)\, d\tau$$
$$+ \Theta_{\tilde{L}^{\bar{f}}}(c', c_\lambda')\Big|_0^{\tau_i^-} \cdot \hat{\delta}(c(\tau), c_\lambda(\tau)) + \Theta_{\tilde{L}^{\bar{f}}}(c', c_\lambda')\Big|_{\tau_i^+}^1 \cdot \hat{\delta}(c(\tau), c_\lambda(\tau)).$$

The integral terms imply that the system obeys the vakonomic extended constrained Euler-Lagrange equations in the smooth regime $t \in (c_t(0), c_t(\tau_i)) \cup (c_t(\tau_i), c_t(1))$. Furthermore, the Lagrangian one-form terms at τ_i imply the jump conditions (expressed in the time domain)

$$\left[\left(\frac{\partial L}{\partial \dot{q}} - \left(\frac{\partial f}{\partial \dot{q}}\right)^T \cdot \lambda\right) dq\right]_{c_t(\tau_i^-)}^{c_t(\tau_i^+)} = 0,$$

on $TQ|\partial R$, and

$$\left[\left(\frac{\partial L}{\partial \dot{q}}\dot{q} - \left(\frac{\partial f}{\partial \dot{q}}\dot{q}\right) \cdot \lambda - L + f \cdot \lambda\right) dt\right]_{c_t(\tau_i^-)}^{c_t(\tau_i^+)} = 0,$$

on $T\mathbb{R}$. Noting that the columns of $\left(\frac{\partial f}{\partial \dot{q}}\right)^T$ are normal to $T\partial R$, the constraint term in the momentum balance is negligible. Using the linearity of f with respect to $\dot{q}$, the energy balance reduces to the conservation of E. Hence, the above conditions are equivalent to those presented in (2.2.3). ■

Remark 2.7: *In the smooth case, the constraint condition* $\Phi(c) = 0$ *simply meant* $\bar{f}(c(\tau)) = 0$ *for all* $\tau \in [0, 1]$. *In the nonsmooth case above, this is not precisely true as the singularity at* τ_i *means* $\bar{f}(c(\tau))$ *does not exist there. In this case, we take* $\Phi(c) = 0$ *to mean* $\bar{f}(c(\tau^+)) = 0$ *and* $\bar{f}(c(\tau^-)) = 0$ *for all* $\tau \in [0, 1]$. *With this definition, it is in fact true* $\Phi^{-1}(0) = \mathcal{T} \times \mathcal{Q}_{ns}([0, 1], \tau_i, \partial R, N)$.

The jump condition (2.2.3) indicates conservation of momentum tangent to ∂R,

which not only admits impulsive changes in momentum normal to ∂C as before, but normal to R as well. That is, at impact, the system may be subject to both impulsive contact forces and impulsive constraint forces. These forces must yield $\bar{f}(c(\tau_i^+)) = 0$, which one might view as being implicitly appended to the jump conditions since $f = 0$ must hold on $t \in (c_t(\tau_i^+), c_t(1))$. Without this condition, we have $(q(c_t(\tau_i^+)), \dot{q}(c_t(\tau_i^+))) \notin TR$ and the system has not been initialized in a way that the DAEs (2.1.8) and (2.1.10) can be solved for $t \in (c_t(\tau_i^+), c_t(1))$. Though it was not mentioned, a similar condition $\bar{f}(c(0)) = 0$ was implicit during our usage of the vakonomic method in the smooth case.

Remark 2.8: *It may be possible to develop results similar to Theorem 2.5 using a variational principle on $\mathcal{M}_{ccns}$, with $\mathcal{M}_{ns}$ as the full space M. We have avoided this choice due to its consequences regarding the structure of the Lagrange multipliers c_λ.*

Using $\mathcal{M}_{ns}$ would result in the jump conditions containing a momentum balance on $T\partial C$ rather than on $T\partial R$. In the general case, impacts include impulsive constraint forces normal to R and thus jump conditions on $T\partial C$ may require impulsive c_λ at τ_i. Though the issue has been explored [74], impulsive generalized functions or, more properly, distributions do not in general admit an inner product. Without belonging to an inner product space, c_λ would no longer meet the necessary conditions of Theorem 2.2.

As a final note, the Lagrange multipliers c_λ in our analysis are discontinuous but not impulsive at τ_i and thus still satisfy $c_\lambda \in \mathcal{L}$.

To formulate the jump condition (2.2.3) in terms of a null space matrix, let us assume that the manifold ∂R can be expressed as the level set $g_{\partial R}^{-1}(0)$ of some function $g_{\partial R} : Q \to \mathbb{R}^{m+1}$. For instance, one could define $g_{\partial R} = (g, g_{\partial C})$ using g and $g_{\partial C}$ from Subsections 2.1.2 and 2.2.1, respectively. Then, given an $n \times (n - m - 1)$ null space matrix $P_{\partial R}(q) : \mathbb{R}^{n-m-1} \to T_q \partial R$ that satisfies (2.1.13) with regards to $g_{\partial R}$ and ∂R

(rather than g and N), we can express the momentum jump condition as

$$P_{\partial R}^{T}(q)\left[\frac{\partial L}{\partial \dot{q}}\right]_{c_t(\tau_i^-)}^{c_t(\tau_i^+)} = 0. \tag{2.2.4}$$

This in combination with $E|_{c_t(\tau_i^-)}^{c_t(\tau_i^+)} = 0$ is equivalent to (2.2.3).

2.3 Forced and Lossful Collisions

This section extends the previous variational methods to include work done at impact. Though the framework we consider could be used to model any type of instantaneous forces at the instant τ_i, we are primarily interested in capturing energy losses due to friction and other sources of dissipation.

2.3.1 Free Systems

Following the structure of Subsection 2.1.3, we define a ***contact force field*** $F^{\partial C} : TQ_e|(\mathbb{R} \times \partial C) \to T^*(\mathbb{R} \times \partial C)$ to model nonconservative impulsive forcing during collisions. As with the exterior force F, the force field $F^{\partial C} = (F_t^{\partial C}, F_q^{\partial C})$ has a time component on the $T^*\mathbb{R}$ portion of the cotangent bundle of TQ_e. Unlike the case of F though, we will show the component $F_t^{\partial C}$ is freely defined and need not satisfy any necessary relation with $F_q^{\partial C}$.

For a system subject to the contact force field at the point of impact, the Lagrange-d'Alembert principle for a path $c \in \mathcal{M}_{ns}$ has the form

$$d\bar{\mathfrak{G}}(c) \cdot \delta c + F^{\partial C}(c(\tau_i), c'(\tau_i)) \cdot \delta c(\tau_i) = 0.$$

Splitting the interval of integration and performing integration by parts yields

$$0 = \int_0^{\tau_i} EL(c'') \cdot \delta c \, d\tau + \int_{\tau_i}^1 EL(c'') \cdot \delta c \, d\tau$$
$$+ \Theta_L(c')\Big|_0^{\tau_i^-} \cdot \hat{\delta} c(\tau) + \Theta_L(c')\Big|_{\tau_i^+}^1 \cdot \hat{\delta} c(\tau) + F^{\partial C}(c(\tau_i), c'(\tau_i)) \cdot \delta c(\tau_i).$$

Clearly $F^{\partial C}$ does not interfere with the integral terms and thus the system still obeys the extended Euler-Lagrange equations in the smooth regime $t \in (c_t(0), c_t(\tau_i)) \cup (c_t(\tau_i), c_t(1))$. Collecting the remaining terms, we see the influence of $F^{\partial C}$ on the jump conditions as

$$\left[\frac{\partial L}{\partial \dot{q}} dq - E \, dt\right]_{c_t(\tau_i^-)}^{c_t(\tau_i^+)} = F_q^{\partial C} dq + F_t^{\partial C} dt, \tag{2.3.1}$$

on $TQ_e|(\mathbb{R} \times \partial C)$. Examining the condition above, we see that the contact force field can impose a discrete jump in the system's momentum tangential to ∂C via the configuration component $F_q^{\partial C}$, and also can impose a discrete jump in the system's energy via the time component $F_t^{\partial C}$. The jump conditions do not contain an equation explicitly indicating the change in momentum normal to ∂C across the impact time. However, the magnitude of such a change could be determined upon solving the above two equations. To see that the structure of $F^{\partial C}$ does permit work done by forces normal to ∂C, just consider the case $F_q^{\partial C} = 0$ and $F_t^{\partial C} \neq 0$. The trajectory labeled "Lossful" in Figure 2.1 depicts an autonomous trajectory $q(t)$ representing this collision model.

The momentum balance in the nonconservative jump condition (2.3.1) can be expressed using a null space matrix in the same manner as in (2.2.2) and (2.2.4). It appears as

$$P_{\partial C}^T(q) \left[\frac{\partial L}{\partial \dot{q}}\Big|_{c_t(\tau_i^-)}^{c_t(\tau_i^+)} - F_q^{\partial C}\right] = 0. \tag{2.3.2}$$

This in combination with $E|_{c_t(\tau_i^-)}^{c_t(\tau_i^+)} = F_t^{\partial C}$ is equivalent to (2.3.1).

2.3.2 Holonomic Constraints

Incorporating a contact force field into the constrained jump conditions (2.2.3) can be done in the same manner as described in Subsection 2.2.1. One could redefine the contact force field as $F^{\partial R} : TQ_e|(\mathbb{R} \times \partial R) \to T^*(\mathbb{R} \times \partial R)$ or leave it as $F^{\partial C}$ with the knowledge that any components of $F_q^{\partial C}$ normal to R will have no bearing on results. We present the following results in terms of $F^{\partial R}$, but are mindful of invariance under the substitution $F^{\partial R} \to F^{\partial C}$. The jump conditions for this case have a structure identical to (2.3.1),

$$\left[\frac{\partial L}{\partial \dot{q}} dq - E\, dt\right]_{c_t(\tau_i^-)}^{c_t(\tau_i^+)} = F_q^{\partial R} dq + F_t^{\partial R} dt, \tag{2.3.3}$$

here restricted to the space $TQ_e|(\mathbb{R} \times \partial R)$. A constrained trajectory representing this collision model, labeled "Lossful", is shown in Figure 2.2.

In terms of a null space matrix, the momentum jump condition above appears, similar to (2.3.2), as

$$P_{\partial R}^T(q) \left[\frac{\partial L}{\partial \dot{q}}\Big|_{c_t(\tau_i^-)}^{c_t(\tau_i^+)} - F_q^{\partial R}\right] = 0.$$

This in combination with $E|_{c_t(\tau_i^-)}^{c_t(\tau_i^+)} = F_t^{\partial R}$ is equivalent to (2.3.3).

2.4 Perfectly Plastic Impacts

The previous theory regarding lossful impacts naturally leads one to consider perfectly plastic impacts. That is, what happens in the case in which an impact removes enough energy from the system that it remains on the contact manifold? Such collisions are called perfectly plastic [43] or perfectly inelastic [81]. The work in [22] describes the underlying structure of these impacts by contrasting the elastic and perfectly plastic cases in a geometric framework. This is done by characterizing collisions in terms of distributions on TQ to which the system must belong before and after impact.

In Subsections 2.2.1 and 2.3.1 regarding free systems, the ***pre-impact distribution***, $\mathfrak{D}^-$, as well as the ***post-impact distribution***, $\mathfrak{D}^+$, was TC. Similarly, in Subsections 2.2.2 and 2.3.2 regarding constrained systems $\mathfrak{D}^-$ and $\mathfrak{D}^+$ were TR. This section discusses cases in which the system is subject to an additional holonomic constraint after impact. In these cases, $\mathfrak{D}^-$ and $\mathfrak{D}^+$ will be distinct.

2.4.1 Free Systems

Consider $S \subseteq \partial C$ is a constraint submanifold of C such that $\mathfrak{D}^+$ is TS. In terms of physical behaviors, the structure of S here is general enough to capture both sticking and sliding contacts on ∂C. As with previous constraint submanifolds, we assume that S can be expressed as the level set $g_S^{-1}(0)$ of some function $g_S : Q \to \mathbb{R}^p$, $p < n$. As in the elastic case for free systems, $\mathfrak{D}^-$ is TC, and thus the pre-impact equations of motion are still the extended Euler-Lagrange equations for all $t \in (c_t(0), c_t(\tau_i^-))$. The jump conditions are identical to the lossful case for free systems, (2.3.1), with the added condition that the post-impact phase lies in the appropriate distribution. That is,

$$\left[\frac{\partial L}{\partial \dot{q}} dq - E\, dt\right]_{c_t(\tau_i^-)}^{c_t(\tau_i^+)} = F_q^{\partial C} dq + F_t^{\partial C} dt,$$

on $TQ_e|(\mathbb{R} \times \partial C)$, and

$$(q(c_t(\tau_i^+)), \dot{q}(c_t(\tau_i^+))) \in TS.$$

This condition on the post-impact momentum can be considered a constraint on the contact force field $F^{\partial C}$. From this viewpoint, force fields that do not satisfy this condition do not model perfectly plastic impacts. Given a force field that does meet the constraints above, following the impact, the system will obey the extended constrained Euler-Lagrange equations (with g_S as the constraint) for all $t \in (c_t(\tau_i^+), c_t(1))$. The trajectory labeled "Perfectly Plastic" in Figure 2.1 depicts an autonomous trajectory $q(t)$ subject to this perfectly plastic collision model.

Remark 2.9: *One should note that the dynamics described above were not derived from a single variational principle. Rather, the results of two variational principles, one for unconstrained lossful collisions and one for smooth constrained systems, were joined at the instant following impact. While obtaining perfectly plastic impact dynamics from a single variational principle remains a subject of interest, it seems unlikely that this is possible. The main difficulty is the lack of smoothness in a path space that describes trajectories subject to constraint distributions of varying dimension.*

While the general formulation above classifies the set of contact force fields that yield perfectly plastic impacts, let us now examine one specific case satisfying the jump conditions. We will place the rigid body impact model used in [38] and [41] in the context of our general framework. Physically, the model used in these works assumes impacting rigid bodies stick at the point of contact due to normal and tangential impact forces (no torques). Under this assumption, angular momentum is conserved about the point of impact, and this conservation can be used to relate pre- and post-impact momenta [39].

For the sake of describing this impact model, momentarily disregard the variational jump conditions (2.3.1) that we have derived and consider the more widely used (but not variational) jump condition

$$\left[\frac{\partial L}{\partial \dot{q}} dq\right]_{c_t(\tau_i^-)}^{c_t(\tau_i^+)} = F^C dq, \tag{2.4.1}$$

on TC, where $F^C : TC \to T^*C$ has been substituted for our usual notion of a contact force field. We will shortly relate this condition to the variational case (2.3.1). In our framework, we use the constraint manifold $S = g_S^{-1}(0)$ to define configurations that satisfy the condition of sticking at the point of contact. Under that definition, the condition of restricting generalized impact forces to components normal and tangential

to the contact surface is equivalent to setting

$$F^C = \left(\frac{\partial g_S}{\partial q}\right)^T \cdot \lambda^C,$$

where $\lambda^C \in \mathbb{R}^p$. Essentially, the impact forces act only in directions normal to the sticking constraint and thus $\left(\frac{\partial g_S}{\partial q}\right)^T$ acts as a basis for F^C. Inserting this force field into (2.4.1) and phrasing the condition $\dot{q}(c_t(\tau_i^+)) \in \mathfrak{D}^+ = TS$ in terms of g_S gives the algebraic system,

$$\begin{aligned} \frac{\partial L}{\partial \dot{q}}\Big|_{c_t(\tau_i^+)} &= \frac{\partial L}{\partial \dot{q}}\Big|_{c_t(\tau_i^-)} + \left(\frac{\partial g_S}{\partial q}\right)^T \cdot \lambda^C, \\ \left(\frac{\partial g_S}{\partial q}\right) \cdot \dot{q}(c_t(\tau_i^+)) &= 0. \end{aligned}$$

Given $q(c_t(\tau_i))$ and $\dot{q}(c_t(\tau_i^-))$, this system is to be solved for $\dot{q}(c_t(\tau_i^+))$ and λ^C. The solution to this system can be represented as a projection. Consider a mapping $Q_S(q) : T_q^*Q \to \eta_S(T_q^*S)$, where $\eta_S : T^*S \to T^*Q$ is a symplectic embedding of T^*S in T^*Q (precise conditions on η_S are given in [68]). We nearly have a null space matrix in $Q_S^T(q) : \mathbb{R}^n \to T_qS$, except that it is $n \times n$ rather than $n \times (n-p)$. Even with its higher dimension, it satisfies the null space matrix property

$$\text{range}(Q_S^T(q)) = \text{null}\left(\frac{\partial g}{\partial q}(q)\right) = T_qS. \tag{2.4.2}$$

In terms of $Q_S(q)$, the algebraic system above reduces to

$$\frac{\partial L}{\partial \dot{q}}\Big|_{c_t(\tau_i^+)} = Q_S \cdot \frac{\partial L}{\partial \dot{q}}\Big|_{c_t(\tau_i^-)}, \tag{2.4.3}$$

yielding the post-impact momentum as a projection of the pre-impact momentum.

Remark 2.10: *In [61], for a Lagrangian of the form $L(q, \dot{q}) = \dot{q}^T M(q)\dot{q} - V(q)$, Q_S*

is calculated explicitly as

$$Q_S = \left(\mathbb{I}_{n\times n} - \left(\frac{\partial g_S}{\partial q}\right)^T \left(\left(\frac{\partial g_S}{\partial q}\right) M^{-1} \left(\frac{\partial g_S}{\partial q}\right)^T \right)^{-1} \left(\frac{\partial g_S}{\partial q}\right) M^{-1} \right).$$

We have derived the conditions for a special case of perfectly plastic impacts using the jump conditions (2.4.1), which presumably are not variational. However, it is easily seen that there exists $F^{\partial C}$ such that the variational jump conditions (2.3.1) are satisfied by the projection (2.4.3). To witness this, just note that if there exists a solution to (2.4.1), then all quantities—momentum and energy both pre and post impact—are known such that the jump conditions (2.3.1) actually define $F^{\partial C}$. In this way, anytime we refer to a force field F^C, it naturally defines an associated contact force field $F^{\partial C}$.

2.4.2 Holonomic Constraints

Similar to S in Subsection 2.4.1, consider $U \subseteq \partial R$ that is a constraint submanifold of R such that $\mathfrak{D}^+$ is TU. As with previous constraint submanifolds, we assume that U can be expressed as the level set $g_U^{-1}(0)$ of some function $g_U : Q \to \mathbb{R}^p$, $p < n$.

Remark 2.11: *For the definition of U to make sense, we assume $p > m$ as well. In general, such as when we deal with the submanifold S, we do not use this assumption.*

As in the elastic case for constrained systems, $\mathfrak{D}^-$ is TR, and thus the pre-impact equations of motion are still the constrained extended Euler-Lagrange equations on $R \subseteq N$ for all $t \in (c_t(0), c_t(\tau_i^-))$. The jump conditions are identical to the lossful case for constrained systems, (2.3.3), with the added condition that the post impact phase lies in the appropriate distribution. That is,

$$\left[\frac{\partial L}{\partial \dot{q}} dq - E\, dt\right]_{c_t(\tau_i^-)}^{c_t(\tau_i^+)} = F_q^{\partial R} dq + F_t^{\partial R} dt,$$

on $TQ_e|(\mathbb{R} \times \partial R)$, and

$$(q(c_t(\tau_i^+)), \dot{q}(c_t(\tau_i^+))) \in TU.$$

The constrained trajectory labeled "Perfectly Plastic" in Figure 2.2 represents this collision model.

Given a mapping $Q_U(q) : T_q^*Q \to \eta_U(T_q^*U)$ that satisfies the same conditions of Q_S in Subsection 2.4.1, we can use a projection to provide a specific impact model that satisfies the conditions above. Like (2.4.3), this model reduces the jump conditions to

$$\frac{\partial L}{\partial \dot{q}}\Big|_{c_t(\tau_i^+)} = Q_U \cdot \frac{\partial L}{\partial \dot{q}}\Big|_{c_t(\tau_i^-)}. \tag{2.4.4}$$

Upon implementing this model, or any other provides $(q(c_t(\tau_i^+)), \dot{q}(c_t(\tau_i^+))) \in \mathfrak{D}^+ = TU$, the system obeys the extended constrained Euler-Lagrange equations (with g_U as the constraint) for all $t \in (c_t(\tau_i^+), c_t(1))$.

2.5 Transition of Constraints

In this final section of the chapter, we discuss the case in which a pre-impact constraint is released following impact. The practice of joining the results of two variational principles at the point of impact is again employed. The results provide equations of motion that can capture, as a point of interest, the dynamics of a bipedal robot simultaneously establishing a new stance leg and lifting the prior step's stance leg as a step is completed.

In this case, we will use S as defined in Subsection 2.4.1 such that $\mathfrak{D}^+$ is TS. We permit $\mathfrak{D}^+ \nsubseteq TR$ since the constraint g associated with R will not be enforced following impact. As in the elastic and perfectly plastic cases for constrained systems, $\mathfrak{D}^-$ is TR and thus the pre-impact equations of motion are still the constrained extended Euler-Lagrange equations on $R \subseteq N$ for all $t \in (c_t(0), c_t(\tau_i^-))$.

Remark 2.12: *In light of the physical behavior this subsection will model (a robot exchanging stance legs) it may seem that the pre-impact constraint submanifold R should belong in the contact set ∂C. After all, the robot has a stance leg in contact prior to impact in this situation. In our approach, we define the contact set in terms of the swing leg that is going to strike and not the currently established stance contact. A "unified" contact set that takes into account contact of both the standing and swinging legs lacks smoothness, particularly at the point of impact (or double-support phase [30]), and cannot be a submanifold as we require of ∂C.*

The jump conditions are identical to the perfectly plastic case for constrained systems, though the appropriate post-impact distribution takes a new value TS. That is,

$$\left[\frac{\partial L}{\partial \dot{q}} dq - E\, dt\right]_{c_t(\tau_i^-)}^{c_t(\tau_i^+)} = F_q^{\partial R} dq + F_t^{\partial R} dt,$$

on $TQ_e|(\mathbb{R} \times \partial R)$, and

$$(q(c_t(\tau_i^+)), \dot{q}(c_t(\tau_i^+))) \in TS.$$

Remark 2.13: *This condition for initializing the system on TS post-impact is largely nonrestrictive. As the variational jump conditions only require conservation of momentum tangent to ∂R, the momenta in any directions normal to ∂R but tangent to S have no bearing on satisfying the conditions above and may be defined post-impact arbitrarily. While the impact model* (2.4.3) *that we focus on initializes the momentum in these directions post-impact at zero, it should be noted the conditions above provide the freedom to do otherwise.*

Recalling the mapping $Q_S(q) : T_q^*Q \to \eta_S(T_q^*S)$ from Subsection 2.4.1, the projection (2.4.3) provides a specific impact model that satisfies the conditions above. Upon implementing this model, or any other that meets the condition $(q(c_t(\tau_i^+)), \dot{q}(c_t(\tau_i^+))) \in \mathfrak{D}^+ = TS$, the system obeys the extended constrained Euler-Lagrange equations (with

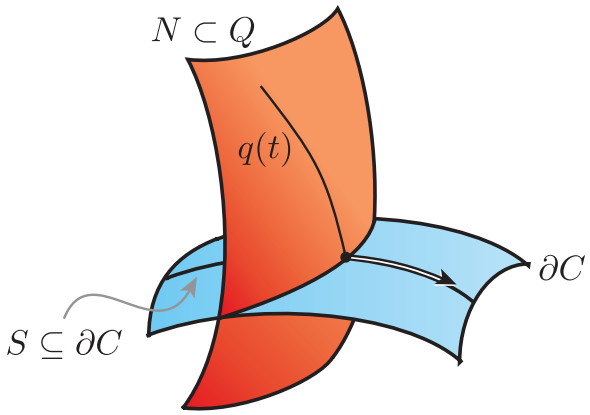

Figure 2.3: A trajectory evolving through a transition of constraints.

g_S as the constraint) for all $t \in (c_t(\tau_i^+), c_t(1))$. A trajectory undergoing a transition of constraints is shown in Figure 2.3.

Chapter 3

Discrete Mechanics and Variational Collision Integrators

In this chapter, we recast all of Chapter 2's results regarding nonsmooth mechanics in a discrete time setting. We will replace the continuous time field with a mesh of discrete time nodes. On this mesh, we develop algebraic equations of motion according to the theory of discrete mechanics [68] yielding structured integration algorithms [42]. Integrators in this class are respected for their ability to preserve the geometric structure of mechanical systems in discrete time.

3.1 Smooth Systems

Prior to deriving integrators for impact mechanics, we examine the free and holonomically constrained systems of Section 2.1 in a discrete time setting. We make reference to the adaptive timestep integrators of [49], which provide a discrete time analogy for the extended configuration space framework.

3.1.1 Free Systems

As in Subsection 2.1.1, we begin with a mechanical system on an n-dimensional configuration manifold Q, this manifold's associated tangent bundle TQ, and a Lagrangian $L : TQ \to \mathbb{R}$. We consider a time-like mesh of $(K+1) \in \mathbb{R}^+$ nodes. On this mesh,

we have the ***discrete path space***

$$\mathcal{M}_d = \mathcal{T}_d \times \mathcal{Q}_d(Q),$$

where

$$\mathcal{T}_d = \big\{t_d : \{0, 1, \ldots, (K-1), K\} \to \mathbb{R} \mid t_d(k+1) > t_d(k)\ \forall k\big\},$$
$$\mathcal{Q}_d(Q) = \big\{q_d : \{0, 1, \ldots, (K-1), K\} \to Q\big\}.$$

The elements $\bar{q}_d \triangleq (t_d, q_d) \in \mathcal{M}_d$ provide mappings t_d and q_d that respectively prescribe a time and a configuration to each of the $(K+1)$ time-like nodes. For the k^{th} node, we will use the notation $t_d(k) = t_k$ and $q_d(k) = q_k$. It should come as no surprise that the integrators we will develop are meant to produce $q_k \approx q(t_k)$.

At the heart of the discrete mechanics approach is the replacement of the tangent bundle TQ with $Q \times Q$. In accordance with this substitution, we define the ***discrete Lagrangian*** $L_d : Q \times Q \to \mathbb{R}$ that approximates the (autonomous) action integral $\mathfrak{G}$ on a finite interval of time $[t_k, t_{k+1}]$ as

$$L_d(q_k, q_{k+1}) \approx \int_{t_k}^{t_{k+1}} L\left(q, \dot{q}\right) dt.$$

Typically, this approximation is made with simple quadrature rules. For instance, the midpoint rule produces

$$L_d(q_k, q_{k+1}) = (t_{k+1} - t_k) L\left(\frac{q_k + q_{k+1}}{2}, \frac{q_{k+1} - q_k}{t_{k+1} - t_k}\right). \tag{3.1.1}$$

In analogy with the nonautonomous approach from the continuous setting, we can define this approximation of the action as a function of the time values as well. This

gives an ***extended discrete Lagrangian*** $\bar{L}_d : Q_e \times Q_e \to \mathbb{R}$ of the form

$$\bar{L}_d(t_k, q_k, t_{k+1}, q_{k+1}) \approx \int_{t_k}^{t_{k+1}} L\,(q, \dot{q})\,dt,$$

where $\bar{L}_d(t_k, q_k, t_{k+1}, q_{k+1}) = L_d(q_k, q_{k+1})$. In terms of the continuous extended Lagrangian, it makes sense to refer to the above approximation as

$$\bar{L}_d(t_k, q_k, t_{k+1}, q_{k+1}) \approx \int_{\tau_k}^{\tau_{k+1}} \bar{L}\,(c, c')\,d\tau,$$

where we have used the notation $\tau_k = c_t^{-1}(t_k)$.

Remark 3.1: *Moving forward, we make extensive use of the abbreviation* $\bar{q}_k \triangleq (t_k, q_k)$ *such that the extended discrete Lagrangian appears as* $\bar{L}_d(\bar{q}_k, \bar{q}_{k+1})$. *This notation is particularly important to keep in mind when viewing abbreviated expressions involving slot derivatives, which appear as*

$$D_i\bar{L}_d(\bar{q}_k, \bar{q}_{k+1}) \triangleq D_i\bar{L}_d(t_k, q_k, t_{k+1}, q_{k+1}).$$

This abbreviation can be counterintuitive, as at times we appear to be taking derivatives with respect to the third and fourth slot of a function with two arguments. Any confusion can be remedied by a substitution of the long form of the extended discrete Lagrangian's arguments, $(t_k, q_k, t_{k+1}, q_{k+1})$.

Summing discrete Lagrangian terms over the entire time-like mesh defines an ***extended discrete action map*** $\bar{\mathfrak{G}}_d : \mathcal{M}_d \to \mathbb{R}$ as

$$\bar{\mathfrak{G}}_d(\bar{q}_d) = \sum_{k=0}^{K-1} \bar{L}_d(\bar{q}_k, \bar{q}_{k+1}).$$

Assuming $\tau_0 = 0$ and $\tau_K = 1$, this discrete action sum provides an approximation to the continuous extended action $\bar{\mathfrak{G}}$. Finally, we define the ***discrete second-order***

submanifold of Q_e as

$$(\ddot{Q}_e)_d = Q_e \times Q_e \times Q_e,$$

which is locally isomorphic to $\ddot{Q}_e$. We now have all of the elements necessary to describe variations of the discrete action with respect to the discrete path.

Theorem 3.1: *Given a C^k discrete Lagrangian, $k \geq 1$, there exists a unique C^{k-2} mapping $EL_d : (\ddot{Q}_e)_d \to T^*Q_e$ and unique C^{k-1} one-forms $\Theta^+_{\bar{L}_d}$ and $\Theta^-_{\bar{L}_d}$ on the discrete phase space $Q_e \times Q_e$, such that for all variations $\delta\bar{q}_d = (\delta t_d, \delta q_d) \in T_{\bar{q}_d}\mathcal{M}_d$ of $\bar{q}_d$ we have*

$$\begin{aligned} d\bar{\mathfrak{G}}_d(\bar{q}_d) \cdot \delta\bar{q}_d = &\sum_{k=1}^{K-1} EL_d(\bar{q}_{k-1}, \bar{q}_k, \bar{q}_{k+1}) \cdot \delta\bar{q}_k \\ &+ \Theta^+_{\bar{L}_d}(\bar{q}_{K-1}, \bar{q}_K) \cdot (\delta\bar{q}_{K-1}, \delta\bar{q}_K) - \Theta^-_{\bar{L}_d}(\bar{q}_0, \bar{q}_1) \cdot (\delta\bar{q}_0, \delta\bar{q}_1), \end{aligned} \tag{3.1.2}$$

where

$$\begin{aligned} EL_d(\bar{q}_{k-1}, \bar{q}_k, \bar{q}_{k+1}) &= [D_3\bar{L}_d(\bar{q}_{k-1}, \bar{q}_k) + D_1\bar{L}_d(\bar{q}_k, \bar{q}_{k+1})]dt_k \\ &\quad + [D_4\bar{L}_d(\bar{q}_{k-1}, \bar{q}_k) + D_2\bar{L}_d(\bar{q}_k, \bar{q}_{k+1})]dq_k, \\ \Theta^+_{\bar{L}_d}(\bar{q}_k, \bar{q}_{k+1}) &= D_3\bar{L}_d(\bar{q}_k, \bar{q}_{k+1})dt_{k+1} + D_4\bar{L}_d(\bar{q}_k, \bar{q}_{k+1})dq_{k+1}, \\ \Theta^-_{\bar{L}_d}(\bar{q}_k, \bar{q}_{k+1}) &= -D_1\bar{L}_d(\bar{q}_k, \bar{q}_{k+1})dt_k - D_2\bar{L}_d(\bar{q}_k, \bar{q}_{k+1})dq_k, \end{aligned}$$

and D denotes the slot derivative. As in [32], we term EL_d the **discrete Euler-Lagrange derivative** *and $\Theta^+_{\bar{L}_d}$ and $\Theta^-_{\bar{L}_d}$ the* **discrete Lagrangian one-forms**. *The latter of these expressions is consistent with the terminology in [68].*

PROOF: Considering $\delta\bar{q}_d \in T_{\bar{q}_d}\mathcal{M}$ with components δt_d and δq_d, we take variations of

the action as

$$d\bar{\mathfrak{G}}_d(\bar{q}_d)\cdot\delta\bar{q}_d = \sum_{k=0}^{K-1}[D_1\bar{L}_d(\bar{q}_k,\bar{q}_{k+1})\cdot\delta t_k + D_2\bar{L}_d(\bar{q}_k,\bar{q}_{k+1})\cdot\delta q_k$$
$$+ D_3\bar{L}_d(\bar{q}_k,\bar{q}_{k+1})\cdot\delta t_{k+1} + D_4\bar{L}_d(\bar{q}_k,\bar{q}_{k+1})\cdot\delta q_{k+1}].$$

Rearranging the terms appropriately (often viewed as the discrete version of integration by parts), the terms EL_d, $\Theta^+_{\bar{L}_d}$, and $\Theta^-_{\bar{L}_d}$ emerge as defined above. ∎

The discrete version of Hamilton's principle provides that discrete trajectories of the mechanical system will correspond with stationary points of the discrete action. That is, a solution $\bar{q}_d \in \mathcal{M}_d$ will yield $d\bar{\mathfrak{G}}_d(\bar{q}_d)\cdot\delta\bar{q}_d = 0$ for discrete variations $\delta\bar{q}_d \in T_{\bar{q}_d}\mathcal{M}_d$ that vanish at the boundary nodes 0 and K. Utilizing (3.1.2), we see that setting discrete variations to zero at the boundaries eliminates the influence of the $\Theta^+_{\bar{L}_d}(\bar{q}_{K-1},\bar{q}_K)$ and $\Theta^-_{\bar{L}_d}(\bar{q}_0,\bar{q}_1)$ terms, and it is sufficient for solutions to produce $EL_d((\bar{q}_{k-1},\bar{q}_k),(\bar{q}_k,\bar{q}_{k+1})) = 0$ for all $k \in \{1,\ldots,K-1\}$. This yields the ***extended discrete Euler-Lagrange (DEL) equations***

$$D_4\bar{L}_d(\bar{q}_{k-1},\bar{q}_k) + D_2\bar{L}_d(\bar{q}_k,\bar{q}_{k+1}) = 0, \tag{3.1.3}$$

$$D_3\bar{L}_d(\bar{q}_{k-1},\bar{q}_k) + D_1\bar{L}_d(\bar{q}_k,\bar{q}_{k+1}) = 0, \tag{3.1.4}$$

for all $k \in \{1,\ldots,K-1\}$. In terms of numerical integration, these equations implicitly define a map $\Psi : Q_e \times Q_e \to Q_e \times Q_e$ such that $\Psi(\bar{q}_{k-1},\bar{q}_k) = (\bar{q}_k,\bar{q}_{k+1})$.

As in the continuous case, the components of the Lagrangian one-form provide expressions for the mechanical system's momentum and energy. However, in the discrete case, we have two one-forms $\Theta^+_{\bar{L}_d}$ and $\Theta^-_{\bar{L}_d}$, and correspondingly two definitions of momentum and energy. Moving forward, we will regard $-D_2L_d(\bar{q}_k,\bar{q}_{k+1})$ and $D_4L_d(\bar{q}_k,\bar{q}_{k+1})$ respectively as ***left and right discrete momenta*** in T^*Q. Further-

more, let us define the ***discrete energies***

$$E^+_{L_d}(\bar{q}_k, \bar{q}_{k+1}) = -D_3\bar{L}_d(\bar{q}_k, \bar{q}_{k+1}),$$
$$E^-_{L_d}(\bar{q}_k, \bar{q}_{k+1}) = D_1\bar{L}_d(\bar{q}_k, \bar{q}_{k+1}).$$

With these definitions we see that, like the continuous time extended Euler-Lagrange equations, (3.1.3) and (3.1.4) define the evolution of the system's momentum and energy, respectively. Unlike the continuous case though, the energy equation is not a redundant result. For arbitrary timesteps, there is no guarantee that solutions to (3.1.3) will also yield (3.1.4). In fact, as discussed in [49] and [56], in some instances there exists no timestep that provides a solution to the extended DEL equations. As a result, in practical applications, fixed timestep integration using (3.1.3) is heavily favored over the extended methods above. Such fixed step methods simply view the discrete dynamics parallel to the autonomous approach in continuous time.

3.1.2 Holonomic Constraints

Returning to the constrained systems of Subsection 2.1.2, we will incorporate the constraint $g : Q \to \mathbb{R}^m$ and its corresponding constraint submanifold $N = g^{-1}(0) \subset Q$ into the framework of the previous subsection. For this, we consider a discrete constrained coordinate path space of the form

$$(\mathcal{M}_{cc})_d = \mathcal{T}_d \times \mathcal{Q}_d(Q) \times \mathcal{L}_d,$$

where $\mathcal{T}_d$ and $\mathcal{Q}_d(Q)$ are as previously defined and

$$\mathcal{L}_d = \big\{\lambda_d : \{0, 1, \ldots, (K-1), K\} \to \mathbb{R}^m\big\}.$$

Using a path of discrete Lagrange multipliers $\lambda_d \in \mathcal{L}_d$, we introduce ***left and right discrete constraint functions*** $g_d^{\pm} : Q \times Q \to \mathbb{R}^m$ of the form

$$g_d^-(q_k, q_{k+1}) = (t_{k+1} - t_k)g(q_k),$$
$$g_d^+(q_k, q_{k+1}) = (t_{k+1} - t_k)g(q_{k+1}),$$

in order to provide the approximation

$$\frac{1}{2}\langle \lambda_k, g_d^-(q_k, q_{k+1})\rangle + \frac{1}{2}\langle \lambda_{k+1}, g_d^+(q_k, q_{k+1})\rangle \approx \int_{t_k}^{t_{k+1}} \langle \lambda, g(q)\rangle dt.$$

The definitions here follow the form of [61]; however, [68] notes that any convex combination of the two inner product terms will suffice. In an extended framework, it makes sense to define the approximation above as a function of the time values as well. This is done with ***extended discrete constraint functions*** $\bar{g}_d^{\pm} : Q_e \times Q_e \to \mathbb{R}^m$ such that

$$\frac{1}{2}\langle \lambda_k, \bar{g}_d^-(\bar{q}_k, \bar{q}_{k+1})\rangle + \frac{1}{2}\langle \lambda_{k+1}, \bar{g}_d^+(\bar{q}_k, \bar{q}_{k+1})\rangle \approx \int_{t_k}^{t_{k+1}} \langle \lambda, g(q)\rangle dt,$$

where $\bar{g}_d^-(\bar{q}_k, \bar{q}_{k+1}) = g_d^-(q_k, q_{k+1})$ and $\bar{g}_d^+(\bar{q}_k, \bar{q}_{k+1}) = g_d^+(q_k, q_{k+1})$. In terms of the extended constraint function $\bar{g}$ associated with g, the above approximation could also be written as

$$\frac{1}{2}\langle \lambda_k, \bar{g}_d^-(\bar{q}_k, \bar{q}_{k+1})\rangle + \frac{1}{2}\langle \lambda_{k+1}, \bar{g}_d^+(\bar{q}_k, \bar{q}_{k+1})\rangle \approx \int_{\tau_k}^{\tau_{k+1}} \langle c_\lambda, \bar{g}(c)\rangle d\tau.$$

Now let us consider, as we did in the continuous case, restrictions of the Lagrangian. Namely, we use the manifold structure of $N_e \times N_e$ to restrict the extended discrete Lagrangian as $\bar{L}_d^{N_e} = \bar{L}_d|_{N_e \times N_e}$. We will compare the discrete dynamics of $\bar{L}_d^{N_e}$ resulting from an action principle on $\mathcal{T}_d \times \mathcal{Q}_d(N)$ with the discrete dynamics of a

discrete augmented Lagrangian $\tilde{L}_d : Q_e \times \mathbb{R}^m \times Q_e \times \mathbb{R}^m \to \mathbb{R}$ derived in $(\mathcal{M}_{cc})_d$.

Remark 3.2: *In the analysis that follows, we make use of an extension to the notation first discussed in Remark 3.1. Namely, we will occasionally make use of the expression*

$$\tilde{q}_k \triangleq (\bar{q}_k, \lambda_k) = (t_k, q_k, \lambda_k) \in \tilde{Q}_e.$$

Theorem 3.2: *Given an extended discrete Lagrangian* $\bar{L}_d : Q_e \times Q_e \to \mathbb{R}$ *with extended discrete holonomic constraints* $\bar{g}_d^{\pm} : Q_e \times Q_e \to \mathbb{R}^m$ *derived from a holonomic constraint* $g : Q \to \mathbb{R}^m$*, denote* $N = g^{-1}(0) \subset Q$*,* $N_e = \mathbb{R} \times N$*, and* $\bar{L}_d^{N_e} = \bar{L}_d|_{N_e \times N_e}$*. The following are equivalent:*

1. $\bar{q}_d = (t_d, q_d) \in \mathcal{T}_d \times \mathcal{Q}_d(N)$ extremizes $\bar{\mathfrak{G}}_d^{N_e} = \bar{\mathfrak{G}}_d|_{N_e \times N_e}$ and thus is a solution of the extended DEL equations for $\bar{L}_d^{N_e}$;

2. $(\bar{q}_d, \lambda_d) \in (\mathcal{M}_{cc})_d$ satisfies the **extended constrained DEL equations**

$$D_4\bar{L}_d(\bar{q}_{k-1}, \bar{q}_k) + D_2\bar{L}_d(\bar{q}_k, \bar{q}_{k+1}) = \frac{1}{2}(t_{k+1} - t_{k-1}) \left(\frac{dg}{dq}\Big|_{q_k} \right)^T \cdot \lambda_k, \tag{3.1.5}$$

$$D_3\bar{L}_d(\bar{q}_{k-1}, \bar{q}_k) + D_1\bar{L}_d(\bar{q}_k, \bar{q}_{k+1}) = 0, \tag{3.1.6}$$

$$g(q_k) = 0, \tag{3.1.7}$$

   for all $k \in \{1, \ldots, K-1\}$;

3. $(\bar{q}_d, \lambda_d) \in (\mathcal{M}_{cc})_d$ extremizes $\tilde{\mathfrak{G}}_d(\bar{q}_d, \lambda_d) = \bar{\mathfrak{G}}_d(\bar{q}_d) - \langle \lambda_d, \Phi(\bar{q}_d) \rangle_{l_2}$ and hence solves the DEL equations for the augmented discrete Lagrangian $\tilde{L}_d^g : \tilde{Q}_e \times \tilde{Q}_e \to \mathbb{R}$ defined by

$$\tilde{L}_d^g(\bar{q}_k, \lambda_k, \bar{q}_{k+1}, \lambda_{k+1}) = \bar{L}_d(\bar{q}_k, \bar{q}_{k+1}) - \frac{1}{2}\langle \lambda_k, \bar{g}_d^-(\bar{q}_k, \bar{q}_{k+1}) \rangle - \frac{1}{2}\langle \lambda_{k+1}, \bar{g}_d^+(\bar{q}_k, \bar{q}_{k+1}) \rangle.$$

PROOF: This proof closely parallels the continuous case of Theorem 2.3. Here, the full space is $M = \mathcal{M}_d$ and the function to be extremized is $\bar{\mathfrak{G}}_d$ as defined in subsection 3.1.1. The constraint is specified by $V = \mathcal{L}_d$ with the l_2 inner product. Set $\Phi : M \to V$ as $\Phi_d(\bar{q}_d)(k) = \frac{1}{2}(\bar{g}_d^+(\bar{q}_{k-1}, \bar{q}_k) + \bar{g}_d^-(\bar{q}_k, \bar{q}_{k+1})) = \frac{1}{2}(t_{k+1} - t_{k-1})g(q_k)$ for all $k \in \{1, \ldots, (K-1)\}$ and at the endpoints $\Phi_d(\bar{q}_d)(0) = \frac{1}{2}\bar{g}_d^-(\bar{q}_0, \bar{q}_1)$ and $\Phi_d(\bar{q}_d)(K) = \frac{1}{2}\bar{g}_d^+(\bar{q}_{K-1}, \bar{q}_K)$. This definition of Φ is such that $\bar{q}_d \in \mathcal{T}_d \times \mathcal{Q}_d(N)$ if and only if $\Phi_d(\bar{q}_d) = 0$ (meaning $g(q_k) = 0$ for all $k \in \{0, \ldots, K\}$). From this it follows $\mathcal{D} = \Phi_d^{-1}(0) = \mathcal{T}_d \times \mathcal{Q}_d(N)$.

The first condition above corresponds with the first condition in Theorem 2.2. That is, $\bar{q}_d \in \mathcal{D}$ is an extremum of $\bar{\mathfrak{G}}_d|_{\mathcal{D}}$. By the Lagrange multiplier theorem, this is equivalent to $(\bar{q}_d, \lambda_d) \in M \times V$ being an extremum of $\tilde{\mathfrak{G}}_d(\bar{q}_d, \lambda_d) = \bar{\mathfrak{G}}_d(\bar{q}_d) - \langle \lambda_d, \Phi_d(\bar{q}_d) \rangle$. Identifying $M \times V$ with $(\mathcal{M}_{cc})_d$ and examining the particular form of $\tilde{\mathfrak{G}}_d : (\mathcal{M}_{cc})_d \to \mathbb{R}$ we see the augmented Lagrangian emerge as

$$\begin{aligned}
\tilde{\mathfrak{G}}_d(\bar{q}_d, \lambda_d) &= \bar{\mathfrak{G}}_d(\bar{q}_d) - \langle \lambda_d, \Phi(\bar{q}_d) \rangle, \\
&= \sum_{k=0}^{K-1} \bar{L}_d(\bar{q}_k, \bar{q}_{k+1}) - \sum_{k=0}^{K} \langle \lambda_d(k), \Phi(\bar{q}_d)(k) \rangle, \\
&= \sum_{k=1}^{K-1} \left[\bar{L}_d(\bar{q}_k, \bar{q}_{k+1}) - \langle \lambda_k, \frac{1}{2}(\bar{g}_d^+(\bar{q}_{k-1}, \bar{q}_k) + \bar{g}_d^-(\bar{q}_k, \bar{q}_{k+1})) \rangle \right] \\
&\quad + \bar{L}_d(\bar{q}_0, \bar{q}_1) - \langle \lambda_0, \frac{1}{2}\bar{g}_d^-(\bar{q}_0, \bar{q}_1)) \rangle - \langle \lambda_K, \frac{1}{2}\bar{g}_d^+(\bar{q}_{K-1}, \bar{q}_K)) \rangle, \\
&= \sum_{k=0}^{K-1} \tilde{L}_d^g(\bar{q}_k, \lambda_k, \bar{q}_{k+1}, \lambda_{k+1}).
\end{aligned}$$

As $(\bar{q}_d, \lambda_d)$ extremizes $\tilde{\mathfrak{G}}_d(\bar{q}_d, \lambda_d)$, it is also a solution to the Euler-Lagrange equations for $\tilde{L}_d^g$, satisfying the third condition. Finally, the second condition follows from $d\tilde{\mathfrak{G}}_d = 0$. To show this, we define the discrete second order submanifold for the

augmented Lagrangian system

$$(\ddot{\tilde{Q}}_e)_d = \tilde{Q}_e \times \tilde{Q}_e \times \tilde{Q}_e.$$

With this definition, we can now express variations $d\tilde{\mathfrak{G}}_d(\bar{q}_d, \lambda_d) \cdot \delta(\bar{q}_d, \lambda_d)$ using the discrete Euler-Lagrange derivative $\widetilde{EL}_d : (\ddot{\tilde{Q}}_e)_d \to T^*\tilde{Q}_e$ and discrete Lagrangian one-forms $\Theta^{\pm}_{\tilde{L}^g_d}$ on $\tilde{Q}_e \times \tilde{Q}_e$ for the augmented discrete Lagrangian $\tilde{L}^g_d$. Using these terms, we have

$$\begin{aligned} d\tilde{\mathfrak{G}}_d(\bar{q}_d, \lambda_d) \cdot \delta(\bar{q}_d, \lambda_d) = &\sum_{k=1}^{K-1} \widetilde{EL}_d(\tilde{q}_{k-1}, \tilde{q}_k, \tilde{q}_{k+1}) \cdot \delta(\tilde{q}_k) \\ &+ \Theta^+_{\tilde{L}^g_d}(\tilde{q}_{K-1}, \tilde{q}_K) \cdot (\delta\tilde{q}_{K-1}, \delta\tilde{q}_K) - \Theta^-_{\tilde{L}^g_d}(\tilde{q}_0, \tilde{q}_1) \cdot (\delta\tilde{q}_0, \delta\tilde{q}_1), \end{aligned}$$

where

$$\begin{aligned} \widetilde{EL}_d(\tilde{q}_{k-1}, \tilde{q}_k, \tilde{q}_{k+1}) = &\, EL_d((\bar{q}_{k-1}, \bar{q}_k), (\bar{q}_k, \bar{q}_{k+1})) \\ &- \left[\frac{1}{2}\lambda_{k-1} \cdot D_3\bar{g}^-_d(\bar{q}_{k-1}, \bar{q}_k) + \frac{1}{2}\lambda_k \cdot D_3\bar{g}^+_d(\bar{q}_{k-1}, \bar{q}_k)\right] dt_k \\ &- \left[\frac{1}{2}\lambda_k \cdot D_1\bar{g}^-_d(\bar{q}_k, \bar{q}_{k+1}) + \frac{1}{2}\lambda_{k+1} \cdot D_1\bar{g}^+_d(\bar{q}_k, \bar{q}_{k+1})\right] dt_k \\ &- \left[\frac{1}{2}\lambda_k \cdot D_4\bar{g}^+_d(\bar{q}_{k-1}, \bar{q}_k) + \frac{1}{2}\lambda_k \cdot D_2\bar{g}^-_d(\bar{q}_k, \bar{q}_{k+1})\right] dq_k \\ &- \left[\frac{1}{2}(\bar{g}^+_d(\bar{q}_{k-1}, \bar{q}_k) + \bar{g}^-_d(\bar{q}_k, \bar{q}_{k+1}))\right] d\lambda_k, \\ \Theta^+_{\tilde{L}^g_d}(\tilde{q}_k, \tilde{q}_{k+1}) = &\, \Theta^+_{\bar{L}_d}(\bar{q}_k, \bar{q}_{k+1}) - \frac{1}{2}\lambda_{k+1} \cdot D_3\bar{g}^+_d(\bar{q}_k, \bar{q}_{k+1})dt_{k+1} \\ &- \frac{1}{2}\lambda_{k+1} \cdot D_4\bar{g}^+_d(\bar{q}_k, \bar{q}_{k+1})dq_{k+1} - \frac{1}{2}\bar{g}^+_d(\bar{q}_k, \bar{q}_{k+1})d\lambda_{k+1}, \\ \Theta^-_{\tilde{L}^g_d}(\tilde{q}_k, \tilde{q}_{k+1}) = &\, \Theta^-_{\bar{L}_d}(\bar{q}_k, \bar{q}_{k+1}) + \frac{1}{2}\lambda_k \cdot D_1\bar{g}^-_d(\bar{q}_k, \bar{q}_{k+1})dt_k \\ &+ \frac{1}{2}\lambda_k \cdot D_2\bar{g}^-_d(\bar{q}_k, \bar{q}_{k+1})dq_k + \frac{1}{2}\bar{g}^-_d(\bar{q}_k, \bar{q}_{k+1})d\lambda_k. \end{aligned}$$

Setting $d\tilde{\mathfrak{G}}_d(\bar{q}_d, \lambda_d)$ and the boundary variations δt_0, δq_0, $\delta\lambda_0$, δt_K, δq_K, and $\delta\lambda_K$ to

zero, collection of like terms of δt_k, δq_k, and $\delta\lambda_k$ yields (3.1.5), (3.1.6), and (3.1.7).

The form of the constraint forces in (3.1.5) results from the following identity

$$\frac{1}{2}\left(D_4\bar{g}_d^+(\bar{q}_{k-1},\bar{q}_k)+D_2\bar{g}_d^-(\bar{q}_k,\bar{q}_{k+1})\right)^T\lambda_k=\frac{1}{2}(t_{k+1}-t_{k-1})\left(\frac{dg}{dq}\Big|_{q_k}\right)^T\cdot\lambda_k,$$

which is produced by evaluating the slot derivatives on the definitions of $\bar{g}_d^{\pm}$. Also, the stationarity condition resulting from variations $\delta\lambda_k$,

$$\bar{g}_d^+(\bar{q}_{k-1},\bar{q}_k)+\bar{g}_d^-(\bar{q}_k,\bar{q}_{k+1})=0,$$

implies (3.1.7), $g(q_k)=0$ for all $k\in\{1,\dots,K-1\}$. This in turn implies that all terms of the form $D_1\bar{g}_d^{\pm}$ and $D_3\bar{g}_d^{\pm}$ in $\widetilde{EL}_d$ are zero for all $k\in\{1,\dots,K-1\}$ and thus they do not appear in (3.1.6). ∎

In the extended constrained DEL equations, (3.1.5) has the structure of (3.1.3) in the extended (free) DEL equations, however, now with the presence of constraint forces. As in the continuous case, these holonomic constraint forces do not influence the energy behavior of the system. This is represented by the equivalence of (3.1.6) and (3.1.4). As in the unconstrained case, it is more common in practice to abandon the energy condition (3.1.6) and perform fixed timestep integration according to (3.1.5) and (3.1.7).

Rather than undertaking the vakonomic approach of Theorem 2.4 in the discrete setting, we note the following. In the continuous setting, vakonomic "hidden" constraints were used to enforce $\dot{q}\in TN$ for all $t\in(c_t(0),c_t(1))$. This condition had important implications for the jump conditions of holonomically constrained elastic impacts. In the discrete setting, where the constraint distribution TN is replaced with $N\times N$, the discrete version of the condition on $\dot{q}$ above amounts to $(q_k,q_{k+1})\in N\times N$ or $(g(q_k),g(q_{k+1}))=(0,0)$. Since the discrete holonomic constraint g_d already yields

this condition, it will be sufficient in the nonsmooth analyses to come.

Remark 3.3: *There are methods that implement a discretized version of the hidden constraints f, for instance, in [11]. However, as mentioned in [59], this practice has yet to reveal any demonstrable advantages.*

The null space methods of Subsection 2.1.2 can be applied in the discrete setting as well. Focusing on the fixed timestep case, we momentarily disregard the energy equation (3.1.6). Given a null space matrix $P(q) : \mathbb{R}^{n-m} \to T_qN$, the constrained DEL equations (3.1.5) and (3.1.7) can be projected down to the n-dimensional set of equations

$$P^T(q_k)\left[D_4\bar{L}_d(\bar{q}_{k-1},\bar{q}_k) + D_2\bar{L}_d(\bar{q}_k,\bar{q}_{k+1})\right] = 0, \tag{3.1.8}$$

$$g(q_k) = 0, \tag{3.1.9}$$

for all $k \in \{1,\dots,K-1\}$. Integration methods that further reduce this system to dimension $(n-m)$ using generalized coordinates on N are discussed in [61].

3.1.3 External Forcing

In this section, we develop a discrete Lagrange-d'Alembert principle for mechanical systems with external forces. We demonstrate this for the free systems of Subsection 3.1.1; however, the following arguments readily apply to any of the discrete variational principles in this chapter.

To incorporate external forces into system dynamics in the discrete setting, we define ***left and right discrete forces*** $F_d^{\pm} : Q_e \times Q_e \to T^*Q_e$ as

$$F_d^+(\bar{q}_k,\bar{q}_{k+1}) = (\bar{q}_{k+1}, F_d^+(\bar{q}_k,\bar{q}_{k+1})),$$
$$F_d^-(\bar{q}_k,\bar{q}_{k+1}) = (\bar{q}_k, F_d^-(\bar{q}_k,\bar{q}_{k+1})).$$

In a discrete sense, these definitions parallel the fiber preserving structure of the forces in Subsection 2.1.3. These discrete forces approximate virtual work from the Lagrange-d'Alembert principle as

$$F_d^-(\bar{q}_k, \bar{q}_{k+1}) \cdot \delta\bar{q}_k + F_d^+(\bar{q}_k, \bar{q}_{k+1}) \cdot \delta\bar{q}_{k+1} \approx \int_{\tau_k}^{\tau_{k+1}} F(c, c') \cdot \delta c \, d\tau.$$

Using this approximation, the ***discrete Lagrange-d'Alembert principle*** takes the form

$$\delta \sum_{k=0}^{K-1} \bar{L}_d(\bar{q}_k, \bar{q}_{k+1}) + \sum_{k=0}^{K-1} F_d^-(\bar{q}_k, \bar{q}_{k+1}) \cdot \delta\bar{q}_k + F_d^+(\bar{q}_k, \bar{q}_{k+1}) \cdot \delta\bar{q}_{k+1} = 0,$$

where the discrete variations at the endpoints vanish, $\delta\bar{q}_0 = \delta\bar{q}_K = 0$. This is equivalent to the ***extended forced DEL equations***

$$D_4 L_d(\bar{q}_{k-1}, \bar{q}_k) + D_2 L_d(\bar{q}_k, \bar{q}_{k+1}) = -(F_q)_d^+(\bar{q}_{k-1}, \bar{q}_k) - (F_q)_d^-(\bar{q}_k, \bar{q}_{k+1}), \tag{3.1.10}$$

$$D_3 L_d(\bar{q}_{k-1}, \bar{q}_k) + D_1 L_d(\bar{q}_k, \bar{q}_{k+1}) = -(F_t)_d^+(\bar{q}_{k-1}, \bar{q}_k) - (F_t)_d^-(\bar{q}_k, \bar{q}_{k+1}), \tag{3.1.11}$$

where we have denoted the discrete force in coordinates as $F_d^\pm = ((F_t)_d^\pm)$.

In practice, there are two major issues with the forced equations (3.1.10) and (3.1.11). First, unlike the continuous case, there is no explicit consistency condition between $(F_q)_d^\pm$ and $(F_t)_d^\pm$. Thus, a poorly defined $F_d^\pm$ could yield solvable equations that do not represent the true momentum and energy behavior of the overlying mechanical system. Secondly, even if a discrete notion of consistency between $(F_q)_d^\pm$ and $(F_t)_d^\pm$ is developed, the challenges regarding the solvability of the extended DEL equations near turning points may persist. While these issues may deem equations (3.1.10) and (3.1.11) unsuitable for integration, the above framework for discrete forcing has been included due to the importance of the extended approach in the nonsmooth case. For smooth forced systems, fixed timestep integration according to (3.1.10) is

recommended.

3.2 Elastic Collisions

In this section, we develop variational collision integrators for the elastic collisions of Section 2.2. The discrete equations of motion presented for free systems match the theory developed in [32].

3.2.1 Free Systems

To model a free system undergoing a single elastic collision in discrete time, we retain the definitions of Q, Q_e, C, and ∂C from Chapter 2. Furthermore, we make use of L_d and $\bar{L}_d$ from Section 3.1. We specify that the collision is fixed with respect to the time-like mesh, say at node j where $j \in \{0, \ldots, K\}$, but allow variations δt_j of the collision time t_j. This specification provides the structure for a ***discrete nonsmooth path space*** of the form

$$(\mathcal{M}_{ns})_d = (\mathcal{T}_{ns})_d(j) \times (\mathcal{Q}_{ns})_d(j, \partial C, Q),$$

where

$$\begin{aligned}(\mathcal{T}_{ns})_d(j) = \Big\{ & t_d : \{0, 1 \ldots, (K-1), K\} \to \mathbb{R} \mid t_d(k) = kh \ \forall k \in \{0, \ldots, j-1\}, \\ & t_d(k) = (k-1)h \ \forall k \in \{j+1, \ldots, K\}, \\ & t_d(j) \in [(j-1)h, jh], \ h \in \mathbb{R} \Big\},\end{aligned}$$

$$(\mathcal{Q}_{ns})_d(j, \partial C, Q) = \big\{ q_d : \{0, 1, \ldots, (K-1), K\} \to Q, \ q_d(j) \in \partial C \big\}.$$

In this path space, the time differences $(t_{k+1} - t_k)$ are fixed for all $k \neq j-1, j$ according to the ***timestep*** $h \in \mathbb{R}$. The collision time t_j is the only variable time value under the

structure of t_d. As a result, we can identify a discrete trajectory $\bar{q}_d = (t_d, q_d) \in (\mathcal{M}_{ns})_d$ with its image (t_j, q_d), where $t_j \in [(j-1)h, jh]$ and $q_d(j) = q_j \in \partial C$. This viewpoint also indicates that $(\mathcal{M}_{ns})_d$ is isomorphic to $[(j-1)h, jh] \times Q \times \cdots \times \partial C \times \cdots \times Q$ (K copies of Q) and thus has a smooth manifold structure.

Remark 3.4: *In this setting, variable timesteps are incorporated in a limited capacity (before and after t_j) to exactly resolve the time of impact. This comes in contrast to the previous section in which variable timesteps were used to enforce discrete energy conservation everywhere. Without this change in the structure of the path space, there is no guarantee that the discrete trajectory would include the impact configuration $q_j \in \partial C$.*

On this path space, the ***nonsmooth discrete action map*** $\bar{\mathfrak{G}}_d : (\mathcal{M}_{ns})_d \to \mathbb{R}$ takes the same form as the extended discrete action map $\bar{\mathfrak{G}}_d$ from Section 3.1. That is,

$$\bar{\mathfrak{G}}_d(\bar{q}_d) = \sum_{k=0}^{K-1} \bar{L}_d(\bar{q}_k, \bar{q}_{k+1}).$$

This definition marks a slight departure in notation from [32]. There, the nonsmooth discrete action map appears as

$$\bar{\mathfrak{G}}_d(t_j, q_d) = \sum_{k=0}^{j-2} L_d(q_k, q_{k+1}) + \sum_{k=j+1}^{K-1} L_d(q_k, q_{k+1}) + \bar{L}_d(\bar{q}_{j-1}, \bar{q}_j) + \bar{L}_d(\bar{q}_j, \bar{q}_{j+1}),$$

to emphasize the fixed nature of the time values t_k for all $k \neq j$. We will keep the shorter notation of $\bar{\mathfrak{G}}_d(\bar{q}_d)$, but note outright that variations of this map will exclude any terms δt_k for all $k \neq j$. The condition $\delta t_k = 0$ for all $k \neq j$ is in accordance with the definition of $(\mathcal{M}_{ns})_d$.

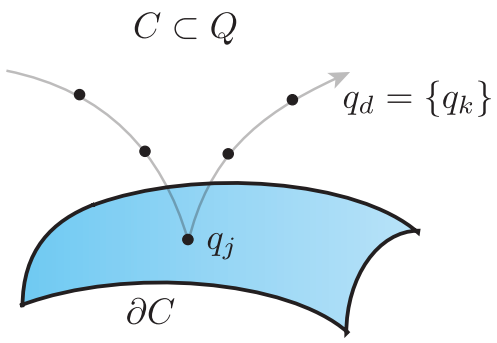

Figure 3.1: A discrete path q_d capturing an elastic collision using discrete variational jump conditions.

Given a variation $\delta\bar{q}_d \in T_{\bar{q}_d}(\mathcal{M}_{ns})_d$, we take variations of $\mathfrak{G}_d$ as follows

$$\begin{aligned} d\bar{\mathfrak{G}}_d(\bar{q}_d)\cdot\delta\bar{q}_d = &\sum_{k=1}^{j-1} EL_d(\bar{q}_{k-1},\bar{q}_k,\bar{q}_{k+1})\cdot\delta q_k + \sum_{k=j+1}^{K-1} EL_d(\bar{q}_{k-1},\bar{q}_k,\bar{q}_{k+1})\cdot\delta q_k \\ &+ \Theta^+_{\bar{L}_d}(\bar{q}_{K-1},\bar{q}_K)\cdot(\delta q_{K-1},\delta q_K) - \Theta^-_{\bar{L}_d}(\bar{q}_0,\bar{q}_1)\cdot(\delta q_0,\delta q_1) \\ &+ [D_3\bar{L}_d(\bar{q}_{j-1},\bar{q}_j) + D_1\bar{L}_d(\bar{q}_j,\bar{q}_{j+1})]\cdot\delta t_j \\ &+ i^*(D_4\bar{L}_d(\bar{q}_{j-1},\bar{q}_j) + D_2\bar{L}_d(\bar{q}_j,\bar{q}_{j+1}))\cdot\delta q_j, \end{aligned}$$

where $i^* : T^*Q \to T^*\partial C$ is the same cotangent lift of the embedding $i : \partial C \to Q$ previously discussed in Subsection 2.2.1. The term preceding δq_j is projected with i^* because, in accordance with the definition of $(\mathcal{Q}_{ns})_d(j,\partial C,Q)$, one cannot take variations of the impact configuration q_j normal to the contact set ∂C.

As in the previous section, the discrete Hamilton's principle specifies that solutions correspond with stationary points of the discrete action. In this case, this means a solution $\bar{q}_d \in (\mathcal{M}_{ns})_d$ will yield $d\mathfrak{G}_d(t_j,q_d)\cdot(\delta t_j,\delta q_d) = 0$ for discrete variations $\delta\bar{q}_d \in T_{\bar{q}_d}(\mathcal{M}_{ns})_d$ with $\delta q_0 = \delta q_K = 0$.

Examining the terms in $d\mathfrak{G}_d(t_j, q_d)$, we have that for all $k \neq j$ it must hold

$$D_4\bar{L}_d(\bar{q}_{k-1}, \bar{q}_k) + D_2\bar{L}_d(\bar{q}_k, \bar{q}_{k+1}) = 0,$$

which is identical to the smooth system DEL equations (3.1.3). In terms of integration, one can use these equations for all $k < j - 1$ without the additional (3.1.4) because the timestep $h \in \mathbb{R}$ predefines all of the time values t_k involved. If, at any point, integrating the equations above yields $q_{k+1} \notin C$, contact has occurred and $k = j - 1$ at this juncture. This inadmissible q_{k+1} is disregarded and to proceed, the equations above are appended with a contact condition to form

$$D_4\bar{L}_d(\bar{q}_{j-2}, \bar{q}_{j-1}) + D_2\bar{L}_d(\bar{q}_{j-1}, \bar{q}_j) = 0, \tag{3.2.1}$$

$$q_j \in \partial C. \tag{3.2.2}$$

Henceforth, we term the set above the ***discrete contact resolution conditions***, as they are to be solved for the impact time t_j and impact configuration q_j. The appended condition $q_j \in \partial C$ is not a product of the stationarity condition $d\bar{\mathfrak{G}}_d(\bar{q}_d) = 0$, but rather of the path space definition for $(\mathcal{M}_{ns})_d$. Using the notation of Subsection 2.2.1, we may express $q_j \in \partial C$ otherwise as $g_{\partial C}(q_j) = 0$. After determining (t_j, q_j), the first post-impact configuration q_{j+1} is solved for according to the ***discrete variational jump conditions***

$$i^*(D_4\bar{L}_d(\bar{q}_{j-1}, \bar{q}_j) + D_2\bar{L}_d(\bar{q}_j, \bar{q}_{j+1})) = 0, \tag{3.2.3}$$

$$D_3\bar{L}_d(\bar{q}_{j-1}, \bar{q}_j) + D_1\bar{L}_d(\bar{q}_j, \bar{q}_{j+1}) = 0. \tag{3.2.4}$$

These equations, representing a conservation of discrete energy and discrete momentum tangent to ∂C, constitute the discrete time version of the jump conditions (2.2.1). Following these conditions, the discrete dynamics can again be integrated for $k > j$,

as they were for $k < j-1$, according to the DEL equations (3.1.3). Figure 3.1 depicts a discrete path subject to the collision model above.

Remark 3.5: *In the integration scheme described above, the benefits of defining t_j as a variable in the path space $(\mathcal{M}_{ns})_d$ appear twofold. First, this definition enables the solution of the exact collision time in the integration process. Second, the energy balance arising from variations δt_j increases the set of equations* (3.2.3) *and* (3.2.4) *(those that determine q_{j+1}) to dimension n. Without this energy balance, the system* (3.2.3) *would surely be underdetermined.*

Though we do not demonstrate it here, this collision integration algorithm and those that follow easily generalize to the case of multiple impacts in a single timestep. Details are contained in [31].

Given the null space matrix $P_{\partial C}(q) : \mathbb{R}^{n-1} \to T_q \partial C$ as defined in Subsection 2.2.1, the momentum balance (3.2.3) in the discrete variational jump conditions may be expressed equivalently as

$$P_{\partial C}^T(q_j) \left[D_4 \bar{L}_d(\bar{q}_{j-1}, \bar{q}_j) + D_2 \bar{L}_d(\bar{q}_j, \bar{q}_{j+1}) \right] = 0. \tag{3.2.5}$$

3.2.2 Holonomic Constraints

To model the constrained elastic collisions of Subsection 2.2.2 in discrete time, we will utilize the definitions of g, $\bar{g}$, R, R_e, and ∂R from that subsection to enforce constraints within the discrete dynamics developed in Subsection 3.2.1. In particular, we begin by defining the ***discrete constrained coordinate nonsmooth path space***

$$(\mathcal{M}'_{ccns})_d = (\mathcal{M}'_{ns})_d \times \mathcal{L}_d,$$

where $\mathcal{L}_d$ is as previously defined and $(\mathcal{M}'_{ns})_d = (\mathcal{T}_{ns})_d(j) \times (\mathcal{Q}_{ns})_d(j, \partial R, Q)$. As in the continuous case, $(\mathcal{M}'_{ccns})_d$ is differentiated from $(\mathcal{M}_{ccns})_d = (\mathcal{M}_{ns})_d \times \mathcal{L}_d$ since it

restricts q_j to ∂R rather than the more general ∂C. With this definition, we develop the following theorem relating the discrete nonsmooth dynamics of $\bar{L}_d^{R_e} = \bar{L}_d|_{R_e \times R_e}$ resulting from an action principle on $(\mathfrak{T}_{ns})_d(j) \times (\mathfrak{Q}_{ns})_d(j, \partial R, N)$ with the discrete nonsmooth dynamics of a discrete augmented Lagrangian $\tilde{L}_d : Q_e \times \mathbb{R}^m \times Q_e \times \mathbb{R}^m \to \mathbb{R}$ derived in $(\mathcal{M}'_{ccns})_d$.

Theorem 3.3: *Given an extended discrete Lagrangian $\bar{L}_d : Q_e \times Q_e \to \mathbb{R}$ on an admissible set C, with a contact set ∂C, subject to extended discrete holonomic constraints $\bar{g}_d^{\pm} : Q_e \times Q_e \to \mathbb{R}^m$ derived from a holonomic constraint $g : Q \to \mathbb{R}^m$, denote $N = g^{-1}(0) \subset Q$, $N_e = \mathbb{R} \times N$, $R_e = \mathbb{R} \times (N \cap C)$, and $\bar{L}_d^{R_e} = \bar{L}_d|_{R_e \times R_e}$. The following are equivalent:*

1. $\bar{q}_d = (t_d, q_d) \in (\mathfrak{T}_{ns})_d(j) \times (\mathfrak{Q}_{ns})_d(j, \partial R, N)$ extremizes $\bar{\mathfrak{G}}_d^{R_e} = \bar{\mathfrak{G}}_d|_{R_e \times R_e}$ and thus is a solution of the DEL equations, discrete contact resolution conditions, and discrete variational jump conditions associated with $\bar{L}_d^{R_e}$;

2. $(\bar{q}_d, \lambda_d) \in (\mathcal{M}'_{ccns})_d$ satisfies the *constrained DEL equations*

$$D_4\bar{L}_d(\bar{q}_{k-1}, \bar{q}_k) + D_2\bar{L}_d(\bar{q}_k, \bar{q}_{k+1}) = \frac{1}{2}(t_{k+1} - t_{k-1}) \left(\frac{dg}{dq}\Big|_{q_k} \right)^T \cdot \lambda_k, \tag{3.2.6}$$

$$g(q_k) = 0, \tag{3.2.7}$$

for all $k \in \{1, \ldots, j-2, j+1, \ldots, K-1\}$, as well as the discrete contact resolution conditions

$$D_4\bar{L}_d(\bar{q}_{j-2}, \bar{q}_{j-1}) + D_2\bar{L}_d(\bar{q}_{j-1}, \bar{q}_j) = \frac{1}{2}(t_j - t_{j-2}) \left(\frac{dg}{dq}\Big|_{q_{j-1}} \right)^T \cdot \lambda_{j-1}, \tag{3.2.8}$$

$$g(q_j) = 0, \tag{3.2.9}$$

$$q_j \in \partial R, \tag{3.2.10}$$

and the discrete variational jump conditions

$$i^*_{\partial R}\left(D_4\bar{L}_d(\bar{q}_{j-1},\bar{q}_j)+D_2\bar{L}_d(\bar{q}_j,\bar{q}_{j+1})\right)=0, \tag{3.2.11}$$

$$D_3\bar{L}_d(\bar{q}_{j-1},\bar{q}_j)+D_1\bar{L}_d(\bar{q}_j,\bar{q}_{j+1})=0, \tag{3.2.12}$$

$$g(q_{j+1})=0, \tag{3.2.13}$$

where $i^*_{\partial R}: T^*Q \to T^*\partial R$ is the cotangent lift of the embedding $i:\partial R \to Q$;

3. $(\bar{q}_d,\lambda_d) \in (\mathcal{M}'_{ccns})_d$ extremizes $\tilde{\mathfrak{G}}_d(\bar{q}_d,\lambda_d) = \mathfrak{G}_d(\bar{q}_d) - \langle\lambda_d, \Phi(\bar{q}_d)\rangle_{l_2}$ and hence solves the DEL equations for the augmented discrete Lagrangian $\tilde{L}^g_d : Q_e \times \mathbb{R}^m \times Q_e \times \mathbb{R}^m \to \mathbb{R}$ defined by

$$\tilde{L}^g_d(\bar{q}_k,\lambda_k,\bar{q}_{k+1},\lambda_{k+1}) = \bar{L}_d(\bar{q}_k,\bar{q}_{k+1}) - \frac{1}{2}\langle\lambda_k,\bar{g}^-_d(\bar{q}_k,\bar{q}_{k+1})\rangle - \frac{1}{2}\langle\lambda_{k+1},\bar{g}^+_d(\bar{q}_k,\bar{q}_{k+1})\rangle.$$

PROOF: For the final time, we walk through an application of Theorem 2.2. Here, the full space M is $(\mathcal{M}'_{ns})_d$ and the function to be extremized is $\bar{\mathfrak{G}}_d$. The constraint is specified by $V = \mathcal{L}_d$ with the l_2 inner product. Set $\Phi : M \to V$ as $\Phi_d(\bar{q}_d)(k) = \frac{1}{2}(\bar{g}^+_d(\bar{q}_{k-1},\bar{q}_k) + \bar{g}^-_d(\bar{q}_k,\bar{q}_{k+1})) = \frac{1}{2}(t_{k+1}-t_{k-1})g(q_k)$ for all $k \in \{1,\ldots,(K-1)\}$ and at the endpoints $\Phi_d(\bar{q}_d)(0) = \frac{1}{2}\bar{g}^-_d(\bar{q}_0,\bar{q}_1)$ and $\Phi_d(\bar{q}_d)(K) = \frac{1}{2}\bar{g}^+_d(\bar{q}_{K-1},\bar{q}_K)$. This definition of Φ is such that $\bar{q}_d \in (\mathcal{T}_{ns})_d(j) \times (\mathcal{Q}_{ns})_d(j,\partial R,N)$ if and only if $\Phi_d(\bar{q}_d)=0$. From this, it follows $\mathcal{D} = \Phi_d^{-1}(0) = (\mathcal{T}_{ns})_d(j) \times (\mathcal{Q}_{ns})_d(j,\partial R,N)$.

The first condition above corresponds with the first condition in Theorem 2.2. That is, $\bar{q}_d \in \mathcal{D}$ is an extremum of $\bar{\mathfrak{G}}_d|_{\mathcal{D}}$. By the Lagrange multiplier theorem, this is equivalent to $(\bar{q}_d,\lambda_d) \in M \times V$ being an extremum of $\tilde{\mathfrak{G}}_d(\bar{q}_d,\lambda_d) = \bar{\mathfrak{G}}_d(\bar{q}_d) - \langle\lambda_d,\Phi_d(\bar{q}_d)\rangle$. Identifying $M\times V$ with $(\mathcal{M}'_{ccns})_d$, the particular form of $\tilde{\mathfrak{G}}_d : (\mathcal{M}'_{ccns})_d \to \mathbb{R}$ yields an augmented Lagrangian of the same form in Theorem 3.2.

In order to show the second and third conditions are equivalent, we evaluate $d\tilde{\mathfrak{G}}_d = 0$ using the same procedure as in Subsection 3.2.1. Using the definitions for

$\tilde{q}_k$, $(\ddot{\tilde{Q}}_e)_d$, $\widetilde{EL}_d$, and $\Theta^{\pm}_{\tilde{L}_g}$ from Theorem 3.2, we express variations $d\tilde{\mathfrak{G}}_d \cdot \delta(\bar{q}_d, \lambda_d)$ as

$$\begin{aligned} d\tilde{\mathfrak{G}}_d(\bar{q}_d, \lambda_d) \cdot \delta(\bar{q}_d, \lambda_d) = &\sum_{k=1}^{j-1} \widetilde{EL}_d(\tilde{q}_{k-1}, \tilde{q}_k, \tilde{q}_{k+1}) \cdot \delta(q_k, \lambda_k) \\ &+ \sum_{k=j+1}^{K-1} \widetilde{EL}_d(\tilde{q}_{k-1}, \tilde{q}_k, \tilde{q}_{k+1}) \cdot \delta(q_k, \lambda_k) \\ &+ \Theta^{+}_{\tilde{L}^g_d}(\tilde{q}_{K-1}, \tilde{q}_K) \cdot (\delta\tilde{q}_{K-1}, \delta\tilde{q}_K) - \Theta^{-}_{\tilde{L}^g_d}(\tilde{q}_0, \tilde{q}_1) \cdot (\delta\tilde{q}_0, \delta\tilde{q}_1) \\ &+ [D_4\tilde{L}^g_d(\tilde{q}_{j-1}, \tilde{q}_j) + D_1\tilde{L}^g_d(\tilde{q}_j, \tilde{q}_{j+1})] \cdot \delta t_j \\ &+ i^*(D_5\tilde{L}^g_d(\tilde{q}_{j-1}, \tilde{q}_j) + D_2\tilde{L}^g_d(\tilde{q}_j, \tilde{q}_{j+1})) \cdot \delta q_j \\ &+ [D_3\tilde{L}^g_d(\tilde{q}_{j-1}, \tilde{q}_j) + D_6\tilde{L}^g_d(\tilde{q}_j, \tilde{q}_{j+1})] \cdot \delta\lambda_j. \end{aligned}$$

The expression above marks our first usage of the slot derivative notation on the augmented discrete Lagrangian $\tilde{L}^g_d$. Notice that this notation is simply shorthand for the terms that appear in the expansion of $\widetilde{EL}_d$ shown in Theorem 3.2. Using the same arguments regarding stationarity from that theorem, the expression above yields (3.2.6), (3.2.7), (3.2.8), (3.2.9), (3.2.10), (3.2.11), (3.2.12), and (3.2.13). Equation (3.2.11) is presented without the presence of constraint forces due to the simplification

$$i^*_{\partial R}\left(\frac{1}{2}(t_{j+1} - t_{j-1})\left(\frac{dg}{dq}\Big|_{q_j}\right)^T \cdot \lambda_j\right) = 0,$$

for all $q_j \in \partial R$. ■

In terms of integrating the discrete dynamics above, the same procedure as in Subsection 3.2.1 applies. One integrates according to (3.2.6) and (3.2.7) until $q_{k+1} \notin C$ is found. At this point, $k = j - 1$ and (3.2.8), (3.2.9), (3.2.10) are solved for t_j, q_j, and λ_{j-1}. Knowing the impact time and configuration, (3.2.11), (3.2.12), and (3.2.13) are solved for q_{j+1} and λ_j. Following this, the system can be integrated according to (3.2.6) and (3.2.7) until another impact occurs. Figure 3.2 depicts a discrete path

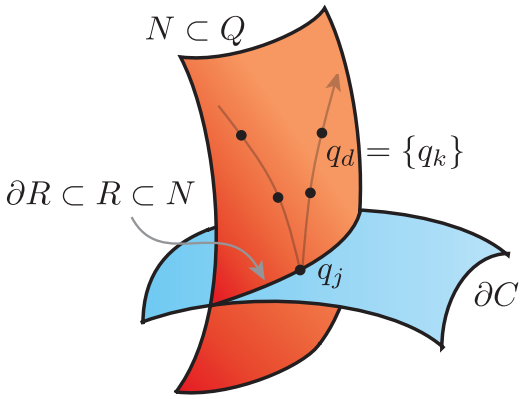

Figure 3.2: A holonomically constrained discrete path q_d capturing an elastic collision using discrete variational jump conditions.

subject to the collision model above.

Given the null space matrix $P_{\partial R}(q) : \mathbb{R}^{n-m-1} \to T_q \partial R$ as defined in Subsection 2.2.2, the momentum balance (3.2.11) in the discrete variational jump conditions may be expressed equivalently as

$$P_{\partial R}^T(q_j) \left[D_4 \bar{L}_d(\bar{q}_{j-1}, \bar{q}_j) + D_2 \bar{L}_d(\bar{q}_j, \bar{q}_{j+1}) \right] = 0. \tag{3.2.14}$$

Also note, as discussed in Subsection 3.1.2, the null space matrix $P(q)$ can be applied to the constrained DEL equations (3.2.6) for all for all $k \in \{1, \ldots, j-2, j+1, \ldots, K-1\}$.

3.3 Forced and Lossful Collisions

Here, we incorporate the contact force fields of Section 2.3 into the discrete dynamics. As a contact force field yields a discrete term in the continuous-time Lagrange-d'Alembert principle, its incorporation into the discrete Lagrange-d'Alembert principle is remarkably easy.

3.3.1 Free Systems

In the spirit of Subsection 2.3.1, we define a discrete contact force field $(F^{\partial C})_d : Q_e \times \mathbb{R} \times \partial C \to T^*(\mathbb{R} \times \partial C)$ to model nonconservative forces in the discrete impact dynamics. Incorporating this force into the discrete Lagrange-d'Alembert principle provides

$$d\bar{\mathfrak{G}}_d(\bar{q}_d) \cdot \delta\bar{q}_d + (F^{\partial C})_d(\bar{q}_{j-1}, \bar{q}_j) \cdot \delta\bar{q}_j = 0.$$

The contact force only influences the stationarity conditions resulting from variations $\delta\bar{q}_j$, that is, the discrete variational jump conditions (3.2.3) and (3.2.4). In the presence of $(F^{\partial C})_d$, these are modified as

$$i^*(D_4\bar{L}_d(\bar{q}_{j-1}, \bar{q}_j) + D_2\bar{L}_d(\bar{q}_j, \bar{q}_{j+1}) + (F_q^{\partial C})_d) = 0, \tag{3.3.1}$$

$$D_3\bar{L}_d(\bar{q}_{j-1}, \bar{q}_j) + D_1\bar{L}_d(\bar{q}_j, \bar{q}_{j+1}) + (F_t^{\partial C})_d = 0, \tag{3.3.2}$$

where $((F_t^{\partial C})_d, (F_q^{\partial C})_d)$ denote the corresponding components of $(F^{\partial C})_d$. These jump conditions maintain the structure of the continuous (2.3.1), capturing the change in system energy and momentum tangent to ∂C across the impact.

As one might expect, given the null space matrix $P_{\partial C}(q) : \mathbb{R}^{n-1} \to T_q\partial C$, we have

$$P_{\partial C}^T(q_j)\left[D_4\bar{L}_d(\bar{q}_{j-1}, \bar{q}_j) + D_2\bar{L}_d(\bar{q}_j, \bar{q}_{j+1}) + (F_q^{\partial C})_d\right] = 0, \tag{3.3.3}$$

which is equivalent to (3.3.1).

3.3.2 Holonomic Constraints

To apply a discrete contact force field to a constrained system, define $(F^{\partial R})_d : Q_e \times \mathbb{R}\times\partial R \to T^*(\mathbb{R}\times\partial R)$. This force field modifies the jump conditions (3.2.11), (3.2.12),

and (3.2.13) to provide

$$i_{\partial R}^{*}\left(D_4\bar{L}_d(\bar{q}_{j-1},\bar{q}_j)+D_2\bar{L}_d(\bar{q}_j,\bar{q}_{j+1})+(F_q^{\partial R})_d\right)=0, \tag{3.3.4}$$

$$D_3\bar{L}_d(\bar{q}_{j-1},\bar{q}_j)+D_1\bar{L}_d(\bar{q}_j,\bar{q}_{j+1})+(F_t^{\partial R})_d=0, \tag{3.3.5}$$

$$g(q_{j+1})=0. \tag{3.3.6}$$

Similar to the continuous case, these results are invariant under the substitution $(F^{\partial R})_d \to (F^{\partial C})_d$.

Given the null space matrix $P_{\partial R}(q) : \mathbb{R}^{n-m-1} \to T_q\partial R$, we have

$$P_{\partial R}^{T}(q_j)\left[D_4\bar{L}_d(\bar{q}_{j-1},\bar{q}_j)+D_2\bar{L}_d(\bar{q}_j,\bar{q}_{j+1})+(F_q^{\partial R})_d\right]=0, \tag{3.3.7}$$

which is equivalent to (3.3.4).

3.4 Perfectly Plastic Impacts

Having established the discrete variational jump conditions for lossful impacts, we turn our attention to deriving discrete dynamics for the perfectly plastic impacts of Section 2.4. The task is slightly more involved than the continuous case, largely because discrete jump conditions apply over an interval of time $[(j-1)h, jh]$ rather than an instant in time. As a result, the action from pre- and post-impact constraints may influence the jump conditions. To accurately capture this influence, we return to the discrete Lagrange-d'Alembert principle, which will be modified in accordance with the ***discrete pre- and post-impact distributions*** $\mathfrak{D}_d^-$ and $\mathfrak{D}_d^+$ on the discrete phase space $Q \times Q$.

3.4.1 Free Systems

Given S as defined in Subsection 2.4.1, we will define jump conditions connecting discrete dynamics on $\mathfrak{D}_d^- = C \times C$ and $\mathfrak{D}_d^+ = S \times S$. Recalling Remark 2.9, we will join two discrete variational principles at the impact time to provide the desired jump conditions. In preparation for this process, consider the path space $(\mathcal{M}_{ns})_d \times \mathcal{L}'_d$ where $(\mathcal{M}_{ns})_d$ is as defined before and

$$\mathcal{L}'_d = \big\{\lambda_d : \{0, 1, \ldots, (K-1), K\} \to \mathbb{R}^p\big\}.$$

Consider a modification of $(\mathcal{M}_{ns})_d \times \mathcal{L}'_d$ in which we identify 0 with j and disregard all elements $\tilde{q}_k$ if $k < j$. We will refer to this new path space as $(\mathcal{M}_{ccns})_d^+$, such that for a path $\tilde{q}_d^+ = (\bar{q}_d^+, \lambda_d^+) \in (\mathcal{M}_{ccns})_d^+$ we can identify it with its image $(t_j, q_j, \ldots, q_K, \lambda_j, \ldots, \lambda_K)$. Similarly, consider a modification to $(\mathcal{M}_{ns})_d$ in which we identify K with j and disregard all elements $\bar{q}_k$ if $k > j$. We will refer to this new path space as $(\mathcal{M}_{ns})_d^-$, such that for a path $\bar{q}_d^- = (t_d^-, q_d^-) \in (\mathcal{M}_{ns})_d^-$ we can identify it with its image $(t_j, q_0, \ldots, q_j)$. Using these modifications, we will concern ourselves with the ***combined path space*** $(\mathcal{M}_1)_d^\pm$ of the form

$$(\mathcal{M}_1)_d^\pm = \{(\bar{q}_d^-, \tilde{q}_d^+) \mid \bar{q}_d^- \in (\mathcal{M}_{ns})_d^-, \tilde{q}_d^+ \in (\mathcal{M}_{ccns})_d^+, \bar{q}_d^-(j) = \tilde{q}_d^+(j)\}.$$

Elements in this path space have the property that the impact time and configuration $\bar{q}_j = (t_j, q_j)$ is identically represented in both paths $\bar{q}_d^-$ and $\tilde{q}_d^+$. This is essentially a discrete notion of continuity when connecting these paths at the impact node.

Using the combined path space, define the ***combined discrete action*** $\tilde{\tilde{\mathfrak{G}}}_d : (\mathcal{M}_1)_d^\pm \to \mathbb{R}$ of the form

$$\tilde{\tilde{\mathfrak{G}}}_d(\bar{q}_d^-, \tilde{q}_d^+) = \sum_{k=0}^{j-1} \bar{L}_d(\bar{q}_k, \bar{q}_{k+1}) + \sum_{k=j}^{K-1} \tilde{L}_d^{g_S}(\tilde{q}_k, \tilde{q}_{k+1}),$$

where $\tilde{L}_d^{g_S}$ is the augmented discrete Lagrangian associated with the constraint g_S. This discrete action approximates the sum of the action integrals from the two variational principles we connected in the continuous case, one for unconstrained lossful collisions and one for smooth constrained systems. All that remains is to incorporate the contact force field to provide a discrete Lagrange-d'Alembert principle of the form

$$d\tilde{\tilde{\mathfrak{G}}}_d(\bar{q}_d^-, \tilde{q}_d^+) \cdot \delta(\bar{q}_d^-, \tilde{q}_d^+) + (F^{\partial C})_d(\bar{q}_{j-1}, \bar{q}_j) \cdot \delta\bar{q}_j = 0.$$

It should be apparent that results away from the impact remain unaffected. That is, the free DEL equations (3.1.3) hold for $k < j-1$ and the constrained DEL equations (3.2.6) and (3.2.7) hold on S for $k > j$. At $k = j-1$, the contact resolution equations have the form

$$D_4\bar{L}_d(\bar{q}_{j-2}, \bar{q}_{j-1}) + D_2\bar{L}_d(\bar{q}_{j-1}, \bar{q}_j) = 0, \tag{3.4.1}$$

$$q_j \in S. \tag{3.4.2}$$

Unlike the case with elastic collisions, the condition (3.4.2) is a result of stationarity. It comes from the variations $\delta\lambda_j^+$, which imply that $g_S(q_j) = 0$.

Remark 3.6: *Frequently, the post-impact constraint g_S is not known a priori; it is determined by the impact configuration q_j. In these cases, the contact resolution conditions* (3.2.1) *and* (3.2.2) *may be substituted for* (3.4.1) *and* (3.4.2) *and solved for (t_j, q_j), which will define g_S and S. Deriving g_S from q_j implies that* (3.4.2) *will automatically be satisfied.*

Finally, the discrete variational jump conditions at $k = j$ are

$$i^*\Bigg(D_4\bar{L}_d(\bar{q}_{j-1},\bar{q}_j) + D_2\bar{L}_d(\bar{q}_j,\bar{q}_{j+1}) \\ -\frac{1}{2}(t_{j+1}-t_j)\left(\frac{dg_S}{dq}\Big|_{q_j}\right)^T\cdot\lambda_j + (F_q^{\partial C})_d\Bigg) = 0, \tag{3.4.3}$$

$$D_3\bar{L}_d(\bar{q}_{j-1},\bar{q}_j) + D_1\bar{L}_d(\bar{q}_j,\bar{q}_{j+1}) + (F_t^{\partial C})_d = 0, \tag{3.4.4}$$

$$g_S(q_{j+1}) = 0. \tag{3.4.5}$$

As in the continuous case, we view the condition (3.4.5) as a constraint on the allowable force fields $(F^{\partial C})_d$.

The constraint term that appears in (3.4.3) may seem out of place considering that the continuous parallel of that equation is the momentum component of (2.3.1). In fact, this term is the reason for developing the Lagrange-d'Alembert principle above rather than using the existing lossful collision results (3.3.1) and (3.3.2). Since the discrete variational jump conditions result from stationarity of the action sum over intervals of time, the work of the constraint forces associated with g_S over the time interval $[t_j, jh]$ must be accounted for.

To derive a discrete version of the impact model (2.4.3) that will satisfy the discrete variational jump conditions above, first consider the discretization of (2.4.1). This takes the form

$$D_4\bar{L}_d(\bar{q}_{j-1},\bar{q}_j) + D_2\bar{L}_d(\bar{q}_j,\bar{q}_{j+1}) - \frac{1}{2}(t_{j+1}-t_j)\left(\frac{dg_S}{dq}\Big|_{q_j}\right)^T\cdot\lambda_j + F_d^C = 0, \tag{3.4.6}$$

where $F_d^C : C\times C \to T^*C$ has been substituted for our common notion of a discrete contact force field. As we did in the continuous setting, consider

$$F_d^C = \left(\frac{\partial g_S}{\partial q}\right)^T\cdot\lambda^C,$$

such that (3.4.6) reduces to

$$D_4\bar{L}_d(\bar{q}_{j-1},\bar{q}_j) + D_2\bar{L}_d(\bar{q}_j,\bar{q}_{j+1}) + \left(\frac{dg_S}{dq}\Big|_{q_j}\right)^T \cdot \left(\lambda^C - \frac{1}{2}(t_{j+1}-t_j)\lambda_j\right) = 0.$$

This condition, in conjunction with $g_S(q_{j+1})$, provides an underdetermined system in the variables q_{j+1}, λ_j, and λ^C. This is representative of our inability to distinguish any difference between impact forces λ^C and constraint forces λ_j in the present model. Given a null space matrix $P_S(q) : \mathbb{R}^{n-p} \to T_qS$, we overcome this difficulty by using

$$P_S^T(q_j)\left[D_4\bar{L}_d(\bar{q}_{j-1},\bar{q}_j) + D_2\bar{L}_d(\bar{q}_j,\bar{q}_{j+1})\right] = 0, \tag{3.4.7}$$

$$g_S(q_{j+1}) = 0, \tag{3.4.8}$$

which is a set of n equations, presumably solvable for q_{j+1}.

As was the case with solutions of the continuous (2.4.3), though the impact model using (3.4.7) and (3.4.8) was not derived with a variational principle, it does constitute a solution to the variational jump conditions (3.4.3), (3.4.4), and (3.4.5). This is presuming we plug solutions q_{j+1} of (3.4.7) and (3.4.8) into (3.4.3) and (3.4.4) to define $(F^{\partial C})_d$.

3.4.2 Holonomic Constraints

Given U as defined in Subsection 2.4.2, we will define jump conditions connecting discrete dynamics on $\mathfrak{D}_d^- = R\times R$ and $\mathfrak{D}_d^+ = U\times U$. Using the same approach as in the previous subsection, consider a modification of $(\mathcal{M}'_{ccns})_d$ in which we identify K with j and disregard all elements $\tilde{q}_k$ if $k > j$. We will refer to this new path space as $(\mathcal{M}'_{ccns})_d^-$, such that for a path $\tilde{q}_d^- = (\bar{q}_d^-, \lambda_d^-) \in (\mathcal{M}'_{ccns})_d^-$ we can identify it with its image $(t_j, q_0, \ldots, q_j, \lambda_0, \ldots, \lambda_{j-1}, \lambda_j^-)$. Similarly, consider a modification to $(\mathcal{M}'_{ns})_d \times \mathcal{L}'_d$ in which we identify 0 with j and disregard all elements $\tilde{q}_k$ if $k < j$. We will refer to this

new path space as $(\mathcal{M}'_{ccns})^+_d$, such that for a path $\tilde{q}^+_d = (\bar{q}^+_d, \lambda^+_d) \in (\mathcal{M}'_{ccns})^+_d$ we can identify it with its image $(t_j, q_j, \ldots, q_k, \lambda^+_j, \lambda_{j+1}, \ldots, \lambda_K)$. Using these modifications, we will concern ourselves with the ***combined path space*** $(\mathcal{M}_2)^\pm_d$ of the form

$$(\mathcal{M}_2)^\pm_d = \{(\tilde{q}^-_d, \tilde{q}^+_d) \mid \tilde{q}^-_d \in (\mathcal{M}'_{ccns})^-_d, \tilde{q}^+_d \in (\mathcal{M}'_{ccns})^+_d, \bar{q}^-_d(j) = \bar{q}^+_d(j)\}.$$

Elements of this path space have Lagrange multipliers $\lambda_k \in \mathbb{R}^m$ for $k < j$ and $\lambda_k \in \mathbb{R}^p$ for $k > j$. At $k = j$, there exists one of each type, $\lambda^-_k \in \mathbb{R}^m$ and $\lambda^+_k \in \mathbb{R}^p$.

Using the combined path space, define the ***combined discrete action*** $\tilde{\tilde{\mathfrak{G}}}_d : (\mathcal{M}_2)^\pm_d \to \mathbb{R}$ of the form

$$\tilde{\tilde{\mathfrak{G}}}_d(\tilde{q}^-_d, \tilde{q}^+_d) = \sum_{k=0}^{j-1} \tilde{L}^g_d(\tilde{q}_k, \tilde{q}_{k+1}) + \sum_{k=j}^{K-1} \tilde{L}^{g_U}_d(\tilde{q}_k, \tilde{q}_{k+1}),$$

where $\tilde{L}^g_d$ and $\tilde{L}^{g_U}_d$ are the augmented discrete Lagrangians associated with g and g_U, respectively. This discrete action approximates the sum of the action integrals from the two variational principles we joined in the continuous case, one for constrained lossful collisions and one for smooth constrained systems. Similar to Subsection 3.4.1, the discrete Lagrange-d'Alembert principle takes the form

$$d\tilde{\tilde{\mathfrak{G}}}_d(\tilde{q}^-_d, \tilde{q}^+_d) \cdot \delta(\tilde{q}^-_d, \tilde{q}^+_d) + (F^{\partial R})_d(\bar{q}_{j-1}, \bar{q}_j) \cdot \delta\bar{q}_j = 0.$$

This principle implies that the constrained DEL equations (3.2.6) and (3.2.7) hold on N for $k < j - 1$ and again on U for $k > j$.

At $k = j - 1$, the contact resolution equations have the form

$$D_4\bar{L}_d(\bar{q}_{j-2}, \bar{q}_{j-1}) + D_2\bar{L}_d(\bar{q}_{j-1}, \bar{q}_j) = \frac{1}{2}(t_j - t_{j-2}) \left(\frac{dg}{dq}\Big|_{q_{j-1}} \right)^T \cdot \lambda_{j-1}, \tag{3.4.9}$$

$$g(q_j) = 0, \tag{3.4.10}$$

$$q_j \in U. \tag{3.4.11}$$

Note that the condition (3.4.10) is redundant as (3.4.11) implies $g(q_j) = 0$ by the property $U \subseteq \partial R \subset R \subset N$.

Lastly, the discrete variational jump conditions at $k = j$ are

$$i^*_{\partial R}\Bigg(D_4\bar{L}_d(\bar{q}_{j-1}, \bar{q}_j) + D_2\bar{L}_d(\bar{q}_j, \bar{q}_{j+1}) - \frac{1}{2}(t_j - t_{j-1}) \left(\frac{dg}{dq}\Big|_{q_j} \right)^T \cdot \lambda_j^- - \frac{1}{2}(t_{j+1} - t_j) \left(\frac{dg_U}{dq}\Big|_{q_j} \right)^T \cdot \lambda_j^+ + (F_q^{\partial R})_d \Bigg) = 0, \tag{3.4.12}$$

$$D_3\bar{L}_d(\bar{q}_{j-1}, \bar{q}_j) + D_1\bar{L}_d(\bar{q}_j, \bar{q}_{j+1}) + (F_t^{\partial R})_d = 0, \tag{3.4.13}$$

$$g_U(q_{j+1}) = 0. \tag{3.4.14}$$

As in the continuous case, we view the condition (3.4.14) as a constraint on the allowable force fields $(F^{\partial R})_d$.

The first of the two constraint terms that appears in (3.4.12) is negligible as a result of

$$i^*_{\partial R}\left(-\frac{1}{2}(t_j - t_{j-1}) \left(\frac{dg}{dq}\Big|_{q_j} \right)^T \cdot \lambda_j^- \right) = 0.$$

The second of the two constraint terms presents the same challenges as the constraint associated with g_S in (3.4.3). We treat it similarly.

Consider the adaptation of (3.4.6) to the constrained case with the form

$$D_4\bar{L}_d(\bar{q}_{j-1},\bar{q}_j)+D_2\bar{L}_d(\bar{q}_j,\bar{q}_{j+1})-\frac{1}{2}(t_j-t_{j-1})\left(\frac{dg}{dq}\Big|_{q_j}\right)^T\cdot\lambda_j^- \\ -\frac{1}{2}(t_{j+1}-t_j)\left(\frac{dg_U}{dq}\Big|_{q_j}\right)^T\cdot\lambda_j^+ + F_d^R=0, \quad (3.4.15)$$

where $F_d^R : R\times R\to T^*R$ has been substituted for our common notion of a discrete contact force field. One way to handle the pre-impact constraint term, which follows the methods for discrete Hamiltonian systems with constraints in [68], is to apply the projection $Q_N(q) : T_q^*Q \to \eta_N(T_q^*N)$ to produce

$$Q_N(q_j)\cdot D_4\bar{L}_d(\bar{q}_{j-1},\bar{q}_j)+D_2\bar{L}_d(\bar{q}_j,\bar{q}_{j+1})-\frac{1}{2}(t_{j+1}-t_j)\left(\frac{dg_U}{dq}\Big|_{q_j}\right)^T\cdot\lambda_j^+ + F_d^R=0.$$

This projection is justified with the argument that the pre-impact right discrete momentum should lie in T^*N. If this is true, it holds

$$D_4\bar{L}_d(\bar{q}_{j-1},\bar{q}_j)-\frac{1}{2}(t_j-t_{j-1})\left(\frac{dg}{dq}\Big|_{q_j}\right)^T\cdot\lambda_j^- = Q_N(q_j)\cdot D_4\bar{L}_d(\bar{q}_{j-1},\bar{q}_j),$$

and thus substitution into (3.4.15) is appropriate.

At this point, we follow the treatment shown in Subsection (3.4.1). That is, we assume

$$F_d^R=\left(\frac{\partial g_U}{\partial q}\right)^T\cdot\lambda^R,$$

such that (3.4.15) further reduces to

$$Q_N(q_j)\cdot D_4\bar{L}_d(\bar{q}_{j-1},\bar{q}_j)+D_2\bar{L}_d(\bar{q}_j,\bar{q}_{j+1})+\left(\frac{dg_U}{dq}\Big|_{q_j}\right)^T\cdot\left(\lambda^R-\frac{1}{2}(t_{j+1}-t_j)\lambda_j^+\right)=0.$$

Using the null space matrix $P_U(q) : \mathbb{R}^{n-p}\to T_qU$ and appending the condition

$g_U(q_{j+1}) = 0$, we have the constrained version of (3.4.7) and (3.4.8) as

$$P_U^T(q_j)\left[Q_N(q_j)\cdot D_4\bar{L}_d(\bar{q}_{j-1},\bar{q}_j) + D_2\bar{L}_d(\bar{q}_j,\bar{q}_{j+1})\right] = 0, \tag{3.4.16}$$

$$g_U(q_{j+1}) = 0. \tag{3.4.17}$$

These n equations constitute a set of sequential projections, presumably solvable for q_{j+1}. First, the pre-impact discrete momentum is restricted to T^*N according to the pre-impact constraint. Second, the jump condition's entire momentum balance is projected onto T^*U as all pre-impact momentum outside of this space will be annihilated by the impact.

The impact model (3.4.16) and (3.4.17) constitutes a solution to the variational jump conditions (3.4.12), (3.4.13) and (3.4.14). Inserting solutions q_{j+1} into (3.4.3) and (3.4.4) recovers the $(F^{\partial R})_d$ that defines this model.

3.5 Transition of Constraints

Lastly, we provide a discrete model for the transition of constraints described in Section 2.5. As in Subsection 3.4.1, we will use S such that $\mathfrak{D}_d^+ = S \times S$. We permit $\mathfrak{D}_d^+ \nsubseteq R \times R$ since the constraint g associated with R will not be enforced following impact. As in the elastic and perfectly plastic cases for constrained systems, $\mathfrak{D}_d^- = R \times R$.

We will retain the combined path space $(\mathcal{M}_2)_d^{\pm}$ as well as the combined discrete action $\tilde{\tilde{\mathfrak{G}}}_d : (\mathcal{M}_2)_d^{\pm} \to \mathbb{R}$, although now enforcing g_S post-impact rather than g_U. In accordance with $\mathfrak{D}_d^- = R \times R$, the constrained DEL equations (3.2.6) and (3.2.7) hold on N for $k < j-1$. At $k = j-1$, the contact resolution equations have the form of (3.4.9) and (3.4.10), but with $q_j \in S$ in place of (3.4.11).

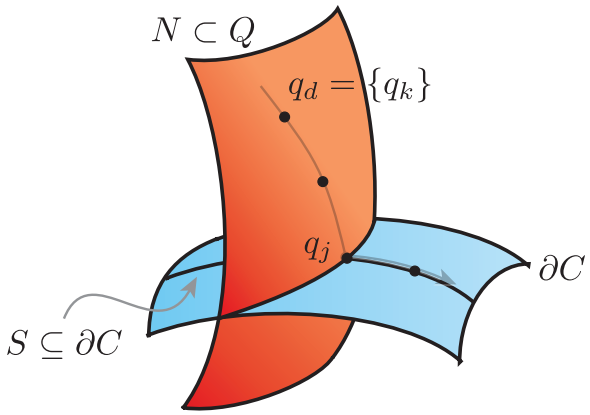

Figure 3.3: A discrete path q_d capturing a transition of constraints using discrete variational jump conditions.

The discrete variational jump conditions at $k = j$ are

$$i^*_{\partial R}\Bigg(D_4\bar{L}_d(\bar{q}_{j-1},\bar{q}_j) + D_2\bar{L}_d(\bar{q}_j,\bar{q}_{j+1}) - \frac{1}{2}(t_j - t_{j-1})\left(\frac{dg}{dq}\Big|_{q_j}\right)^T \cdot \lambda_j^- \\ -\frac{1}{2}(t_{j+1} - t_j)\left(\frac{dg_S}{dq}\Big|_{q_j}\right)^T \cdot \lambda_j^+ + (F_q^{\partial R})_d\Bigg) = 0, \quad (3.5.1)$$

$$D_3\bar{L}_d(\bar{q}_{j-1},\bar{q}_j) + D_1\bar{L}_d(\bar{q}_j,\bar{q}_{j+1}) + (F_t^{\partial R})_d = 0, \quad (3.5.2)$$

$$g_S(q_{j+1}) = 0, \quad (3.5.3)$$

which mirrors (3.4.12), (3.4.13), and (3.4.14) but with S in place of U. Figure 3.3 depicts a discrete path subject to the transition of constraints model above.

Using Subsection (3.4.2)'s arguments, one impact model that satisfies the jump conditions above is

$$P_S^T(q_j)\left[Q_N(q_j)\cdot D_4\bar{L}_d(\bar{q}_{j-1},\bar{q}_j) + D_2\bar{L}_d(\bar{q}_j,\bar{q}_{j+1})\right] = 0, \quad (3.5.4)$$

$$g_S(q_{j+1}) = 0. \quad (3.5.5)$$

As with the continuous jump conditions (2.4.3), this model initializes the post-impact

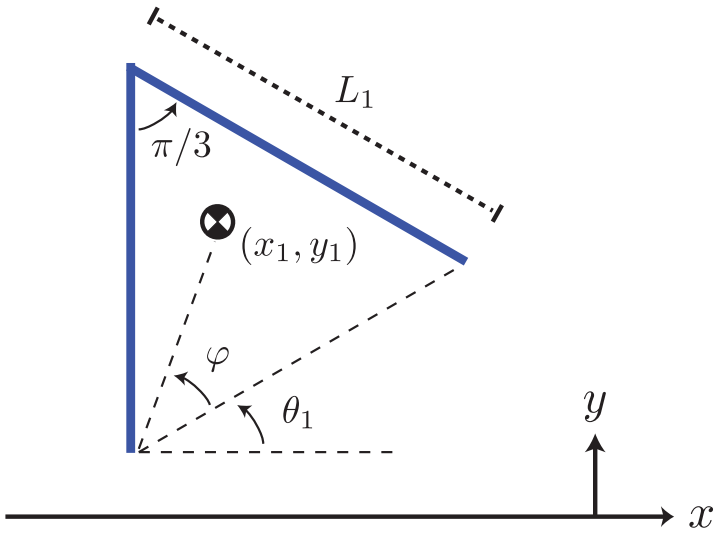

Figure 3.4: A simple rigid body wedge model.

discrete momenta at zero in all directions normal to R. Upon implementing this model or any other that meets the condition $(q_j, q_{j+1}) \in \mathfrak{D}_d^+ = S \times S$, the system obeys the constrained DEL equations (3.2.6) and (3.2.7) on S for $k > j$.

3.5.1 Variational Collision Integration Example

The discrete dynamics in the previous subsection provide a variational collision integrator (VCI) for the transition of constraints behavior. Since this VCI will be utilized for modeling bipedal robots in the subsequent Chapters 4 and 5, here we examine an example of its usage. Specifically, the behavior of the rigid body wedge pictured in Figure 3.4 undergoing a transition of constraints is captured with the VCI and compared with a benchmark simulation.

The free configuration space Q for the wedge is 3-dimensional with coordinates (x_1, y_1, θ_1). Note that the angle φ pictured in the model is just a relevant constant, $\varphi = \arctan(\sqrt{3}/2)$. Physically we model the wedge in frictional contact with the line $y = 0$, first with its left "foot" and then transitioning to its right "foot." Geometrically,

this means that prior to impact the wedge evolves on

$$R = \left\{ q \,\middle|\, x_1 - \sqrt{\frac{7}{16}} L_1 \cos(\theta + \varphi) = 0,\, y_1 - \sqrt{\frac{7}{16}} L_1 \sin(\theta + \varphi) = 0,\, \theta_1 \geq 0 \right\}.$$

Presuming a clockwise rotation, the wedge eventually reaches the boundary ∂R where $\theta_1 = 0$. After undergoing the transition of constraints the system evolves on

$$S = \left\{ q \,\middle|\, x_1 + \sqrt{\frac{7}{16}} L_1 \cos(\theta - \varphi) - L_1 = 0,\, y_1 + \sqrt{\frac{7}{16}} L_1 \sin(\theta - \varphi) = 0 \right\}.$$

The Lagrangian for this system has the form $L(q, \dot{q}) = \dot{q}^T M \dot{q} - V(q)$, where M is the diagonal 3×3 mass matrix defining the system's kinetic energy and $V(q)$ is the gravitational potential energy. Using m to signify the total mass of the wedge and assuming the rods that compose the wedge are isotropic and infinitely thin, the diagonal elements of M are $(m,\, m,\, J)$ where

$$J = \frac{13}{48} m L_1^2.$$

The potential energy of the wedge is $V(q) = mgy_1$, where g is the gravitational constant. In simulation, the following parameter values were used: $m = 2$ kg, $L_1 = 0.2$ m, and $g = 9.81$ m/s^2.

For the purpose of comparison with VCI, a benchmark simulation was produced by taking an analytical solution to the continuous time jump conditions (2.4.3) and integrating the pre-impact phase backward in time and the post-impact phase forward in time. This practice of patching intervals of smooth integration together with analytical jump conditions is representative of the hybrid systems approach for nonsmooth systems [41, 4]. For the smooth patches of integration, the benchmark simulation utilized the variational Störmer-Verlet method with a timestep of $h = (t_{k+1} - t_k) = 4 \times 10^{-4}$ s. Though the choice is not unique [68], one discrete

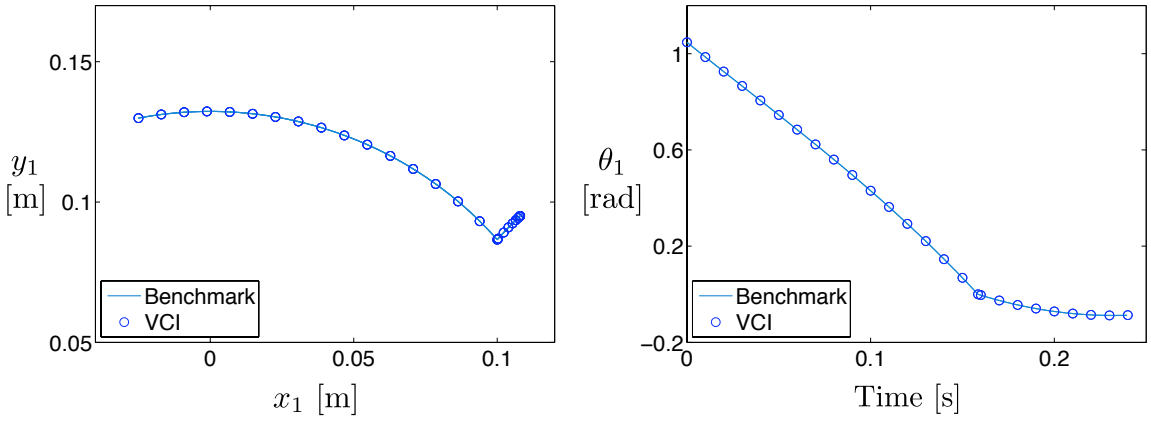

Figure 3.5: Evolution of the wedge's center of mass in the plane (left) and orientation over time (right) for the benchmark and VCI simulations.

Lagrangian that produces Störmer-Verlet is

$$L_d(q_k, q_{k+1}) = \frac{t_{k+1} - t_k}{2}\left(L\left(q_k, \frac{q_{k+1} - q_k}{t_{k+1} - t_k}\right) + L\left(q_{k+1}, \frac{q_{k+1} - q_k}{t_{k+1} - t_k}\right)\right).$$

The VCI simulation utilized this same discrete Lagrangian, but was initialized at $t = 0$ rather than the contact time. The VCI simulation used a timestep of $h = 1 \times 10^{-2}$.

Position and orientation results comparing the simulations are shown in Figure 3.5. Initially evolving on R, the VCI detected an inadmissible configuration with $\theta_1 < 0$ after the sixteenth timestep. Thus, the integrator set $j = 16$ and solved for $q_j \in \partial R$ (with $\theta_1 = 0$) and $t_j = 0.158$ s. This evaluation of the collision time matches that used by the benchmark within 3.75×10^{-5} s. Using the jump conditions (3.5.4), (3.5.5), the VCI determined the first post impact configuration $q_{j+1} \in S$ and then continued integration on S where $\theta_1 < 0$ is permitted. It should be noted that even with the use of a larger timestep in the smooth regimes and adaptive timestepping through the collision, the VCI closely matches the behavior determined by the benchmark simulation. This matching behavior is further supported by the energy plot in Figure 3.6. The change in the discrete energy of the VCI simulation through the jump

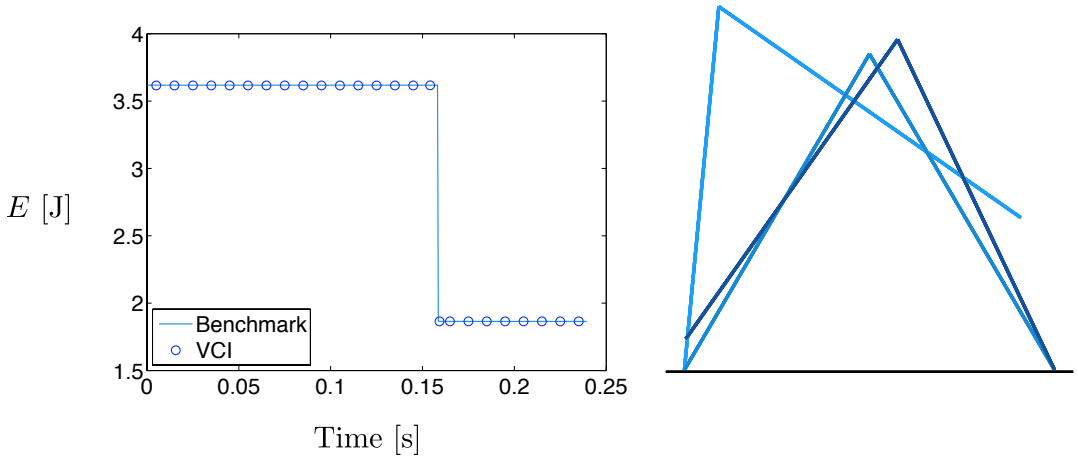

Figure 3.6: Energy behavior and snapshots of the wedge progressing through a transition of constraints. The VCI accurately captures the loss in kinetic energy resulting from collision. The slowing of the system is reflected in the snapshots, which have been taken from the VCI simulation at even 0.06 s intervals.

conditions, $(F_t^{\partial R})_d$, matches the benchmark's analytical solution within 1.41×10^{-3} percent error.

A final note is made regarding post-processing steps for the VCI simulation. Since holonomic constraints have been used to model frictional contacts, it must be checked that all contacts have been accounted for and only feasible contacts have been simulated. For the model above, the wedge is a single rigid body and there is only one contact surface in the plane. Hence, there is only one type of contact, rigid body to surface, which has been accounted for in all instances. In terms of feasibility, it must be checked that the unconstrained acceleration of any points of contact are persistently "into" the contact surface, the frictional constraint forces tangential to the contact surface fall within some physically realizable bounds, and at no point has the paradox of Painlevé [85] been encountered. For the simple wedge, no red flags were raised in post-processing. Note that if a simulation fails one of these post-processing checks it does not stonewall the VCI method. It simply implies an additional behavior, a collision or perhaps a constraint release, must be added to the model.

Chapter 4

Discrete Nonsmooth Mechanics and Optimal Control

In this chapter, we extend the structured integration results of Chapter 3 to generate optimal controls for nonsmooth mechanical systems. Optimal control generation is done according to the method of discrete mechanics and optimal control (DMOC) [47, 48, 51, 62, 52], which relies on variational integrators to discretize standard optimal control problems. After a review of DMOC for smooth systems, we describe the modifications necessary to incorporate nonsmooth impact mechanics. The nonsmooth version of DMOC is demonstrated in the task of determining locally optimal gaits for bipedal robot models.

4.1 The DMOC Method

First introduced in [47], the DMOC method uses discrete mechanics to recast standard optimal control problems in discrete time. The discretized problem has the structure of an equality-constrained nonlinear optimization problem and is solvable with sequential quadratic programming (SQP) methods [36].

4.1.1 Smooth Systems

In the traditional case for DMOC we assume we are dealing with smooth mechanical systems as in Section 2.1, and thus inherit the definitions of Q, TQ, and L from that section. The continuous time optimal control problem solved by DMOC seeks the local minima of a cost function J while using controls $u : \mathbb{R} \to T^*Q$ to move the mechanical system from a given initial phase $(q^0, \dot{q}^0)$ to a given final phase $(q^T, \dot{q}^T)$ in a specified time T. It is assumed that J is the integral of a performance metric $Z : \Delta \to \mathbb{R}$ where

$$\Delta = \big\{((q_1, v_1), (q_2, u_2)) \in TQ \times T^*Q \,|\, q_1 = q_2\big\}.$$

For brevity we write elements of Δ excluding the redundant coordinate in Q. Using this notation the optimal control problem is formally stated

$$\text{Minimize } J(q(t), u(t)) = \int_0^T Z(q(t), \dot{q}(t), u(t))\, dt,$$

subject to $(q(0), \dot{q}(0)) = (q^0, \dot{q}^0)$, $(q(T), \dot{q}(T)) = (q^T, \dot{q}^T)$, and the appropriate forced Euler-Lagrange equations of motion. Treating u as an external force field F_q, the system dynamics have precisely the form of (2.1.16).

Using the machinery from 3.1, the DMOC method moves all aspects of the problem above to the discrete time setting. That is, $q(t)$ is replaced by a discrete path $q_d \in \mathcal{Q}_d(Q)$ and the influence of $u(t)$ is captured with $u_d = \{u_k^{\pm}\}$, a discrete path of left and right discrete forces $u_k^{\pm} : Q \times Q \to T^*Q$ at each time node. Similar to the discrete forces $F_d^{\pm}$ defined in Subsection 3.1.3, the $u_k^{\pm}$ provide the approximation

$$u_k^- \cdot \delta q_k + u_k^+ \cdot \delta q_{k+1} \approx \int_{t_k}^{t_{k+1}} u(t) \cdot \delta q(t)\, dt.$$

The boundary conditions $(q^0, \dot{q}^0)$ and $(q^T, \dot{q}^T)$ are discretized through a combina-

tion of continuous and discrete Legendre transformations. Following the treatment in [47], we make use of the ***standard Legendre transformation*** $\mathbb{F}L : TQ \to T^*Q$ defined as

$$\mathbb{F}L(q, \dot{q}) = (q, D_2L(q, \dot{q})),$$

as well as the ***left and right discrete Legendre transforms*** $\mathbb{F}^{u\pm}L_d : Q \times Q \to T^*Q$ defined as

$$\mathbb{F}^{u+}L_d(q_k, q_{k+1}) = (q_{k+1}, D_2L_d(q_k, q_{k+1}) + u_k^+),$$
$$\mathbb{F}^{u-}L_d(q_k, q_{k+1}) = (q_k, -D_1L_d(q_k, q_{k+1}) - u_k^-).$$

With these definitions, we enforce the boundary conditions at the momentum level (in T^*Q) as

$$(q^0, D_2L(q^0, \dot{q}^0)) = (q_0, -D_1L_d(q_0, q_1) - u_0^-), \tag{4.1.1}$$
$$(q^T, D_2L(q^T, \dot{q}^T)) = (q_K, D_2L_d(q_{K-1}, q_K) + u_{K-1}^+). \tag{4.1.2}$$

For a discrete time approximation of J, we follow the same method by which we approximated the action map $\bar{\mathfrak{G}}$ with $\bar{\mathfrak{G}}_d$ in Subsection 3.1.1. That is, we introduce a discrete performance metric $Z_d : T^*Q \times T^*Q \to \mathbb{R}$ providing the approximation

$$Z_d(q_k, u_k^-, q_{k+1}, u_k^+) \approx \int_{t_k}^{t_{k+1}} Z(q(t), \dot{q}(t), u(t))\, dt.$$

Using Z_d we approximate J with a discrete cost function J_d and state the discretized optimal control problem:

$$\text{Minimize } J_d(q_d, u_d) = \sum_{k=0}^{N-1} Z_d(q_k, u_k^-, q_{k+1}, u_k^+),$$

subject to (4.1.1), (4.1.2), and the appropriate forced DEL equations of motion. Treating $u_k^{\pm}$ as a discrete external force field $(F_q)_d^{\pm}$, the system dynamics have precisely the form of (3.1.10). As mentioned, this discretized problem is an equality-constrained nonlinear optimization problem and can be solved using SQP.

4.1.2 Nonsmooth Systems

In this subsection, we extend the DMOC method to handle systems with collisions. To simplify the process, we assume advanced knowledge of the number of collisions N_c to take place in the time interval $[0, T]$, the set of collision times $\{t_\ell\}$ where $\ell \in \{1, \ldots, N_c\}$, and the desired collision model (elastic, lossful, perfectly plastic) to be enforced at each t_ℓ.

Remark 4.1: *Generalizing the following method to problems with a variable number of collisions, variable collision times, or variable collision models could be achieved with the use of dynamic programming, but remains outside the scope of this thesis.*

The search for optimal trajectories will only be performed in the space of admissible configurations, giving rise to the constraint $q(t) \in C$ for all $t \in [0, T]$. Furthermore, we require that at the collision times t_ℓ, the corresponding system configuration is on the contact set ∂C. We express this constraint as $g_{\partial C}(q(t_\ell)) = 0$ for all $\ell \in \{1, \ldots, N_c\}$.

Using the assumptions and constraint definitions above, we modify the continuous time optimal control problem as

$$\text{Minimize } J(q(t), u(t)) = \int_0^T Z(q(t), \dot{q}(t), u(t))\, dt,$$

subject to $(q(0), \dot{q}(0)) = (q^0, \dot{q}^0)$, $(q(T), \dot{q}(T)) = (q^T, \dot{q}^T)$, the appropriate forced Euler-Lagrange equations of motion, $q(t) \in C$ for all $t \in [0, T]$, $g_{\partial C}(q(t_\ell)) = 0$ for all $\ell \in \{1, \ldots, N_c\}$, and the appropriate variational jump conditions at each t_ℓ.

All of the elements of this optimization problem held in common with the problem for smooth systems are discretized in the same fashion as in the previous subsection. To handle the collisions, we require that the mesh of time has been defined such that each t_ℓ has an associated time node t_k. In this case, we discretize the admissibility constraint $q(t) \in C$ as $g_{\partial C}(q_k) \geqslant 0$ for all $k \in \{0, \ldots, K\}$ and the contact conditions $q(t_\ell) \in \partial C$ as $g_{\partial C}(q_k) = 0$ for all $k \in \{k \,|\, t_k = t_\ell, \ell \in \{1, \ldots N_c\}\}$. Additionally, we enforce the discrete variational jump conditions associated with the appropriate collision model at each t_k associated with some t_ℓ. These discrete variational jump conditions replace the forced DEL equations at these nodes.

As a final note, we mention that in practice the added constraints for the nonsmooth case, both equality and inequality, do not change the solution method. The nonsmooth version of DMOC is still solvable with SQP.

Remark 4.2: *Though it is not regularly stated, admissibility constraints similar to* $g_{\partial C}(q_k) \geqslant 0$ *are frequently used in DMOC for smooth systems to prevent mass intersection and other physical impossibilities.*

Remark 4.3: *The variational jump conditions presented in Chapter 3 were absent of external forcing. To accurately capture the influence of the control forces* u *through collisions, one simply extends the theory of Subsection 3.1.3 to the nonsmooth cases in Sections 3.2, 3.3, 3.4, and 3.5.*

4.2 Optimal Gait Search for Bipedal Robots

In this section, we describe a specific usage of the DMOC method for nonsmooth systems in regards to bipedal robot models. Results are presented for two 4-link rigid body biped models, a six-degree-of-freedom planar model and an eleven-degree-of-freedom model in three dimensions.

4.2.1 Bipedal Gait Optimization Problem

In this specific application of the DMOC method, we seek locally optimal periodic gaits for a given biped model. The cost function we will locally minimize is the ***specific cost of transport*** [30], a standard metric in locomotion problems defined as

$$\eta = \int_0^T \frac{P_{\text{control}}}{W_{\text{robot}} \cdot V_{\text{fwd}}} dt,$$

where P_{control} is the instantaneous power exerted by the control forces, W_{robot} is the total weight of the robot, and V_{fwd} is the forward velocity of the center of mass. In our analysis to come, we will assume T is the period of a single step. This means we can recast the integral form above as

$$\eta = \frac{E_{\text{control}}}{W_{\text{robot}} \cdot L_{\text{step}}},$$

where E_{control} is the energy exerted by the control forces over the course of a step and L_{step} is the length of the step. Note that the cost η is dimensionless (the numerator units are J, and the denominator is in N $\times$ m). It should be apparent that the dependence of η on $q(t)$, $\dot{q}(t)$, and $u(t)$ follows the structure specified in the definition of J, and thus setting $J = \eta$ is permitted.

In order to search for periodic gaits, the notion of specified boundary conditions $(q^0, \dot{q}^0)$ and $(q^T, \dot{q}^T)$ is replaced with a ***periodicity relation*** $\rho : TQ \to TQ$ such that $(q(T), \dot{q}(T)) = \rho(q(0), \dot{q}(0))$. Noting that the stance leg of a bipedal robot switches over the course of one step, defining ρ usually entails rearranging information in the generalized coordinate system. For instance, the initial position and velocity of the knee joint on a robot's "right" leg will depend on the final position and velocity of the knee joint on the robot's "left" leg. The configuration component of ρ can be used to define a discrete periodicity relation $\rho_d : Q \times Q \to Q \times Q$ such that

$(q_{K-1}, q_K) = \rho_d(q_0, q_1)$.

We will assume the trajectory defining the periodic gait has a single collision ($N_c = 1$), which we will model using the transition of constraints jump conditions defined in Section 2.5. Given that trajectories are periodic and contain only a single collision per period, the choice of the collision time t_ℓ is somewhat arbitrary. In particular, the solution (q_d, u_d) for a given choice of t_ℓ can be shifted in time to provide a solution for other choices $t_\ell + ah \in [0, T]$, where $a \in \mathbb{Z}$. Furthermore, changing t_ℓ by an increment other than ah may slightly change results, but not the underlying continuous trajectory they represent.

4.2.2 4-Link Planar Biped Results

This subsection provides results from an optimal gait search for the planar biped model shown in Figure 4.1. The free configuration space Q for this model is six-dimensional with coordinates $(x_1, y_1, \theta_1, \theta_2, \theta_3, \theta_4)$. Physically, this model has point feet and walks along the flat line $y = 0$ in the plane. In the geometric terms of Section 2.5, this means that prior to impact the system evolves on

$$R = \{q \,|\, x_1 = 0,\, y_1 = 0,\, y_1 + L_1(c_1 - c_{123}) + L_2(c_{12} - c_{1234}) \geq 0\},$$

where we have introduced the shorthand $c_1 = \cos(\theta_1)$, $c_{12} = \cos(\theta_1 + \theta_2)$, $c_{123} = \cos(\theta_1 + \theta_2 + \theta_3)$, and $c_{1234} = \cos(\theta_1 + \theta_2 + \theta_3 + \theta_4)$. The manifold R is the set of configurations where the position of one point foot is fixed on the contact surface $y = 0$ and the height of the other point foot is positive (above the contact surface). At the double-support phase, in which both point feet are on the contact surface, we have $q \in \partial R$ where

$$\partial R = \{q \,|\, x_1 = 0,\, y_1 = 0,\, y_1 + L_1(c_1 - c_{123}) + L_2(c_{12} - c_{1234}) = 0\}.$$

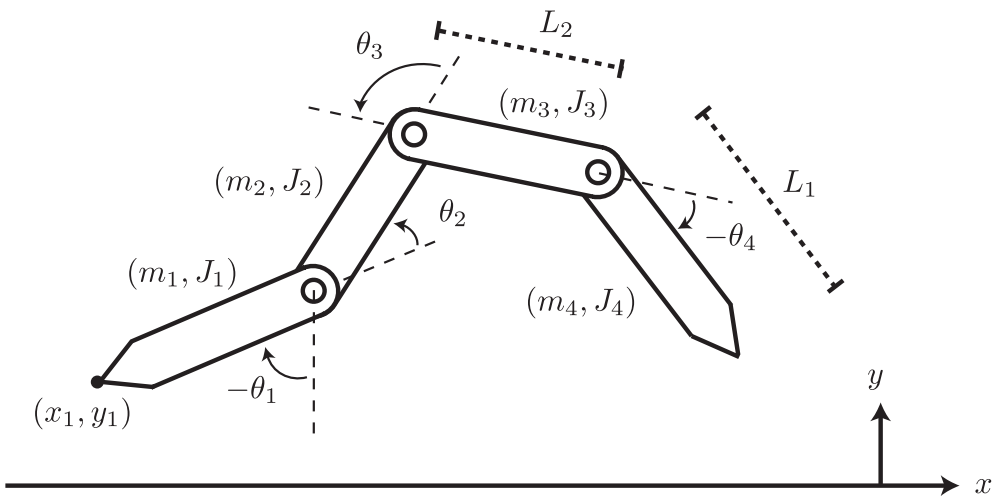

Figure 4.1: A 4-link planar biped model.

Following impact, the biped has established a new stance foot and evolves on

$$S = \{q \,|\, x_1 + L_1(s_{123} - s_1) + L_2(s_{1234} - s_{12}) - L_{\text{step}} = 0,$$
$$y_1 + L_1(c_1 - c_{123}) + L_2(c_{12} - c_{1234}) = 0\},$$

where we have abbreviated sine in the same fashion as cosine above.

The constant L_{step} in the definition of S indicates the step length of the robot during the double-support phase. While the DMOC framework permits changes in this variable, for simplicity during the optimization it has been fixed at 0.56 m. The remaining parameters in the model have been fixed in the optimization as $L_1 = L_2 =$ 0.5 m, $m_1 = m_4 = 2$ kg, $m_2 = m_3 = 3$ kg, $J_1 = J_4 = \frac{1}{24} m_1 L_1^2$, $J_2 = J_3 = \frac{1}{24} m_2 L_2^2$. Note that the moments of inertia, as defined, indicate an assumption of anisotropism for the links (they have higher mass density towards their center). Finally, the period of the step is fixed at $T = 0.9$ s and is represented in discrete time with $K = 80$ timesteps.

The Lagrangian for this system has a similar form as that of the example in

Subsection 3.5.1. That is, $L(q, \dot{q}) = \dot{q}^T M(q)\dot{q} - V(q)$ where $\dot{q}^T M(q)\dot{q}$ is the kinetic energy of the system and $V(q)$ is the gravitational potential energy. In this case, closed form expressions for $M(q)$ and $V(q)$ have a significant level of complexity. For this reason, for the implementation of DMOC, calculations of L and its partial derivatives were performed using the tree structure framework of [46]. Using this method, one does not need an unwieldy analytical expression for L, as it can be constructed from simpler rigid body Lagrangians. To move the Lagrangian L to the discrete time setting, L_d was defined according to the midpoint rule as in (3.1.1).

During the walking motion, control torques are applied at the stance leg's point of contact, both knee joints, and the hip joint. Under these control inputs, the robot is fully actuated on the respective constraint submanifolds R and S. It should be noted, however, that an underactuated version of this problem was solved with the DMOC method in [73].

Results from the gait search optimization are shown in Figure 4.2. The overall small deviations in system energy (note the y axis scale on the figure) indicate an efficient use of work done by the control inputs. This notion is also supported by optimal cost associated with the gait pictured, a specific cost of transport $\eta = 1.59 \times 10^{-3}$. For reference, this is roughly two orders of magnitude smaller than that of average human walking. As we will see, though, such dominance in performance may be difficult to maintain as additional complexity is added to the model.

As in Subsection 3.5.1, post processing steps were performed to ensure that the model remained in the space of feasible contact forces as well as admissible configurations throughout the gait. Given the weight of the robot and the permission of link "intersections" in the plane (links may pass through one another), these conditions represent relatively weak constraints on the gait for this model.

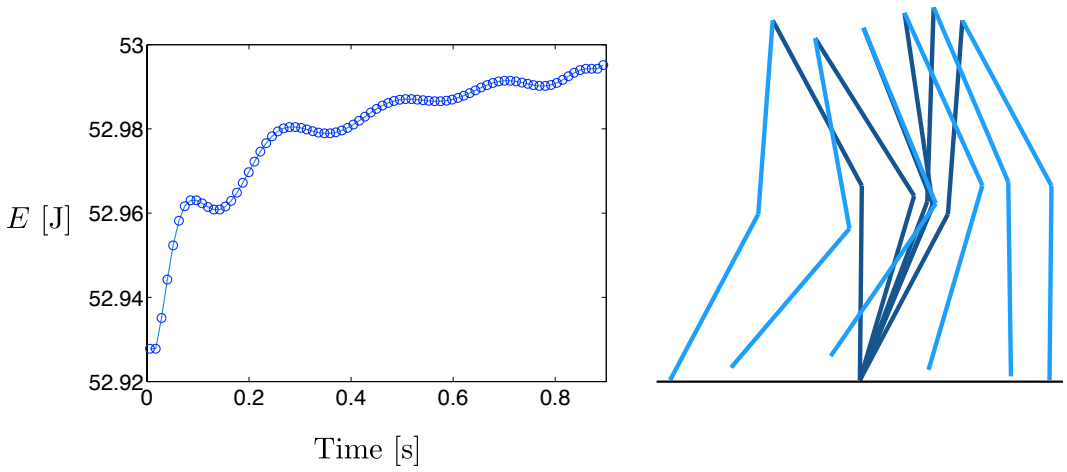

Figure 4.2: Energy behavior and snapshots for one step of the planar biped's locally optimal periodic gait determined by DMOC.

4.2.3 4-Link Three-Dimensional Biped Results

This subsection provides results from an optimal gait search for the planar biped model shown in Figure 4.3. The free configuration space Q for this model is eleven-dimensional with coordinates $(x_1, y_1, z_1, \theta_1, \ldots, \theta_8)$. Physically, this model has point feet and walks along the plane $z = 0$ in three-dimensional Euclidean space. While we do not explicitly present the definitions of R, ∂R, and S that correspond with this behavior, they are based on the respective positions of the robot's feet in the same manner as described in the last subsection.

Working in three dimensions, the definition of S depends on both the step length L_{step} and the step width W_{step} during the double-support phase. In the optimization process they have been specified as $L_{\text{step}} = 0.45$ m and $W_{\text{step}} = 0.2$ m. The remaining parameters in the model have been fixed in the optimization as $L_1 = L_2 = 0.5$ m,

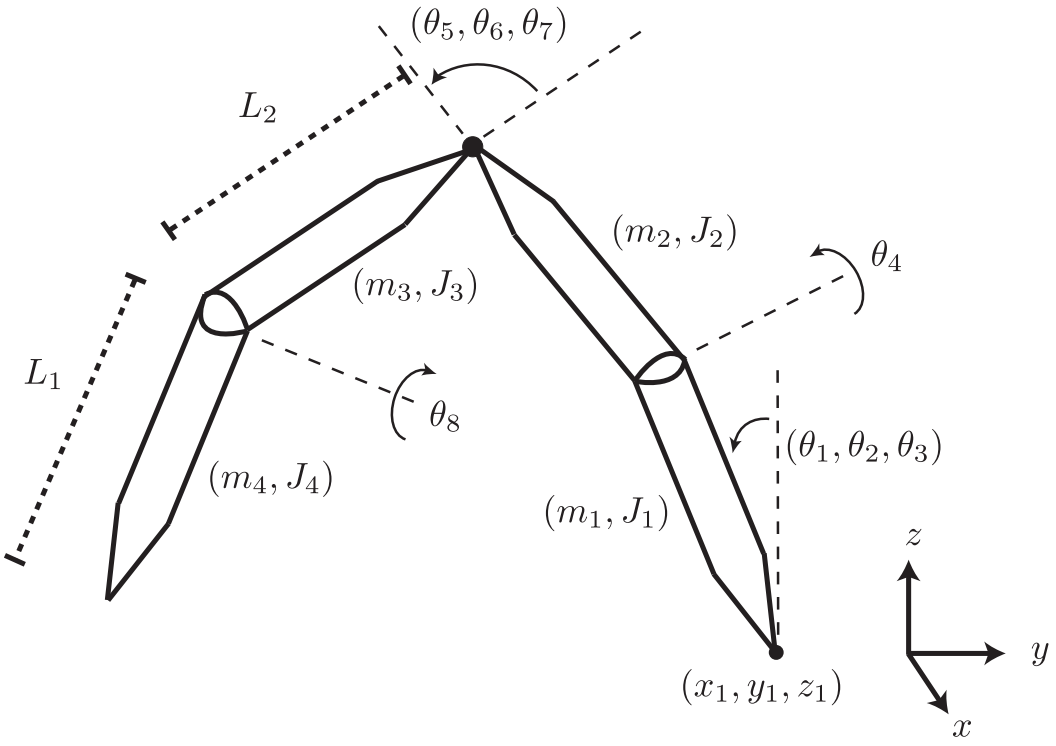

Figure 4.3: A 4-link three-dimensional biped model with revolute joint knees and a spherical joint hip. The triple $(\theta_1, \theta_2, \theta_3)$ represents the ZYZ Euler angles of the body frame of first link with respect to the inertial frame, and $(\theta_5, \theta_6, \theta_7)$ represents the ZYZ Euler angles of the body frame of the third link with respect to the body frame of the second.

$m_1 = m_4 = 2$ kg, $m_2 = m_3 = 3$ kg,

$$J_1 = J_4 = \begin{pmatrix} \frac{31}{1000}m_1L_1^2 & 0 & 0 \\ 0 & \frac{31}{1000}m_1L_1^2 & 0 \\ 0 & 0 & \frac{3}{500}m_1L_1^2 \end{pmatrix},$$

$$J_2 = J_3 = \begin{pmatrix} \frac{31}{1000}m_2L_2^2 & 0 & 0 \\ 0 & \frac{31}{1000}m_2L_2^2 & 0 \\ 0 & 0 & \frac{3}{500}m_2L_2^2 \end{pmatrix}.$$

These inertias, again indicating an assumption of anisotropy for the links composing the biped, were generated using two slender cones (joined at their respective bases) to define the geometry of each link. The period $T = 0.9$ s and mesh of time with $K = 80$ timesteps were retained from the previous example.

The Lagrangian for this system, also having the form $L(q, \dot{q}) = \dot{q}^T M(q)\dot{q} - V(q)$, was handled in the same manner as in the case of the planar biped. Calculations of L and its partial derivatives were performed using the tree structure framework, and L_d was defined according to the midpoint rule. Control torques are applied to the system about each of the θ coordinates, $\theta_1, \ldots, \theta_8$. As in the planar case, this indicates the model is fully actuated on both R and S.

Results from the gait search optimization are shown in Figure 4.4. Again the overall small deviations in system energy indicate an efficient use of work done by the control inputs. However, the specific cost of transport for this gait, $\eta = 9.04 \times 10^{-2}$, indicates a significant drop in efficiency from the planar case. This decrease in efficiency may be attributed to constraints placed on the system by frontal plane dynamics. A number of more efficient gaits were found in the optimization process, but each was ruled inadmissible during post-processing due to either infeasible constraint forces at the point of contact or link intersections during the step. These behaviors were not problematic in the planar case, where only the saggital plane dynamics were captured.

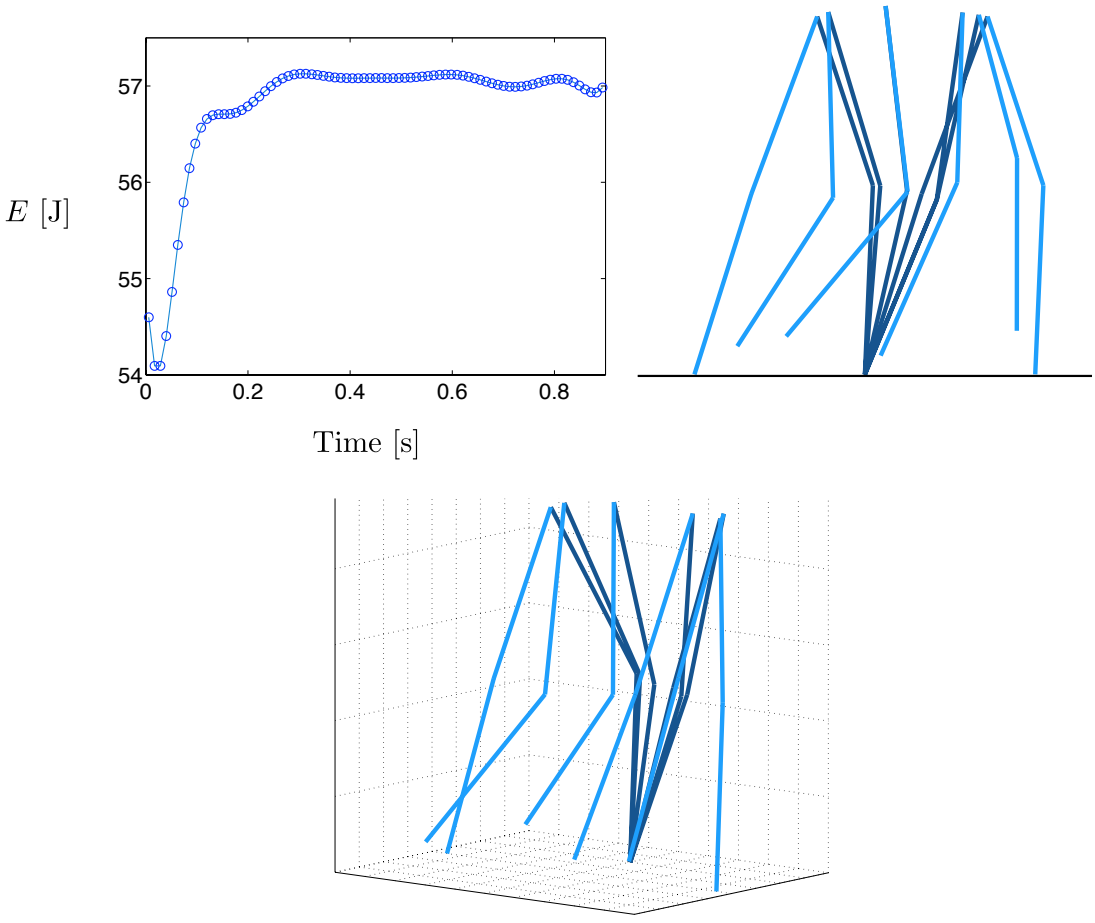

Figure 4.4: Energy behavior and snapshots for one step of the three-dimensional biped's locally optimal periodic gait determined by DMOC.

It is possible that by performing further optimizations or making modifications to the model, a more efficient feasible gait could be identified. Additionally, the method suggested in Remark 4.1 could rule out infeasible results during an optimization, rather than in post-processing. In any case, the gait presented here is feasible and more than twice as efficient as human walking.

Chapter 5

Design of Dynamics Optimization

In this chapter, we present a multilayered design optimization scheme, termed design of dynamics (DD), to determine mechanical system designs that reduce the cost of optimal control. The scheme leverages the results of Chapter 4 by making use of DMOC in the "inner" layer optimization. The "outer" layer, for which function evaluations are assumed to be costly, uses optimization with surrogate functions [45, 6]. DD results are presented for the task of optimizing the knee joint placement of the 4-link planar biped model from Subsection 4.2.2.

5.1 Design of Dynamics

Typically the task of a controls engineer is to achieve some desired performance from a dynamical system through the use of sensors and inputs. Classically, the system model, or plant, defining the system dynamics and available sensors/actuators is assumed to be fixed. Modern control theory provides an impressive set of tools to analyze and control fixed plants, and we postulate that the same tools can provide additional benefits when utilized in the system design process. An example of this is the following DD optimization scheme, which uses DMOC, an optimal control scheme for fixed plants, to perform design optimization.

Formally, the problem considered by DD is that of optimizing a given set of design

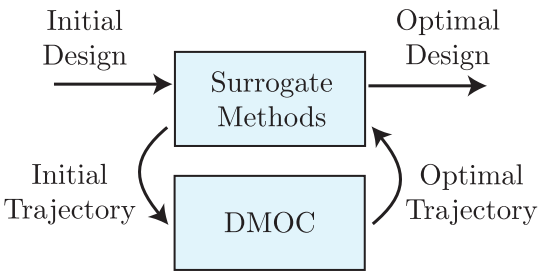

Figure 5.1: The multilayered DD optimization scheme.

parameters β to reduce the cost of optimal control J for a given mechanical system. We propose solving this problem using a multilayered optimization as pictured in Figure 5.1. The "outer" loop of this scheme performs the optimization of β in design space by making function calls to the "inner" loop. The inner loop calculates the cost of optimal control J associated with a particular design by solving the DMOC optimization problem from Section 4.1. Given that each outer loop function evaluation requires the solution of an optimization problem, the outer loop optimization should be performed with a method sensitive to this computational expense. The use of surrogate functions, as described in the next section, is such a method.

Remark 5.1: *In its current definition, the DD scheme is applicable to any mechanical system with quantifiable design parameters that can be treated with the DMOC method. As the class of problems handled with DMOC grows, so will the applicability of DD.*

One issue of note with the proposed DD scheme is the sensitivity of the inner loop to the initial guess provided to SQP as it solves the DMOC problem. For DMOC problems with many local minima, meaning many locally optimal control policies, the cost J determined with SQP will be dependent on both the design parameters β in use and the initial guess for q_d and u_d. This makes the DD scheme, as it is currently expressed, most suitable for problems with a low number of local minima, or at least minima with large basins of attraction relative to initial conditions. In

practice, there is no standard way to determine these attributes a priori for a given DMOC problem. Thus, it remains a subject of future work to adapt the DD scheme to handle problems with a dense population of local minima in design space, as well as to adapt the DMOC framework to be less sensitive to the user's initial guess.

5.2 Optimization with Surrogate Functions

In this section, we discuss the properties of surrogate function optimization methods as motivation for their use in the outer loop of DD. In the outer loop optimization problem, consider that there is no analytical expression for the gradient of J with respect to β. Furthermore, the computational expense associated with outer loop function calls implies that numerical approximations of the gradient would be impractical. It is due to these factors that standard gradient-based optimization methods, SQP or otherwise, are not applicable in this setting. However, surrogate methods [15, 6] have been developed to handle precisely these challenges in optimization.

The basic algorithm underlying the use of surrogate functions in optimization is as follows. Given some function $f(x)$ to be optimized, perform the following:

1. Choose a surrogate s that approximates f using a finite number of function evaluations $f(x_i)$, where the samples x_i belong to a finite set $\{x_1, \ldots, x_d\}$. The definition of s is provided by a user's choice of interpolation or smoothing function.

2. Using some prescribed rules, determine additional sample locations. One obvious rule [6] is to calculate the minimum of s and sample there. More sophisticated implementations may add randomly generated points to globally sample the space [65].

3. Add the newly determined sample points to the set $\{x_1, \ldots, x_d\}$ and perform

all necessary new function evaluations $f(x_i)$.

4. Check for convergence. A criteria for convergence is typically expressed in terms of the improvement in min $f(x_i)$ provided by the function evaluations performed in step 3.

5. Return to step 1 and update the surrogate s. Repeat steps until convergence.

This basic algorithm provides many user freedoms, which has led to several studies regarding customized use and expansion of the method. A means to appropriately select an initial set of samples $\{x_1, \ldots, x_d\}$ has been examined in [77, 53]. Various choices for basis functions defining the structure of s are compared in [45]. Convergence properties, particularly those gained by incorporating pattern search methods into the algorithm above, are examined in [15]. Also, there exists an open source Matlab optimization package [63] that makes use of statistical kriging functions [86], a popular choice of basis for the surrogate s.

5.3 Knee Joint Placement Optimization Results

In this section, we present results from the implementation of DD regarding the knee joint placement of the planar bipedal robot model in Subsection 4.2.2. Here, the inner loop optimization of DD is performed with the DMOC code from that example. The outer loop optimization of DD is performed using the "strawman" algorithm (SA) of [65].

SA is one of the simplest implementations of optimization with surrogate functions. It is used here for illustrative purposes in spite of the performance benefits associated with more complex surrogate methods. In terms of the steps outlined in the previous subsection, SA restricts the sampling in step 2 to a single sample at the minimum of the surrogate s. The remainder of the steps remain unchanged, implying

that SA still provides user freedoms in terms of the choice of initial samples, the structure of the surrogate, and the criteria for convergence.

For the use of SA in the DD example to come, the one-dimensional design optimization was simply initialized with two samples in a promising region of design space. The surrogate s was chosen to be a cubic spline passing through the function evaluations $J(\beta_i)$. Convergence was determined when the addition of a sample produced less than a 1×10^{-5} percent change in $\min J(\beta_i)$.

To apply DD optimization in the task of knee joint placement, the biped model in Figure 4.1 was parameterized using $\beta = L_1$. The total height of the biped was kept fixed in the design process by defining $L_2 = 1 - \beta$ such that the biped remained 1 m tall for all values of β. The practice of equating the cost of optimal control J and the dimensionless specific cost of transport η was retained from Subsection 4.2.2. Results for the DD optimization of J over β are shown in Figure 5.2.

Using SA in the outer loop, DD produced a locally optimal design in nine function evaluations. The specific cost of transport associated with this design is $\eta = 4.44 \times 10^{-4}$, an 11.1 percent improvement over the worst of our samples $J(\beta_i)$ and a 72.1 percent improvement over the results in Subsections 4.2.2. Though the example problem considered here is low dimensional, the efficiency of DD in this instance motivates its development for and use on problems of higher complexity.

DMOC results, in terms of energy behavior and gait snapshots, for the locally optimal design produced by DD are pictured in Figure 5.3. As in Figure 4.2, the scale on the energy plot indicates low overall fluctuation in system energy and efficient use of work done by the controls. In terms of the influence of the knee joint placement on efficiency, the robot seems to leverage high knees and short thighs by lowering its stance thigh in the first half of the step. This lowering motion may make it easier to lift the swing leg and save energy required from the controls.

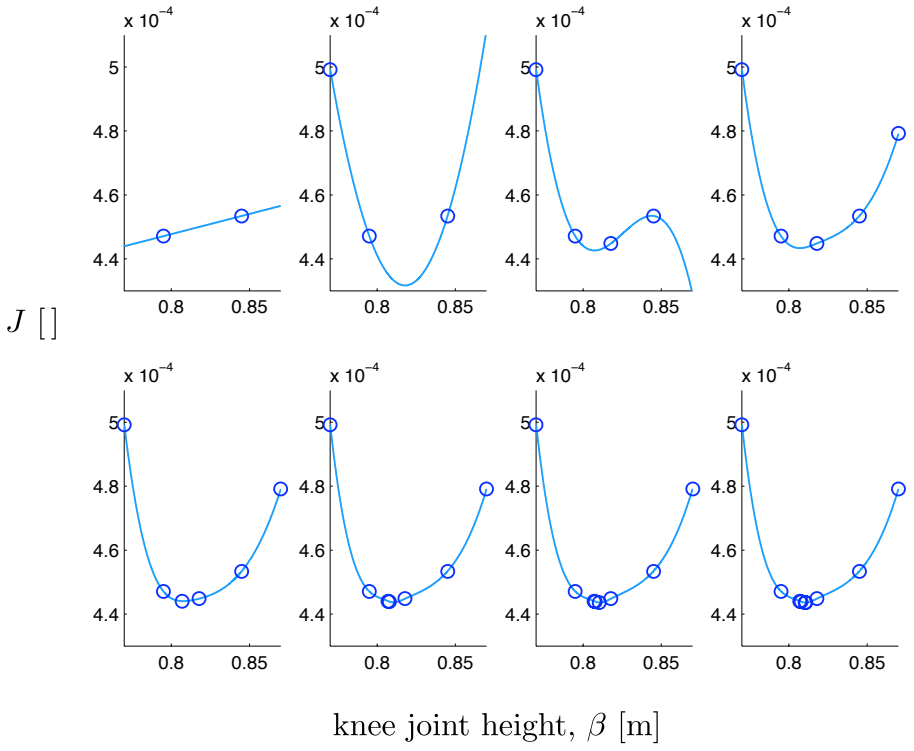

Figure 5.2: Progression of the "strawman" surrogate method in the outer loop of DD. The optimal knee joint placement is determined in nine function evaluations.

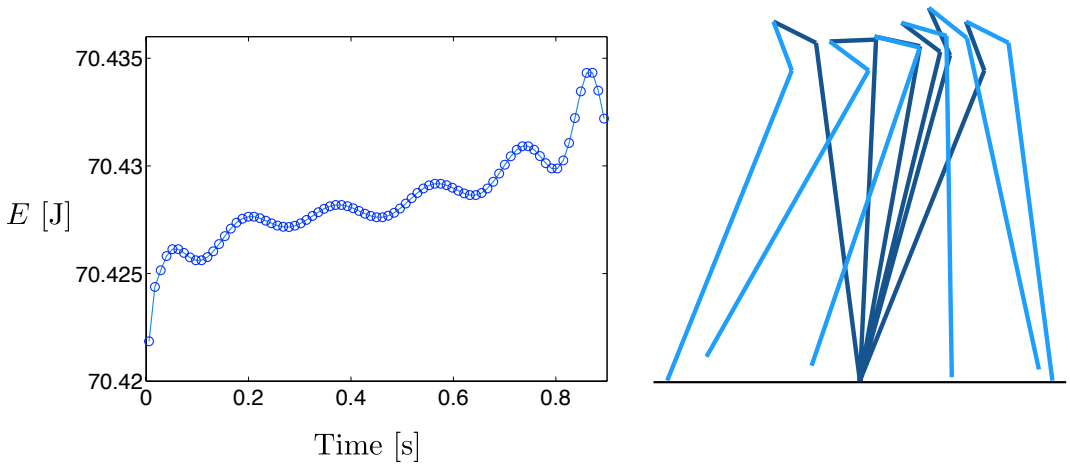

Figure 5.3: Energy behavior and snapshots for one step of the locally optimal gait of the locally optimal design produced by DD.

Chapter 6

Future Directions

There are several future directions to pursue in order to extend the applicability and utility of the theory and methods presented in this thesis. Though a variety of behaviors have been captured with variational nonsmooth mechanics here, a number of relevant behaviors have yet to be modeled. Adding complexity to the system constraints (making them nonholonomic for instance) and contact conditions (examining compliant patch contacts for instance) provides challenging important problems.

Another task is to develop more computationally feasible variational collision integration methods. The adaptive time stepping used in the integrators derived in this thesis makes them ill suited for large systems with a high density of collision events over time. Defining a symplectic method that captures impact mechanics using fixed time steps would increase applicability and attract more users.

Improvements in the DMOC method for nonsmooth systems could be made in more than one regard. As mentioned in Remark 4.1, dynamic programming could improve the DMOC optimization process by allowing changes in collision time and collision model within the optimization. This improvement will allow DMOC to handle problems where the timing of impacts and behavior of the system during impact is not known a priori.

A second improvement for DMOC is applicable to the method as a whole, not just the nonsmooth case. Casting the DMOC problem with such a large number

of equality constraints (a set of DEL equations at each time node) increases computational expense and can actually create additional local minima in the trajectory optimization process. By leveraging ideas like differential flatness, one may be able to decrease the dimension of the DMOC problem in terms of both optimization variables and number of constraints.

For the DD method, improvements could be made in terms of sensitivity to inner loop initialization. The inner loop requires both design parameters and an initial condition to compute a cost. The outer loop is only interested in the influence of the parameters on cost, and thus a means to minimize or remove the influence of the inner loop initial condition must be explored.

Bibliography

[1] R. Abraham, J. E. Marsden, and T. S. Ratiu. *Manifolds, Tensor Analysis and Applications*, volume 75 of *Appl. Math. Sci.* Springer-Verlag, New York, second edition, 1988.

[2] V. Acary and B. Brogliato. *Numerical Methods for Nonsmooth Dynamical Systems: Applications in Mechanics and Electronics*, volume 35. Springer Lecture Notes in Applied and Computational Mechanics, 2008.

[3] N. M. Alexandrov, J. E. Dennis, R. M. Lewis, and V. Torczon. A trust-region framework for managing the use of approximation models in optimization. *Structural Optimization*, 15(1):16–23, 1998.

[4] A. D. Ames and R. D. Gregg. Stably extending two-dimensional walking to three dimensions. In *Proc. ACC, New York*, 2007.

[5] C. Audet and J. E. Dennis. Analysis of generalized pattern searches. *SIAM J. on Optimization*, 13(3):889–903, 2003.

[6] J. F. M. Barthelemy and R. T. Haftka. Approximation concepts for optimum structural design—a review. *Structural and Multidisciplinary Optimization*, 5(3):129–144, 1993.

[7] H. Baruh. *Analytical Dynamics*. WCB/McGraw-Hill, 1999.

[8] A. Bemporad and M. Morari. Control of systems integrating logic, dynamics, and constraints. *Automatica*, 35(3):407–427, 1999.

[9] M. Benzi, G. Golub, and J. Liesen. Numerical solution of saddle point problems. *Acta Numerica*, 2005.

[10] P. Betsch and S. Leyendecker. The discrete null space method for the energy consistent integration of constrained mechanical systems. II. Mulitbody dynamics. *Int. J. Num. Meth. Eng.*, 67:499–552, 2006.

[11] P. Betsch and P. Steinmann. Constrained dynamics of geometrically exact beams. *Comput. Mech.*, 31(1–2):49–59, 2003.

[12] J. T. Betts. Survey of numerical methods for trajectory optimization. *AIAA J. Guidance, Control, and Dynamics*, 21(2):193–207, 1998.

[13] T. Binder, L. Blank, H. G. Bock, R. Bulirsch, W. Dahmen, M. Diehl, T. Kronseder, W. Marquardt, J. P. Schlöder, and O. v. Stryk. Introduction to model based optimization of chemical processes on moving horizons. In M. Grötschel, S. O. Krumke, and J. Rambau, editors, *Online Optimization of Large Scale Systems: State of the Art*, pages 295–340. Springer, 2001.

[14] A.m. Bloch, J. Ballieul, P. Crouch, and J. E. Marsden. *Nonholonomic Mechanics and Control*, volume 24. Interdisciplinary Applied Mathematics, Springer-Verlag, 2003.

[15] A. J. Booker, J. E. Dennis Jr., P. D. Frank, D. B. Serafini, V. Torczon, and M. W. Trosset. A rigorous framework for optimization of expensive functions by surrogates. *Structural and Multidisciplinary Optimization*, 17(1):1–13, 1999.

[16] N. M. Bou-Rabee and J. E. Marsden. Reduced Hamilton-Pontryagin variational integrators. *Found. Comput. Math.*, 9:1–23, 2008.

[17] M. S. Branicky, V. S. Borkar, and S. K. Mitter. A unified framework for hybrid control: Model and optimal control theory. *IEEE Trans. Auto. Control*, 43(1):31–45, 1998.

[18] K. E. Brenan, S. L. Campbell, and L. R. Petzold. *Numerical Solution of Initial-Value Problems in Differential-Algebraic Equations*. Prentice Hall, 1989.

[19] B. Brogliato. *Nonsmooth Impact Mechanics: Models, Dynamics and Control*, volume 220 of *Lecture Notes in Control and Inform. Sci.* Springer, New York, 1996.

[20] B. Brogliato. *Nonsmooth Mechanics*. Springer, 1999.

[21] B. Brogliato. On the control of non-smooth complementarity dynamical systems. *Phil. Trans. R. Soc. Lond A*, 359:2369–2383, 2001.

[22] F. Bullo and M. Zefran. Modeling and controllability for a class of hybrid mechanical systems. *IEEE Transactions on Robotics and Automation*, 18(4):563–573, 2002.

[23] G. Buttazzo and D. Percivale. On the approximation of the elastic bounce problem on riemannian manifolds. *Journal of Differential Equations*, 47:227–275, 1983.

[24] A. Chatterjee and A. Ruina. A new algebraic rigid-body collision law based on impulse space considerations. *Journal of Applied Mechanics-Transactions of the ASME*, 65(4):939–951, 1998.

[25] C. Chevallereau and Y. Aoustin. Optimal reference trajectories for walking and running of a biped robot. *Robotica*, 19(5):557–569, 2001.

[26] C. Chevallereau, J.W. Grizzle, and C. Shih. Asymptotically stable walking for a five-link underactuated 3D bipedal robot. *IEEE Trans on Robotics*, 25(1):37–50, 2008.

[27] F. Cirak and M. West. Decomposition contact response (dcr) for explicit finite element dynamics. *Int. J. for Num. Methods in Eng.*, 64:1078–1110, 2008.

[28] S. Collins, A. Ruina, R. Tedrake, and M. Wisse. Efficient bipedal robots based on passive-dynamic walkers. *Science*, 307(5712):1082–1085, 2005.

[29] P. A. M. Dirac. On generalized hamiltonian dynamics. *Can. J. Math.*, 2:129–148, 1950.

[30] V. Duindam. *Port-Based Modeling and Control for Efficient Bipedal Walking Robots*. PhD thesis, University of Twente, 2006.

[31] R. Fetecau. *Variational Methods for Nonsmooth Mechanics*. PhD thesis, California Institute of Technology, 2003.

[32] R. Fetecau, J. E. Marsden, M. Ortiz, and M. West. Nonsmooth lagrangian mechanics and variational collision integrators. *SIAM Journal on Dynamical Systems*, 2:381–416, 2003.

[33] A. F. Filippov. Differential equations with discontinuous right-hand side. *American Mathematical Society Translations*, 42:199–231, 1964.

[34] A. F. Filippov. Classical solutions of differential equations with multivalued right-hand side. *SIAM J. Control Optim.*, 5:609–621, 1967.

[35] L. Geppert. Qrio, the robot that could. *IEEE Spectrum*, 41(5):34–37, 2004.

[36] Philip E. Gill, Walter Murray, and Michael A. Saunders. SNOPT: an SQP algorithm for large-scale constrained optimization. *SIAM Rev.*, 47(1):99–131 (electronic), 2005.

[37] D. E. Goldberg. *Genetic algorithms in search, optimization and machine learning*. Addison-Wesley, 1989.

[38] A. Goswami, B. Espiau, and A. Keramane. Limit cycles in a passive compass gait biped and passivity-mimicking control laws. *Journal of Autonomous Robots*, 4:273–286, 1997.

[39] A. Goswami, B. Thuilot, and B. Espiau. Compass-like biped robot part i: Stability and bifurcation of passive gaits. Technical Report 2996, INRIA, 1996.

[40] R. D. Gregg and M. W. Spong. Reduction-based control with application to three-dimensional bipedal walking robots. *Proc. ACC, Seattle*, 2008.

[41] J. W. Grizzle, G. Abba, and F. Plestan. Asymptotically stable walking for biped robots: analysis via systems with impulse effects. *IEEE Trans. Aut. Control*, 46:51–64, 2001.

[42] E. Hairer, C. Lubich, and G. Wanner. *Geometric numerical integration*, volume 31 of *Springer Series in Computational Mathematics*. Springer-Verlag, Berlin, second edition, 2006.

[43] Y. Hurmuzlu. Dynamics of bipedal gait; Part I—objective functions and the contact event of a planar five-link biped. Part II—stability analysis of a planar five-link biped. *ASME Journal of Applied Mechanics*, 60(2):331–344, 1993.

[44] Y. Hurmuzlu, F. Genot, and B. Brogliato. Modeling, stability and control of biped robots—a general framework. *Automatica*, 40(10):1647–1664, 2004.

[45] R. Jin, W. Chen, and T. W. Simpson. Comparative studies of metamodelling techniques under multiple modelling criteria. *Structural and Multidisciplinary Optimization*, 23(1):1–13, 2001.

[46] E. R. Johnson and T. D. Murphey. Discrete and continuous mechanics for tree representations of mechanical systems. *IEEE Trans. on Robotics*, 25(6):1249–1261, 2008.

[47] O. Junge, J. E. Marsden, and S. Ober-Blöbaum. Discrete mechanics and optimal control. *Proc. IFAC Conf, Prague*, 2005.

[48] O. Junge, J. E. Marsden, and S. Ober-Blöbaum. Optimal reconfiguration of formation flying spacecraft—a decentralized approach. *Proc. CDC*, 45:5210–5215, 2006.

[49] C. Kane, J. E. Marsden, and M. Ortiz. Symplectic energy-momentum integrators. *J. Math. Phys.*, 40:3353–3371, 1999.

[50] C. Kane, E. A. Repetto, M. Ortiz, and J. E. Marsden. Finite element analysis of nonsmooth contact. *Computer Meth. in Appl. Mech. and Eng.*, 180:1–26, 1999.

[51] M. Kobilarov, M. Desbrun, J. E. Marsden, and G. S. Sukhatme. A discrete geometric optimal control framework for systems with symmetries. *Robotics: Science and Systems*, 3:1–8, 2007.

[52] M. Kobilarov and G. S. Sukhatme. Optimal control using nonholonomic integrators. *Proc. IEEE Int. Conf. on Robotics and Automation*, 2007.

[53] J. R. Koehler and A. B. Owen. Computer experiments. In S. Ghosh and C. R. Rao, editors, *Handbook of Statistics 13: Design and Analysis of Experiments*, pages 261–308. Elsevier Science, 1996.

[54] V. V. Kozlov and D. V. Treschev. Billiards. a genetic introduction to the dynamics of systems with impacts. *AMS Transl. Ser.*, 1991.

[55] T. Lee, M. Leok, and N. H. McClamroch. Lie group variational integrators for the full body problem. *Comput. Methods Appl. Mech. Engrg.*, 196(29-30):2907–2924, 2007.

[56] A. Lew. *Variational time integrators in computational solid mechanics*. PhD thesis, California Institute of Technology, 2003.

[57] A. Lew, J. E. Marsden, M. Ortiz, and M. West. Asynchronous variational integrators. *Archive for Rat. Mech. An.*, 167:85–146, 2003.

[58] A. D. Lewis and R. M. Murray. Variational principles for constrained systems: theory and experiment. *Int. J. Nonlinear Mech.*, 30(6):793–816, 1995.

[59] S. Leyendecker. *Mechanical integrators for constrained dynamical systems in flexible multibody dynamics*. PhD thesis, Kaiserslautern University of Technology, 2006.

[60] S. Leyendecker, P. Betsch, and P. Steinmann. The discrete null space method for the energy consistent integration of constrained mechanical systems. III. Flexible multibody dynamics. *Multibody System Dynamics*, 19:45–72, 2008.

[61] S. Leyendecker, J. E. Marsden, and M. Ortiz. Variational integrators for constrained mechanical systems. *Z. Angew. Math. Mech.*, 88:677–708, 2008.

[62] S. Leyendecker, S. Ober-Blöbaum, J. E. Marsden, and M. Ortiz. Discrete mechanics and optimal control for constrained multibody dynamics. *Proc. of the 6th International Conference on Multibody Systems, Nonlinear Dynamics, and Control, ASME International Design Engineering Technical Conferences*, Proceedings of IDETC/MSNDC 2007:1–10, 2007.

[63] S. N. Lopenhaven, H. B. Nielsen, and J. Sondergaard. DACE – a Matlab kriging toolbox. Technical Report IMM-TR-2002-12, Technical University of Denmark, 2002.

[64] J. Lygeros, K. H. Johansson, S. N. Simic, J. Zhang, and S. S. Sastry. Dynamical properties of hybrid automata. *IEEE Trans, on Automatic Control*, 48(1):2–17, 2003.

[65] A. L. Marsden, M. Wang, J. E. Dennis Jr., and P. Moin. Optimal aeroacoustic shape design using the surrogate management framework. *Optimization and Engineering*, 5(2):235–262, 2004.

[66] Alison L. Marsden, Meng Wang, John E. Dennis Jr., and Parviz Moin. Optimal aeroacoustic shape design using the surrogate management framework. *Optim. Eng.*, 5(2):235–262, 2004. Special issue on surrogate optimization.

[67] J. E. Marsden and T. S. Ratiu. *Introduction to Mechanics and Symmetry*, volume 17 of *Texts in Applied Mathematics*. Springer-Verlag, New York, second edition, 1999.

[68] J. E. Marsden and M. West. Discrete mechanics and variational integrators. *Acta Numerica*, 10:357–514, 2001.

[69] R. McLachlan and M. Perlmutter. Integrators for nonholonomic mechanical systems. *J. Nonlinear Sci.*, 16(4):283–328, 2006.

[70] J.-J. Moreau. Une formulation du contact à frottement sec; application au calcul numérique. *C. R. Acad. Sci. Paris Sér. II*, 302:799–801, 1986.

[71] J.-J. Moreau. Free boundaries and nonsmooth solutions to some field equations: variational characterization through the transport method. In *Boundary control*

and boundary variations (Nice, 1986), volume 100 of *Lecture Notes in Comput. Sci.*, pages 235–264. Springer, New York, 1988.

[72] S. Ober-Blöbaum, O. Junge, and J. E. Marsden. Discrete mechanics and optimal control: an analysis. *ESAIM: Control, Optimisation and Calculus of Variations*, 2009.

[73] D. Pekarek and J. E. Marsden. Variational collision integrators and optimal control. *Proc. of the 18th International Symposium on Mathematical Theory of Networks and Systems (MTNS)*, 2008.

[74] C. K. Raju. Products and compositions with the dirac delta function. *Journal of Physics A: Mathematical and General*, 15(2):381–396, 1982.

[75] W. Raza and K. Y. Kim. Evaluation of surrogate models in optimization of wire-wrapped fuel assembly. *J. of Nuclear Science and Technology*, 44(6):819–822, 2007.

[76] L. Roussel, C. Canudas-de Wit, and A. Goswami. Generation of energy optimal complete gait cycles for biped robots. *Proc. IEEE Conf. on Robotics and Automation*, 1998.

[77] J. Sacks, W. J. Welch, T. J. Mitchell, and H. P. Wynn. Design and analysis of computer experiments. *Statistical Science*, 4(4):409–423, 1989.

[78] Y. Sakagami, R. Watanabe, C. Aoyama, S. Matsunaga, N. Higaki, and K. Fujimura. The intelligent asimo: System overview and integration. *Proc. IEEE/RJS international conference on intelligent robots and systems*, 3:2478–2483, 2002.

[79] M. S. Shaikh and P. E. Caines. On the hybrid optimal control problem: Theory and algorithms. *IEEE Trans. Auto. Control*, 52(9):1587–1603, 2007.

[80] J. C Simo, P. Wriggers, and R. L. Taylor. A perturbed lagrangian formulation for the finite-element solution of contact problems. *Comput. Methods Appl. Mech. Engrg*, 50(2):163–180, 1985.

[81] M. W. Spong and F. Bullo. Controlled symmetries and passive walking. *IEEE Trans. Aut. Control*, 50(7):1025–1031, 2005.

[82] M. Srinivasan and A. Ruina. Computer optimization of a minimal biped model discovers walking and running. *Nature*, 439(7072):72–75, 2006.

[83] A. Stern, Y. Tong, M. Desbrun, and J. E. Marsden. Computational electromagnetism with variational integrators and discrete differential forms. *Numer. Math.*, 2007.

[84] D. E. Stewart. Convergence of a time-stepping scheme for rigid-body dynamics and resolution of Painleve's problem. *Arch. Rational Mech. Anal*, 145:215–260, 1998.

[85] D. E. Stewart. Rigid-body dynamics with friction and impact. *SIAM Review*, 42(1):3–39, 2000.

[86] G. S. Watson. Smoothing and interpolation by kriging and with splines. *Mathematical Geology*, 16(6):601–615, 1984.

[87] L. C. Young. *Lectures on the Calculus of Variations and Optimal Control Theory.* Corrected printing, Chelsea, 1980, 1969.